CAPITAL UNIVERSITY OF SCIENCE AND TECHNOLOGY, ISLAMABAD

Comparative Analysis of Modified Inc.Cond MPPT Algorithms based-on Direct Control

by

Noman Barkat

A thesis submitted in partial fulfillment for the
degree of Master of Science

in the
Faculty of Engineering
Department of Electrical Engineering

2022

I am dedicating this thesis to teachers who strengthen me and put me on the right path. I am also dedicating to my Parents who supports me and always prayed for me and older brother and sisters who have inspired and motivates me in all situation.

CERTIFICATE OF APPROVAL

Comparative Analysis of Modified Inc.Cond MPPT Algorithms Based-on Direct Control

by

Noman Barkat

(MEE193003)

THESIS EXAMINING COMMITTEE

S. No.	Examiner	Name	Organization
(a)	External Examiner	Dr. Tahir Nadeem Malik	HITEC, Taxila
(b)	Internal Examiner	Dr. Noor Muhammad Khan	CUST, Islamabad
(c)	Supervisor	Dr. Umer Amir Khan	CUST, Islamabad

Dr. Umer Amir Khan
Thesis Supervisor
May, 2022

Dr. Noor Muhammad Khan
Head
Dept. of Electrical Engineering
May, 2022

Dr. Imtiaz Ahmad Taj
Dean
Faculty of Engineering
May, 2022

Author's Declaration

I, **Noman Barkat** hereby state that my MS thesis titled "**Comparative Analysis of Modified Inc.Cond MPPT Algorithms Based-on Direct Control**" is my own work and has not been submitted previously by me for taking any degree from Capital University of Science and Technology, Islamabad or anywhere else in the country/abroad.

At any time if my statement is found to be incorrect even after my graduation, the University has the right to withdraw my MS Degree.

(Noman Barkat)

Registration No: MEE193003

Plagiarism Undertaking

I solemnly declare that research work presented in this thesis titled "**Comparative Analysis of Modified Inc.Cond MPPT Algorithms Based-on Direct-control**" is solely my research work with no significant contribution from any other person. Small contribution/help wherever taken has been duly acknowledged and that complete thesis has been written by me.

I understand the zero tolerance policy of the HEC and Capital University of Science and Technology towards plagiarism. Therefore, I as an author of the above titled thesis declare that no portion of my thesis has been plagiarized and any material used as reference is properly referred/cited.

I undertake that if I am found guilty of any formal plagiarism in the above titled thesis even after award of MS Degree, the University reserves the right to withdraw/revoke my MS degree and that HEC and the University have the right to publish my name on the HEC/University website on which names of students are placed who submitted plagiarized work.

(Noman Barkat)

Registration No: MEE193003

List of Publications

It is certified that following publication(s) have been made out of the research work that has been carried out for this thesis:-

1. **N. Barkat**," A Comparative Study of Different Modified Incremental Conductance MPPT Algorithms Under very Fast-Changing Atmospheric Conditions for Solar Charging Station," *2021 16th International Conference on Emerging Technologies (ICET)*, pp. 1-6. IEEE, 2021

(Noman Barkat)

Registration No: MEE193003

Acknowledgement

First, I am very thankful to Allah who blessed me with strenght, patience and knowledge during the period of my studies. I would like to express my gratitude to my primary supervisor, Dr. Umer Amir Khan, who guided me throughout this thesis and provided understanding at every stage and correct my direction.

I would also like to thank my family members: my mother, my father and my siblings who supported me, encouraged me, motivates me and offered deep insight into the study. I wish to acknowledge those people for helping me finalize the thesis. I also want to extend my special thanks to Dr. Noor Muhammad Khan and Dr. Imtiaz Ahmad Taj for supporting me. Again i would like to show my deep appreciation to my supervisors who helped me finalize my thesis.

(Noman Barkat)

Abstract

Solar energy is vital to achieve clean, green, and sustainable energy. It has many applications in the domain of solar transportation. For instance, solar electric cars and solar buses. These vehicles consume energy from solar cells installed over their roofs. The efficiency of installed solar cells can be improved by tracking them on their maximum power point (MPPT). In the literature, many techniques are presented to achieve maximum energy from solar cells. However, among these the incremental conductance algorithm is the most efficient algorithm for solar cars. It is more efficienct, easy to implement, and provide quick response under fast-changing irradiance level. For MPPT operation, multiple modified IncCond algorithms are proposed in the literature. Yet, these modified IncCond algorithms are neither simulated against the rapidly changing atmospheric conditions nor compared with each other for the selection of the best IncCond algorithm for solar car application. In this thesis, a comparative study is conducted among the five selected modified incremental conductance algorithms under fast-changing solar irradiance and varying temperature conditions. Moreover, comparison of voltage, current and power of each IncCond algorithm is also extracted and tested to validate the performance of best algorithm. In addition, these algorithms are ranked according to their performance with respect to following performance testing parameters (PTP). Like, convergence speed, steady-state oscillation, system complexity, efficiency, length of the algorithm, accuracy, performance under varying temperatures, and detection of fast change in solar irradiance in order to improve the efficiency of solar cars. Whereas, the selection of the best algorithm for solar car is made on the basis of extracted power, performance efficiency, tracking accuracy and behaviour under varying temperature conditions. To sum up all the discussion, it can be concluded, this comparative study would provide realistic analysis for the implementation of the best algorithm for the solar car applications. The overall simulations are performed in MATLAB/SIMULINK environment.

Contents

List of Figures

List of Tables

Abbreviations

AC	Alternating Current
AI	Artificial Intelligence
ANN	Artificial Neural Network
CdTe	Cadmium Telluride
CIGS	Copper Indium Gallium Selenide
CPG	Constant Power Generation
DC	Direct Current
DOD	Depth of discharge
DSASS	Dual Scaled Adaptive Stepsize
EAS	Enhanced Auto-scaling Stepsize
FLC	Fuzzy Logic Controller
GA	Genetic Algorithm
GOW	Grey Wolf Optimization
I	Current
Impp	Current at max. power point
Inc.Cond	Incremental conductance
I-V curve	Current and Voltage curve
LF	Lyapunov Function
LS	Large Step Size
LSA	Lyapunov Stability Analysis
LVD	Low Voltage Disconnect
Mono c-Si	Monocrystalline and Silicon
MPPT	Maximum Power Point Tracking
NAVSS	New Advance Variable Step Size

NB	Negative Big
NS	Negative Small
P	Power
PB	Positive Big
PBV	Petroleum-based Vehicles
Pmpp	Power at max. power point
PO	Perturb and Observe
Poly c-Si	Polycrystalline Silicon
PS	Positive Small
PSO	Particle Swarm Optimization
PTP	Performance Testing Parameters
P-V curve	Power and Voltage curve
PV	Photovoltaic
PWM	Pulse Width Modulation
QBC	Quadratic Boost Converter
SEPIC	Single-ended Primary-inductor Converter
SMC	Sliding Mode Cotroller
SOC	State of Charge
SS	Small Step Size
STC	Standard Test Condition
V	Voltage
Vmpp	Voltage at max. power point
VSS	Variable Step size
VSS-VSF	Variable Step Size based on variable step size
ZE	Zero

Symbols

V_{oc}	Open-circuit Voltage
I_{sc}	Short-circuit Current
V_{pv}	Voltage of Photovoltaic array
I_{pv}	Current of Photovoltaic array
P_{pv}	Power of Photovoltaic array
V_{ref}	Reference Voltage
ΔI	Change in Current
ΔV	Change in Voltage
ΔP	Change in Power
Δd	Change in Dutycycle
$d(k)$	Dutycycle at time $'k'$
$d(k-1)$	Dutycycle at time $'k-1'$
Δs	Change in Slope
$S(k)$	Slope at time $'k'$
$S(k-1)$	Slope at time $'k-1'$
Δe	Change in Error
z	Minimum slope value
e	Small Tolerance
$\sigma(\alpha)$	Signum Function
α	Sliding surface

Chapter 1

Introduction

Electricity is the key element of the development of any country and also generated electricity must be cheap and environment friendly. Electricity generation technologies generate Co_2 and other greenhouse gases. Due to this carbon footprint increase and global warming increases, approximately 40% of global Co_2 produce by electricity generation through, burning the fossil fuels like (coal, oil, petroleum, natural gas, bitumen's and heavy oil) to run our Electricity Generation Power Plant. Combustion of these fossil fuels causes the production of Carbon Dioxide, the heat-trapping, green-houses gas responsible for Global Warming. A carbon footprint is the total amount of Carbon Dioxide and other Greenhouse gases produced over the full supply chain of the production of electricity using Fossil fuels. It is determined by gram carbon dioxide equivalent per kilowatt-hours of electricity generation [1] . Last 2 to 3 years, the largest demand of increase in energy consumption, 41% was achieved by renewables. The second-largest contribution to pull off the 36% energy consumption was by natural gas. The overall share of energy needs, oil remained in first place with 33% of the whole energy need of the world. The remaining contribution came from coal (27%), hydropower (6%), natural gas (24%), nuclear power (4%), and renewables are only (5%). To draw more attention to overcome the environmental problems, it is important to achieve the maximum demands of energy must be fulfilled by renewable and on small scale, renewable energy plants must be developed for attraction and encourage the whole

world to shift their complete fossil fuel-based energy generation system to renewable energy system [2]. Figure 1.1 shows that 84% still fossil fuel is contributed to the world's primary energy consumption in 2019-2021.
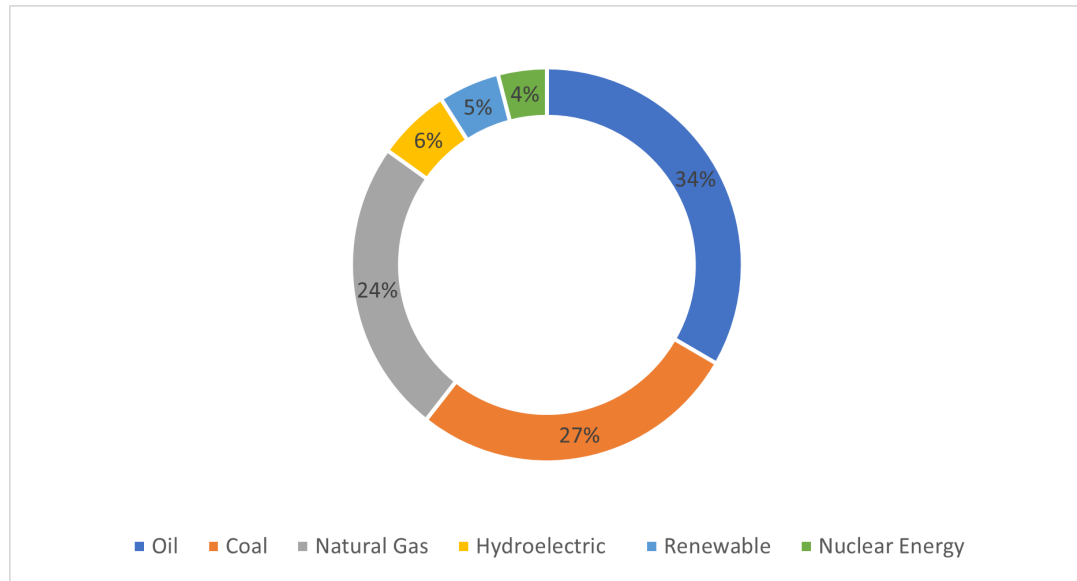
FIGURE 1.1: Primary Global Energy Consumption 2019-21 [2]

To generate electricity without affecting the environment, Renewable Energy Sources are used for the production of electricity. Renewable Energy Sources include Hydro energy, Solar energy, Wind energy, Tidal energy, Geothermal energy, and Biomass energy. All of these sources produce Green, emission-free, and also cheap Electricity.

Renewable energy sources have intermittent behavior which is not in human control, there is not always the sunny day, not every day the speed of wind is constant. The sunlight changes as the sun move from east to west, and our PV system must give maximum power. To do so we need to track the sun mechanically or use a different method to operate the PV system at its the maximum power.

1.1 Basic Idea of Solar Energy

The researcher has been working on the development of improving the design and manufacturing of the components of renewable energy in two directions one is to

develop high-performance material and the second is improving and optimization of the technique of energy conversion. A Solar (PV) renewable energy source, the PV system converts the solar energy (Sunlight energy) to generate electricity, the working principle of the Solar PV is photovoltaic effect, a photon the basic unit of light impacting a surface made of special material generates the release of an electron. PV systems are vary in size from a small rooftop or portable system to a massive utility-scale generation plant. PV system produces pure DC power which is used to run DC load, if DC power is excessive, it can be stored in a battery known as a stand-alone PV system. Another option is that this DC power is converted into AC power by using DC- AC power converter, satisfying AC load requirements, and delivering the power to Conventional AC Power Grid known as grid-connected PV systems [3].
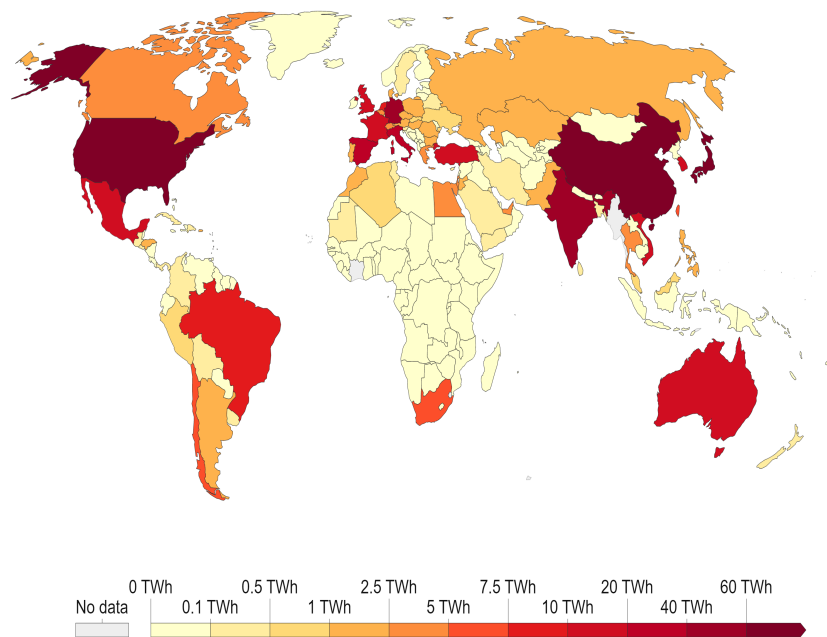
FIGURE 1.2: Energy Produces by whole world using Renewable Energy Sources 1985-20 [3]

PV system is a renewable energy source, the amount of solar power which is reaching the earth in 1 -hour is more than the planet's total energy requirements for the whole year. PV systems operate silently to generate power as compared to

other power generation systems. PV systems need little maintenance, remove the dust from the PV panels to perform well. Figure 1.2 shows the data of energy production from 1985 - 20 by the whole world, in which large energy demands are achieved by Hydro, Wind, and less contribution of Solar energy as compared to other renewable energy sources. Pakistan has immense potential for producing electricity through solar power. Installed solar power capacity in Pakistan is around 1.03 tegawatt's. But currently only produces a meager 1.16% of its electricity through solar power and 64% with fossil fuels. Other electricity sources include hydropower at 27% and nuclear at 5%. Solar energy applications are listed down:

1. Solar Electricity.

2. Solar Water Heating.

3. Solar Heating.

4. Solar Lighting.

5. Solar Ventilation.

6. Portable Solar.

7. Solar Transportation.

A huge amount of air pollution emitted from transportation which contribute to smog,to harm our health and contain greenhouse gases that cause climate change. Use of gasoline and diesel fuel creates harmful by-products like nitrogen dioxide, carbon monoxide,benzene and formaldehyde. By shifting our gasoline and diesel fuel vehicles to electric vehicles and these vehicles are charged by solar energy.

For charging of an electric vehicle, solar charging stations are constructed in which two or more charging slots are available depending on installed solar power. Figure 1.3 represent the solar charging station. This solar charging station made by solar panels and this is called static solar charging station. The second kind of solar charging is, the solar cells are mounted on the roof of a car. These cells are

operated by some dc-dc converter, and these converter energise the load. These solar cells are highly efficient which regulates charging process and required less charging stop.

In Pakistan Sigma motor's develop a solar electric car having maximum range of 200km in one full charge. The electrical specifications include AC electric motor to drive the wheels, battery capacity is 72V and 100Ah. The solar power installed on car hood and roof is about 300 to 500 watts which increase the range of the solar vehicle up to 12km.

Figure 1.4 shows the general diagram of the solar car. The roof of car is made of solar cells and these cells are highly efficient compare to ordinary PV cell. To operate the PV cell at its maximum efficiency a peak power tracker is also installed in controller. Peak power tracker means maximum power point tracking controller which control the flow of power from PV cell to battery and from battery to load. The charging of the battery is done by these PV cells or some solar charging station. Battery pack is used to continuous operation of the motor.

FIGURE 1.3: Solar Charging Station
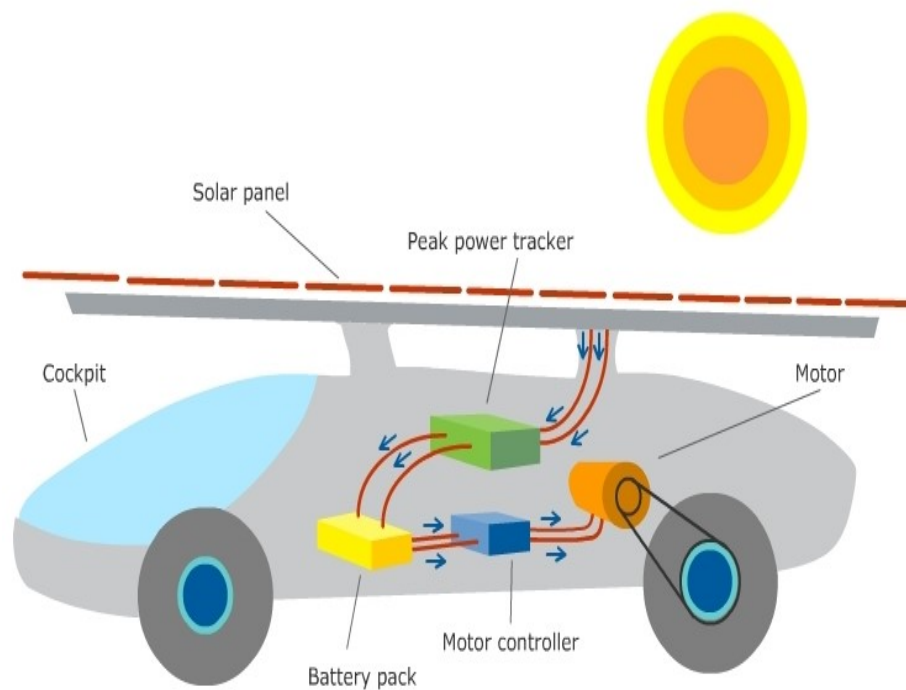
FIGURE 1.4: General image of Solar electric vehicle

1.2 History of Photovoltaic

Photosynthesis is the process by which green plants and certain other organisms convert light energy into chemical energy. Similarly, we convert light energy from Sun, into electricity for our use. The Photovoltaic Effect, the ability to generate electrical current using solar rays, was initially discovered in 1839 by Alexander Becquerel. But kind of energy is around us from the beginning of life on earth. Since then, Photovoltaic (PV) technology (solar panels) has made progress substantially, with modules becoming more and more efficient and cost-effective.

In 1954 the first generation of semiconductor silicon-based PV cell was born, with an efficiency of 6%, and adopted in space applications. Much of this work was done leading up to the 1970s. Continued adoption and investment in technology over time, caused the efficiency of solar panels to increase from 15% to 21%. A Photovoltaic (PV) panel or module incorporate of many silicon cells connecting
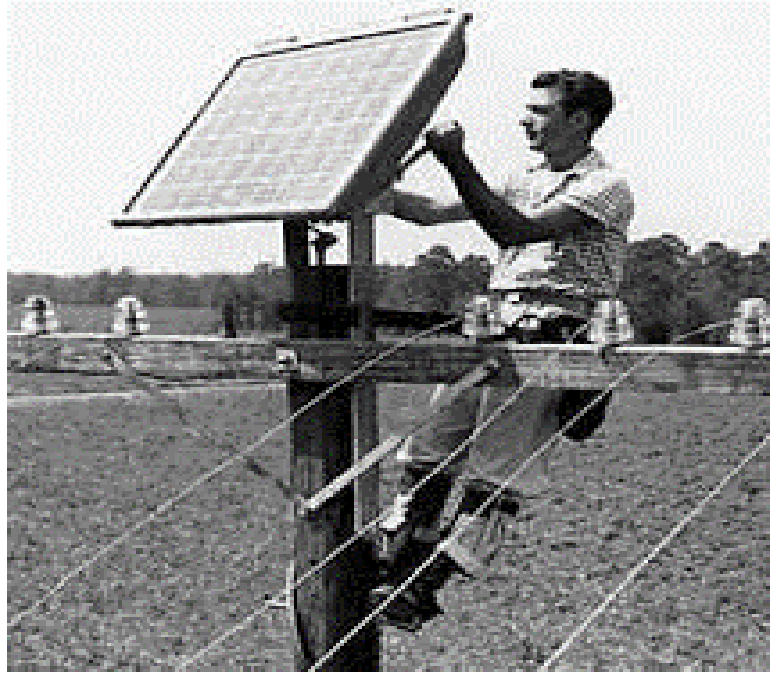
FIGURE 1.5: PV module in 1954 by Bell laboratories [4]

in the combination of series and parallel to form a Photovoltaic panel or module. When (PV) panel or module is reveal to sunlight these cells generates a direct current of electricity with no moving parts, noise, and emission of Co_2 and other greenhouse gases. The first PV module was installed in 1954 by Bell laboratories [4]. Figure 1.5 shows the first PV module install on an electric pole.

1.3 Background

Among others sustainable energy sources, Solar energy is the emission free and noiseless renewable source. The photovoltaic module consists of many solar collector, the solar collector is also called a photovoltaic (PV) cell shown in figure 1.6. PV cell transform the energy of solar radiations into DC-electric power.

PV cell changes their electrical properties of voltage, current, and resistance when there is a change in light. It incorporates semiconductor material that is energized by subjected to solar light, surrendering free electrons and holes. When it is connected with any circuit, it can produce an electric current that circulates in the circuit and feed to connected loads [4].
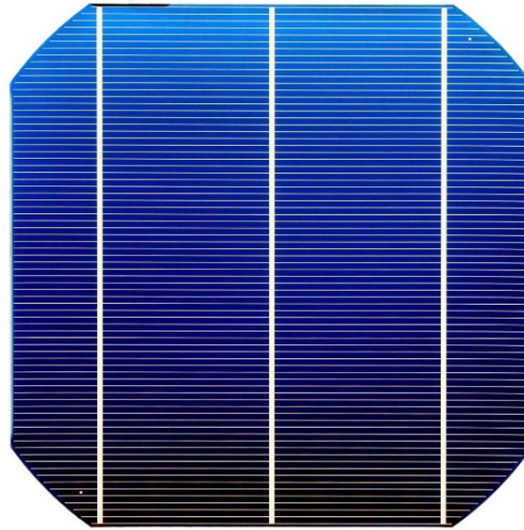
FIGURE 1.6: PV cell which combines to form a PV module [3]

The solar cell working function is the photovoltaic effect, that transform light energy into electrical energy. They are fabricated either in a single layer also called a single junction or in multiple layers called multi-junctions for absorbing the sunlight. These cells are made of crystalline silicon which is commonly known as wafer-based cells either in Monocrystalline or Polycrystalline. Many other materials are used in the fabrication of PV cells include Cadmium Telluride (CdTe), Amorphous silicon, and Copper Indium Gallium Selenide (CIGS), these kinds of solar cells are called thin film [5].

One solar cell produces 0.5 to 0.6 V as an open-circuit voltage. For the operation of real solar application, it is needed that solar cells are must be combine in the groups to produce much amount of current and voltage to satisfy the load requirement.

There are two topologies for the connection of solar cells either in series to rise up the sum of output voltage or in parallel to enlarge the output current. Connection of solar cells in series and parallel forms a PV module. In the coming sections, it will be discussed in detail how cells and modules in series or parallel form an array [6].

Solar modules or arrays may work in different topologies one is stand-alone topology, in which PV modules are directly connected to load or through DC to DC

converters to meet the power requirements of load. The second topology is grid-connected, in which the whole PV system is linked to a utility grid using a DC-AC converter to match the grid frequency and voltage for proper functioning of the PV system in grid-connected mode [6]. The third is the hybrid mode which is the combination of the stand-alone and the grid-connected. In this topology power is flow from PV module to battery and grid, battery to grid and also when PV is not generating any power but battery is not fully charge and grid have cheap electricity then power is flow from grid to battery.

1.4 Classification Of PV System

PV systems are categorized according to their functional operational and functional requirements, their component configurations, and how the equipment is connected to other sources, and loads. There are three main classifications of the PV system listed down.

1. Off-Grid PV system.

2. Grid-Tied PV system.

3. Grid-Hybrid PV system.

1.4.1 Off-Grid PV System

Off-grid systems are also called Stand-alone PV systems. These systems are best for those customers who can't easily connect or near to the main grid. This may be because of their geographical location. The off-grid PV system is for small villages or towns. These PV systems usually fulfil the low power loads like lighting, refrigerating, etc. Off-grid systems are accommodate with multiple storage devices and other charging sources such as wind turbines, and a small generator to charge up the battery for later use.

When there is no power generated from the solar array and also at night when

the PV system not contributing to the generation of electricity. Micro-grid an example of an off-grid PV system. Micro-grid is may or may not connect with the conventional power grid. It has many generations of sources include solar panels, wind turbines, small Biogas plants, diesel generators, and energy storages devices [7].

1.4.2   Grid-Tied PV System

Photovoltaic systems are designed and easily adjustable to operate in two ways. Here PV system is connected with a load and electric utility grid also called a conventional electric power grid. The flow of power is now two-way, the load is operated by both PV system and grid power. The system is connected with a utility power grid system through an inverter, which makes sure some important parameters like voltage level, frequency, and phase must same when PV system want to connect with the grid.

PV system injects power into the grid when sur-plus is available. There is no need for a battery storage unit as these systems are connected directly to the utility grid. The major purpose of a grid-connected PV system is to feedback into the utility grid during peak hours and replace the peaker-plant which is very expensive to operate and achieve the load demands. Also able to supply the cheap electricity to the consumers.

1.4.3   Grid-Hybrid PV System

Here PV system has storage backup and is also connected with a utility power grid system, commonly recognized by Grid-hybrid PV system. This kind of PV setup is on the consumer side having load sharing with PV system power, grid supply, and power from batteries. Consumer install PV system to generate its electricity and achieve the requirement of the load. Consumer priority is that the full load is driven by only PV system power, its second priority is if PV is not producing much energy then meets the load demands by energy store in batteries and then

come to the utility grid power.

In this topology the power flow is in many way like if battery is full charge and PV array generating surplus electricity then this power is flow from PV array to the grid. When PV modules are not generating any power and battery is not fully charge but gird have cheap electricity then the power flow is from grid to battery. With connecting to the conventional power grid consumer can also sell their electricity to the grid and reduce their utility bills and most importantly when there is a power demand peak occurs PV system delivers power into the grid to reduce the expense of the peaker plant [7].

1.5 Basic Of a PV Electric Cell

Solar cells transform solar radiations into electrical energy due to the photovoltaic effect. It gives rise to free electrons and holes inside the solar material which are collected at the end-side metal contact of a solar cell. Solar cells would change their behavior when place in sunlight, due to this its electrical properties of current, voltage, and resistance change. Solar cell are made of two type of semiconductors N and P-type silicon and form differnt layers of p-n junction created by the silicon and some impurities in it. Conduction paths are made on upper and lower side of the PV cell by copper and aluminum. The Solar cells are cut in square form to utilize maximum bar of silicon ingots. Solar cell must be operate at its maximum efficiency, to do so it is essential to implement the MPPT (maximum power point) algorithm [8].

1.6 Components Of PV System

Photovoltaic (PV) systems generally consist of six individual components. The installation of these components decides how efficient the solar panels are.

1. Solar PV Array.

2. Charge Controller.

3. Battery bank.

4. Inverter.

5. In a Grid-tied case net meter is also a part of the PV system.

1.6.1 Photovoltaic (PV) Array

PV array is a linked collection of photovoltaic modules, and photovoltaic modules are made of multiple interconnected PV cells. These PV cells can convert solar energy into electrical energy and these cells are made of a semiconductor like silicon, the semiconductor has a mixed property seen in metal and insulator material, which make possible the phenomena that cause the photoelectric effect.

The PV cells are made of a p-n junction, which contains two different layers. The positive side is N-type layer, it is doped with a material that has more than four electrons in its valence layer like Phosphor. On the negative side, the P-type layer is doped with a different material that has less than four electrons in the valence shell, the last valence shell has lacks one electron.

The two-layer junction develops a region called the Depletion region in the junction zone, where free electrons have occupied the holes, while the n-type zone has become positive due to the loss of the free electrons and the p-type zone negative due to the loss of the holes. Then this depletion layer is already formed and a slightly electrical field between the two sides is generated, impeding the move from more free electrons from the n-type region to the p-type region.

Now for the current generation, it is required to apply extra energy, which is coming from the sunlight (Photons), into the depletion region. By this energy, electron-hole pair is produced which is isolated by the electric field that exists between the two layers, figure 1.7 shows the extraction of the electron [9].

The flow of the current in PV cell is completed in three main stages figure 1.8. Solar (PV) modules have many solar cells are connected in series and parallel
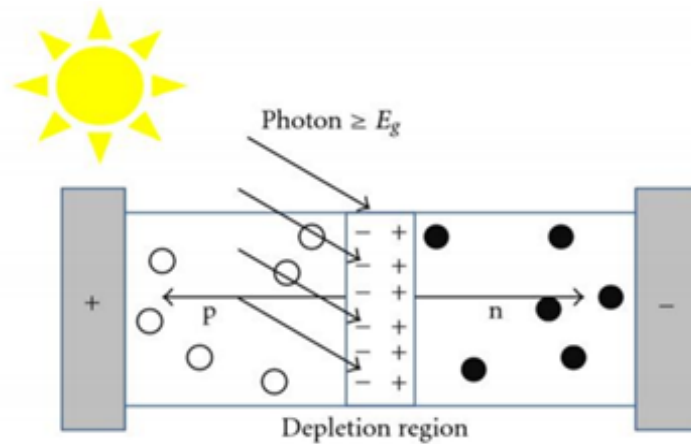
FIGURE 1.7: Extraction of electrons in PV cell [9]

to achieve a certain amount of voltage and current to create a certain amount of power which is according to the load requirement, in a practical PV system several PV modules are connected in series or parallel combinations which are called PV Array.
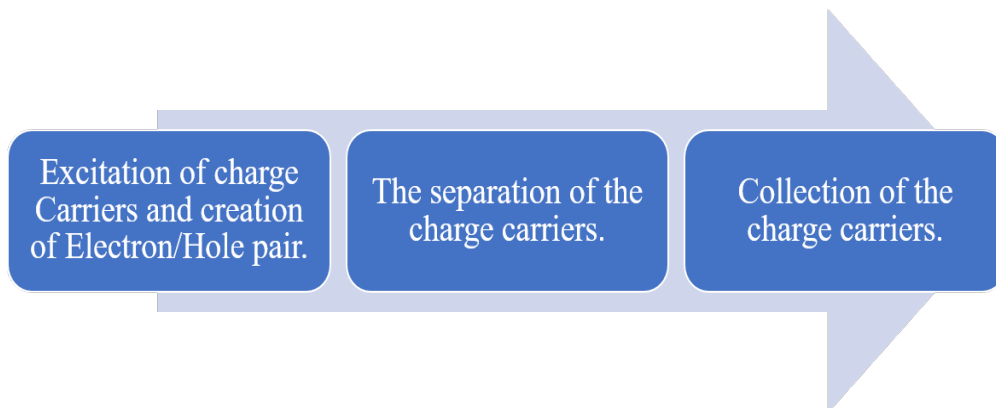
FIGURE 1.8: Three stage of flow of extracted electrons

PV system output power depends on ambient conditions (Irradiance 1000 W/m^2 and Temperature 25℃). With the change of weather conditions the output production power of the PV system change accordingly. As the irradiance increases, the output power of the PV system increase and if irradiance level is decrease the output generated power is also reduce. But when temperature rises output of the PV cell is badly affected. Because high temperature reduce the output current of the PV cell. Figure 1.9 shows how a change in irradiance and temperature affects the PV array production.[9]
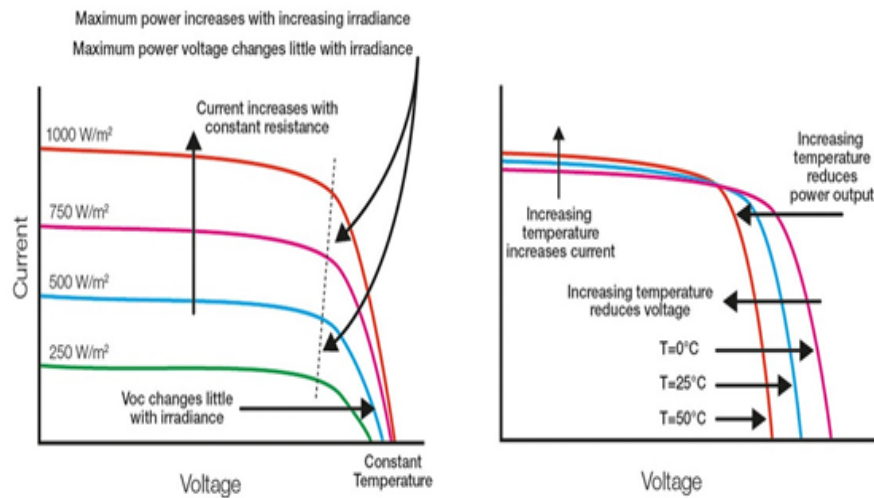
FIGURE 1.9: Effect of Irradiance and Temperature on a PV system [9]

1.6.1.1 Photovoltaic (PV) Technologies

The PV technologies are distributed into three generations.

1.6.1.1.1 First Generation

1. Monocrystalline silicon (Mono c-Si)

   The monocrystalline silicon (Mono c-Si) is made from pure silicon crystal. Its properties have high efficiency of sunlight conversion up to 22-24%. These cells are typically black or blue. The Mono c-Si has a durability of 25 years. However, its slice is made of single crystals with unvarying properties and is acquired by a complicated and expensive procedure which makes this material quite expensive. Disadvantages of the Mono c-Si, its efficiency will gradually decrease about 0.5% per year, so replacement of operating modules might be needed sooner.

2. Polycrystalline silicon (Poly c-Si)

   The polycrystalline silicon (Poly c-Si) cells are constructed by gathering multiple grains of silicon crystal, a structure that is less ideal than monocrystalline. Using smaller segment of silicon is cheaper and easy to produce so

it is not so expensive and due to multi-crystalline, it has relatively lower efficiency. Polycrystalline cells have a long life span of more than 25 years[10, 11].

3. Heterojunction cells (HJT)

This is also monocrystalline silicon type, multiple busbars (MBB), and passivation type (PERC) cell which is currently the most efficient (20-22%), due to the high purity N-type silicon cell base and no losses from busbar finger shading. However, recent mono PERC cells with MBB and the latest heterojunction (HJT) cells have achieved efficiency levels well above 22%. Panels built using these heterojunction (HJT) cells, half-cut and multi-busbar monocrystalline PERC cells for producing 415 watt panels having 22.2% efficiency. 60 cell poly or multicrystalline panels are generally the least efficient and equally the lowest cost panels.

1.6.1.1.2 Second Generation

1. Copper Indium Gallium Selenide (CIGS)

CIGS PV has become a popular new material for solar cell manufacturing and has an efficiency quite close to the polycrystalline silicon about 20% and the manufacturing procedure is relatively cheap. Its main disadvantage is the toxicity and shortage of the material. The CIGS cells are constructed by tine film deposition on a substrate, which is flexible. As compared to CdTe cells, the CIGS cells have good resistance against heat

2. Cadmium Telluride, CdTe (Thin-film)

Cd-Te PV is the second generation of PV technology it has a lower cost per kW-hour relative to first-generation. As for efficiency is concerns CdTe cells are around 16% efficient. The main advantage of thin-film CdTe is that they absorbed a shorter wavelength of sunlight from the silicon cells. Some environmental concerns related to the supply of tellurium and the potentially toxic impact of cadmium at a stage of CdTe panel discarding [10, 11].
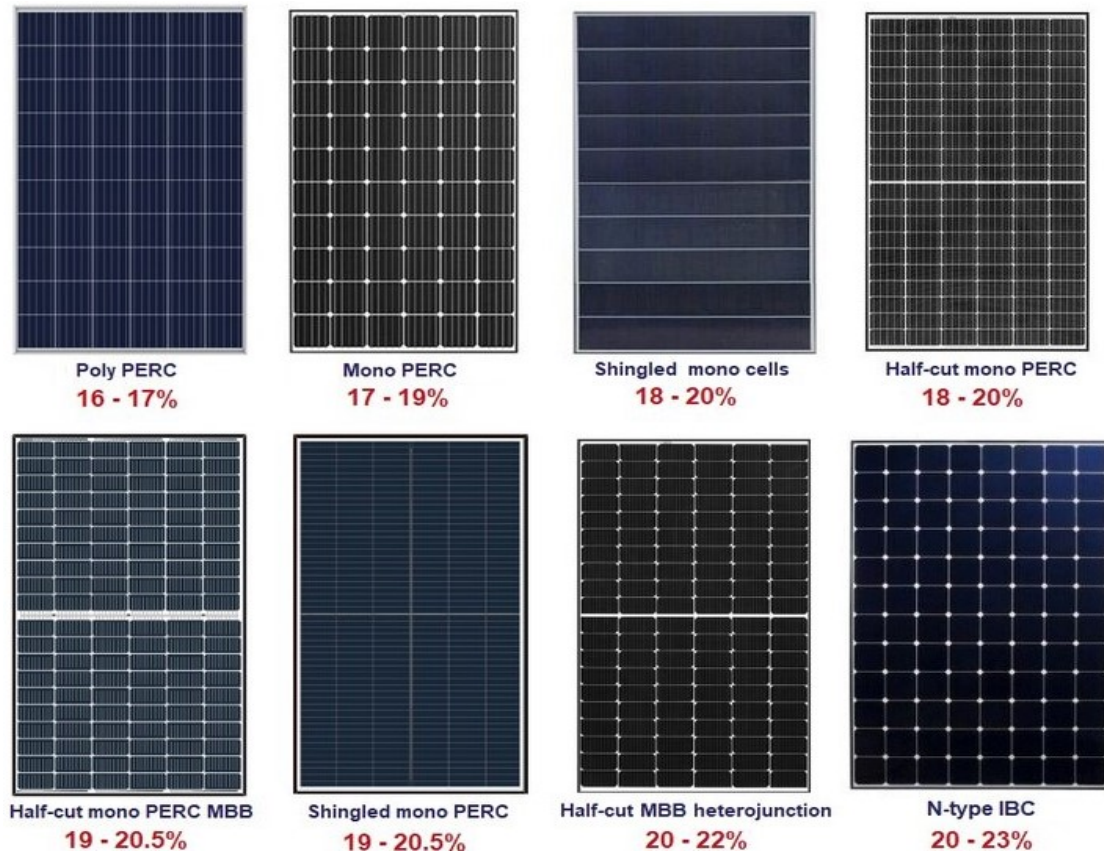
FIGURE 1.10: Technologies of different solar PV modules with their efficiencies
[11]

1.6.1.1.3 Third Generation .

Multi-junction PV modules have very high efficiency, obtained by stacking multiple p-n junctions on top of each other to absorb different wavelengths of light. Its record efficiency is 45% but technology is very expensive. These types of PV modules are used for Space technology in satellites. Figure 1.10 shows the PV technologies [12].

1.6.2 Charge Controller

A charge controller is a key component of the PV system and an electronic device that can interface three ways with PV system PV module, battery, and loads. The charge controller performs multiple functions to prevent any damage in the PV system including the constant voltage to the battery, constant supply to a load, and extracting the maximum power from the PV array.

The charge controller protects the PV system in many ways. For proper operation of batteries, the Charge controller ensures that the electrical parameters around the batteries remain between as the manufactures prescribed specification/limits. During high PV output, a charged battery can damage if the charge controller charges it that damages the battery, and cause severe problems inside the battery like gas formation, overheating, and capacity loss.

Charge controllers prevent this problem by disconnecting the PV array from batteries is known as overcharging prevention. During the low solar irradiance, PV array output is low, and load requirements are high. In this situation, a battery can be over-discharged, which will affect the battery life. Here a charger controller can disconnect the batteries from loads and connect the batteries with a PV array for charging whatever amount of power is produced by the PV array, this operation is known as discharging prevention.
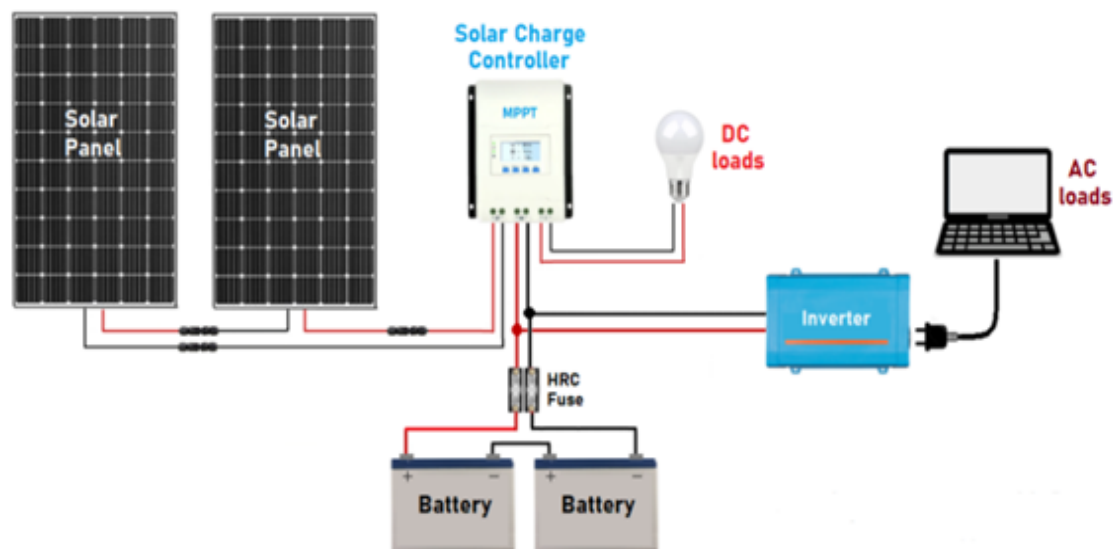
FIGURE 1.11: Complete the PV systems components [12]

Battery charged at a certain level of the voltages, for optimal performance the battery voltage must be within limits. For this purpose, the charge controller regulates the voltages of the PV array to charge the battery with limited voltage and supply constant voltage to load, to do so it can also perform the max. power point tracking (MPPT) for voltage regulation by applying MPPT techniques.

The charge controller also performs current regulations to limit the charging current of batteries. The below figure shows the interface of the charge controller with batteries and loads [12]. Charge-controller has implemented effective load management by using low voltage disconnect (LVD). As the capacity and service life of batteries are affected by ambient conditions, the charge controllers with temperature compensation features are very essential in the design of a PV system. Figure 1.11 shows the PV modules and their Fundamental components interacting with each other.

Charger controllers are rated according to the max. input voltage and charging current. There are two categories of charge controllers on basis of extraction of power from PV module, charger controllers can use to charge batteries and drive different loads from the PV array.

1. Pulse Width Modulation (PWM).

2. Max. Power Point Tracking (MPPT).

1.6.2.1   Pulse Width Modulation (PWM)

PWM controllers are the earliest and primal charge controllers used for the proper operation of the PV systems at the start. These controllers are simple in design structure, implementation and less expensive than an MPPT controller. In the PWM charge controller, the PV array is connected to the battery by using a switch to control the battery charging. The switch may be Mosfet, IGBT, or a simple transistor, it open until the battery achieves absorption charge voltage.
The switch opens and closes rapidly depending on the switching frequency to control the current and charge the battery at a constant voltage using a simple PWM signal. The advantages of the PWM controller are cheaper, is best for a small system where efficiency is not a concern, and performs well when a battery is close to its full charge. The main drawback of the PWM charge controller it reduces the PV array voltages to match the charging voltage of the battery by this operation PV array voltage dropdown to optimal operating voltage (V_{mpp}) which

reduces the power and efficiency of the PV array. And also, by using this type of charge controller we are not able to fast charging of the battery.

1.6.2.2 Max. Power Point Tracking (MPPT)

This type of charge controller is advanced and robust than a PWM controller and it can operate the PV array at its max. power point with optimal voltage. MPPT charge controllers are 30% more efficient than PWM controllers. MPPT is an efficient DC to DC converter, PV systems have intermittent behavior its output change with the change in irradiance. To operate the PV array on MPP, the max. power point tracker search through the PV array voltage (V_{mpp}) to find the best combination of voltage and current to generate the max. power.
MPPT is designed to track frequently the max. power point of PV array and regulate the voltage overall output will increase and efficiency is higher than 90%, whatever the weather condition or irradiance value. Using different MPP tracking techniques in the MPPT controller to increase the output generated power of the PV array. They are highly efficient, best for large systems, perform well in a colder, cloudy environment.

When the PV array voltages are higher than battery voltage this situation is ideal for the MPPT controller. As for as disadvantages are a concern, more expensive than PWM controller, complex in implementation, and shorter lifespan due to more components are involved in circuit [12, 13].

1.6.3 Battery Bank

Integration of energy storage devices with renewable energy sources is very important and difficult because renewable energy sources are intermittent in nature. Many energy storage devices are used to overcome the intermittency of renewable energy sources and battery is one of them and has become an essential part of a PV system. It produces DC direct current. PV modules depend on solar irradiance and can not generate power at night in this case, we need backup supplies

such as a battery storage device to meet the load demand [14]. Batteries have two categories primary or secondary. Primary batteries are used one time only and are not rechargeable.

Zinc-carbon, dry cell, and Alkaline are some types of primary batteries. Secondary batteries are also called rechargeable or reusable batteries. Lead-acid, Nickel-Cadmium, Nickel-Metal, and Lithium-ion are secondary batteries [15]. In PV system batteries interacts with charge controller, for the battery when PV array output exceeds from load demands and also the battery is not full charge available. At night or when PV array power is not available battery operates the load.

1.6.4 Inverters

An inverter is another essential component of a PV system, it is responsible for the effective transformation of constant and variable DC output of the PV array into clarified sinusoidal AC power, with a frequency of either 50 or 60 Hz. PV system is not directly connected with the grid because the grid operates at a fixed frequency and voltages.

In PV systems an inverters are classified by size, topology, and mode of operation. The size of the inverter depends on the power rating, the topology of the inverter is, how many inverters are used in the PV system as a single-stage single-PV array, Multi-stage multi-PV array, and then Multi-strings of PV array with Multi-stage inverters [12]. The mode of an inverter is important to understand in PV system operation. There are three modes of inverter described below:

1. Stand-alone Inverters

   In this mode, no charge-controller is involved, the PV system only operates the AC-loads by using an inverter that also performs the MPPT operation. Here variable DC output of PV array consider as an input of the inverter, and the inverter converts variable DC into fixed AC power for a stable and smooth operation of AC-load. The inverter also monitor the output power of the PV array and enable the MPPT tracking process.

2. Grid-Tied Inverters

   Here PV system is connected with a Conventional electric grid using a grid-tied inverter, which also operates the local AC loads. The flow of power is now two-way. Ac loads demands are achieved by the PV system and also conventional grid supplies the power to loads.

   In this mode of an inverter, a charge controller and batteries are not used, the PV system gives the power through an inverter to load and also to the grid. When the PV system produces subsidiary power, this power is given to the conventional grid.

3. Bimodal Inverters

   This kind of system is a combination of both stand-alone and grid-tied systems also known as the Hybrid PV system. Charge controllers, batteries, and grid power are used to operate both AC and DC loads. This mode also has a two-way power flow that gives and takes power from the grid.

   It is very useful when grid power is disconnected, now the load is operating by the battery's power or PV array power if available. These inverter can operate in parallel with grid and also drive the load at same time. The extra power generated by the PV modules are feed to storage devices, if the storage devices are fully charged then this extra power is give to gird.

1.6.5   Net Meter

Net metering is used when a PV system is in grid-tied and hybrid mode. The purpose of net metering is to calculate the injected power by the PV system and how much power is consumed by the load if the load is using grid power. The consumer installs the PV system and connects it with the grid, it needs a net meter to connect to the conventional grid. Net meter generates bills by calculating, how much power is consumed by the consumer and how much power is injected into the grid by the consumer. Net meter measure the flowing of current in two directions for billing purposes. This concept is about Advance metering infrastructure (AMI) used in the implementation of Smart-gird in any country.

1.7 PV Module Performance Parameter

The electrical characteristic of the PV module is the same as a single PV cell has. PV cell electrical properties can be seen and constituted by voltage, current, and power. The PV module performance has been affected by weather conditions including sunny days, cloudy weather, solar irradiance in both kinds of weather and temperature. Consider a model of PV module, which is constructed in Matlab/Simulink software of 1000 watts of power using one module in series and three in parallel.

In figure 1.12 shows the effect of changing irradiance at constant temperature 25℃, on the power production to voltage P-V curves available at distinct values of irradiance. Different values of solar irradiance are 1000, 800, 600, and 400 watts per meter square (W/m^2). During high irradiance, we extract maximum power from the PV module and vice versa. While figure 1.13 portrays the effect of temperature on P-V side-by-side with I-V characteristics curves having different values of temperature at 25,50,75 and 100℃ with constant irradiance of 1000W/m^2. Detail related to parameters that effect the output of the PV module are discussed in coming chapter.

1.7.1 PV Module Performance in Fast-Changing Irradiance

As all renewable energy sources have a dependency on weather conditions, solar energy systems also have this snag due to changing solar irradiance and temperature over a day and every season of weather. For operating the PV system at its maximum point many algorithms and techniques are presented to control the optimized point at which max. power is extracted from the PV array.

The PV array output power is varying as irradaince is changing, if irradiance is high the generated power by the PV array is large and if irradiance is low the output power is reduced.
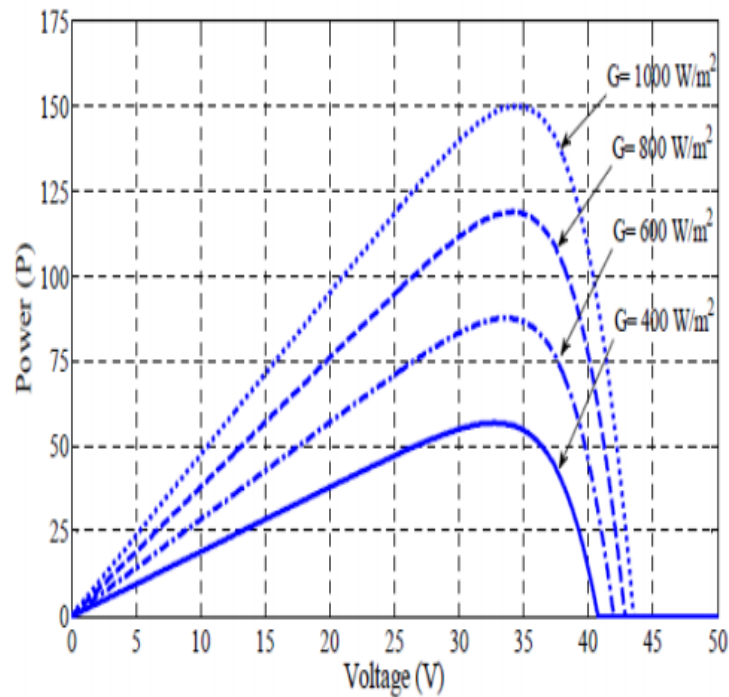
FIGURE 1.12: P-V characteristics under different irradiance values [17]

These algorithms are known as Maximum Power Point Techniques (MPPT) to operate the PV system at its max. efficiency and these techniques are discussed in detail in the coming chapter along with their strength and weaknesses.

As mentioned above PV system power generation has been affected by atmospheric conditions. During the whole day, solar irradiance changes gradually or maybe fast [17, 19]. It is important to track the continuous change in solar irradiance for controlling the operation of solar modules to optimize the extracted energy in such a manner that PV panels are working at the point where they are generating the maximum power.

Temperature have negative effect on the PV array output at normal temperature PV array produces great power according to the available irradiance but with rise of the temperature the generated power is reducing whatever the irradiance level.

Due to this, overall system efficiency is low many techniques are developed but only to deal with change in solar irradiance not to deal with temperature. Some cooling systems are develop to reduce the temperature of the PV array. Some of them are mentioned in chapter 3.
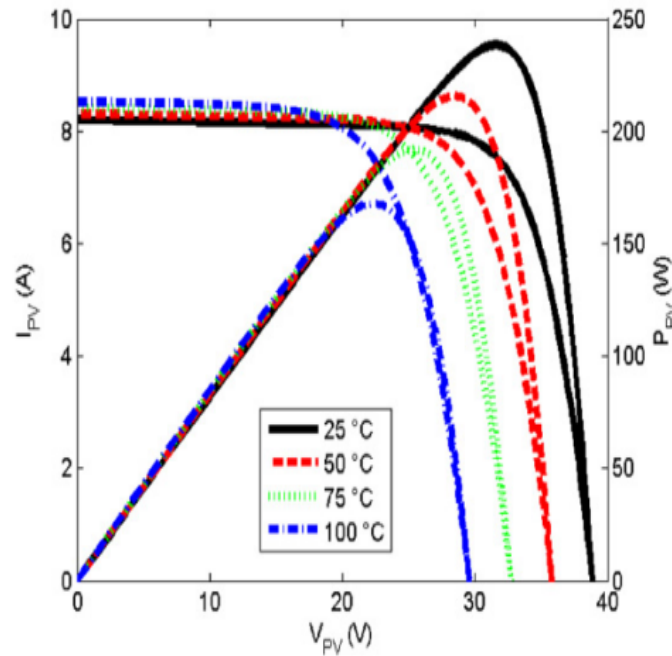
FIGURE 1.13: At fixed irradiance 1000W/m^2 and different temperature values show the P-V and I-V curves of the PV module [17]

1.8   Need Of MPP Tracking for PV Systems

PV systems have intermittent production of electric power. The conversion with low radiation (in general less than 17%), as well as the nonlinear characteristic of PV cell. The nonlinear behaviour of a PV cell depends on irradiation and temperature in its operation which changes the quantity of generated electric power. PV systems are expensive so is necessary to get more benefit as possible.

An MPP technique operates the PV array at its max. power generation point by adjusting the voltages of the PV array. The closer the PV module voltage to its Voltage at Max.power point (VMPP) the more power will be extracted [16].

The PV array voltages are adjusted by changing the dutycycle generated by MPPT techniques with some DC to DC converters like boost, buck, flyback, buck-boost converter. As irradiance changes so the V$_{MPP}$ is also shifting, now the MPPT algorithm must search for the V$_{MPP}$ when solar irradaince level is shifted.

Figure 1.14 shows the input solar irradiance of the PV system and figure 1.15 shows the performance of the PV system with and without the MPP technique.
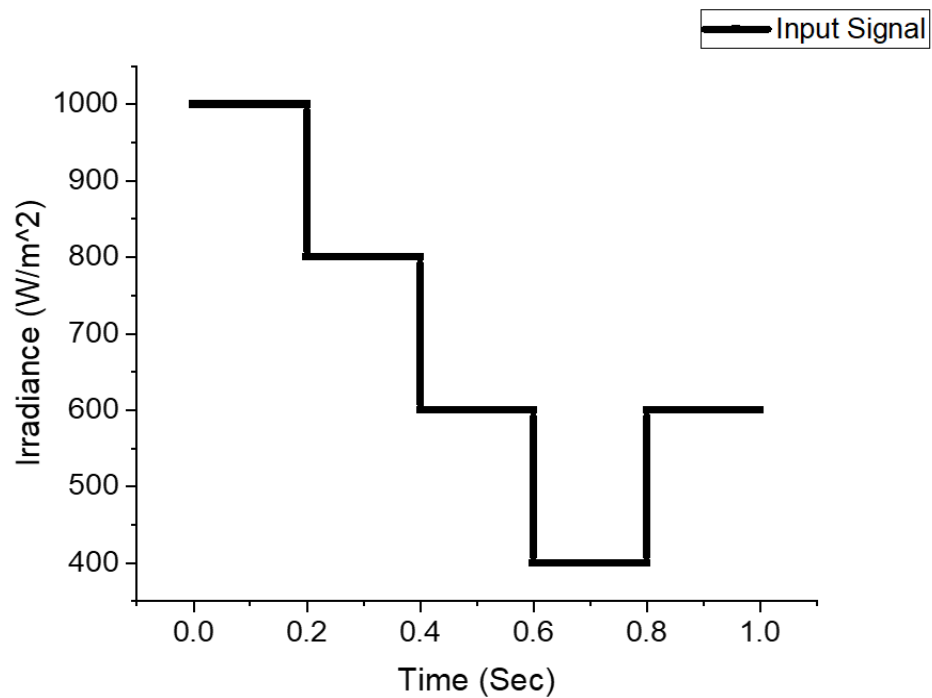
FIGURE 1.14: Input irradiance signal for PV array

The system is considered the same as mentioned in figure 1.12 and load resistance is 10 ohms.

In figure 1.15 response of without-MPP technique, the PV array power output is constant, at distinct irradiance values it generates less amount of power as compared to with-MPP technique. If extra power is available in a PV system, then it must be extracted for reduction of its nonlinear actions and also a proper charge controller is used for the operation of connected load and fast charging of a battery for the later use.

1.9 Maximum Power Point Tracking (MPPT) Methods

To keep the Solar PV system working at its maximum efficiency all the time, Maximum power point techniques aim to be used for the max. power extraction from a PV system. There are many methods used to track the MPP point. Some
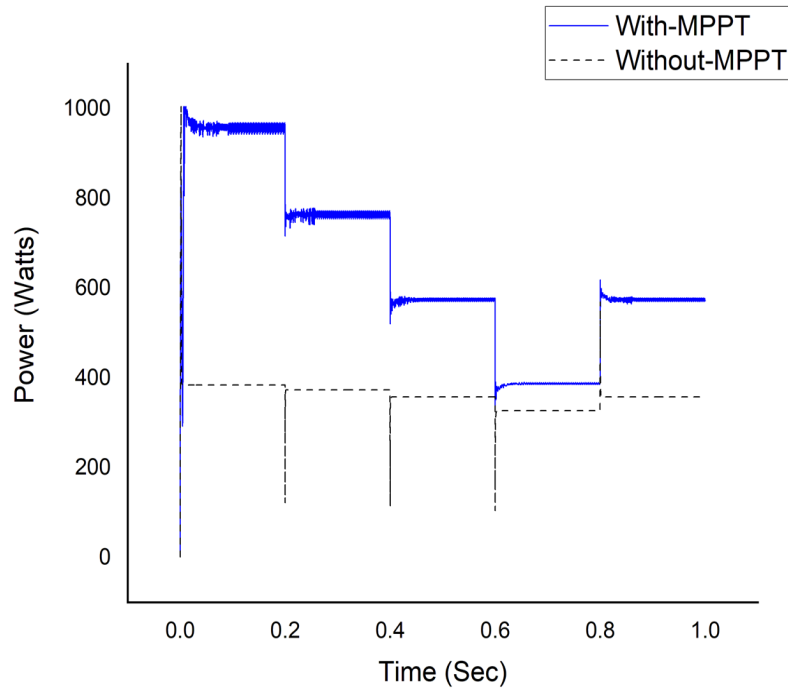
FIGURE 1.15: Power production response using Mppt and without-Mppt

of the methods are very efficient in tracking, there are two main methods, direct methods, and in-direct methods. The in-direct method includes Fixed voltage and Fractional Open-circuit voltage, and the direct method incorporates Perturb and Observe (P&O), Incremental Conductance (Inc.Cond), some advanced MPP tracking techniques are Fuzzy-logic, Artificial Neural Network (ANN), Genetic Algorithm, and Particle Swarm Optimization (PSO) [20].

Control procedures are also used for tracking, Sliding-Mode technique, and Adaptive Back-Stepping. These techniques are varying in the speed of convergence and response, complexity, cost, hardware implementation, sensors required, and efficiency and effectiveness.

1.9.1 Fixed or Constant Voltage Method

This is the type of MPPT tracking method that was used initially, consideration is made to adjust the operating voltage of the PV module. Select the operating voltage of the PV module by assuming on a seasonal basis for summer and winter.

Fix voltage value was used for the higher MPP expected in winter and summer. It was not very accurate but it run the PV systems [20].

1.9.2 Fractional Open-Circuit Voltage

This is the second type of indirect MPP method, which is one of the most common MPPT techniques. This technique also makes assumptions for operating the PV module at MPP, (V_{MPP})voltage at MPP is obtained by multiplying open-circuit voltage of PV module (V_{OC}) with a constant L. The value varies with PV cell technology, L is equal to 0.7 or 0.8. So $V_{MPP} = L \times V_{OC}$ to calculate the voltages at MPP point.

As change is occur in weather or ambient conditions the V_{OC} of the PV module changes and the P-V curve in figure 1.7 also shift in the same manner, but the ratio of MPP and V_{OC} remain the same and MPP is a fraction of V_{OC}. It has disadvantages, for measuring the V_{OC} of PV module load must be disconnected for every measurement which causes power loss.

To avoid disconnection of load, a pilot cell is used. The pilot cell represents the V_{OC} of the whole PV module that is also an assumption to adjust the voltage accordingly.

1.9.3 Perturbation and Observation (P&O)

Perturb and Observe is a direct method, which is also called the Hill climbing method. Perturb and observation is the most common direct method because of their easy implementation in software and hardware. Perturb means change, and change is made in the voltage of the PV module to operate the PV at MPP. Output Power may decrease or increase at every perturbation [20]. If power is increasing when perturbation in voltage of PV module then operation point is at the left side of the P-V curve, increase the reference voltage (V_{ref}) and if power is decreasing then operation point is at the right side and V_{ref} must be decreased
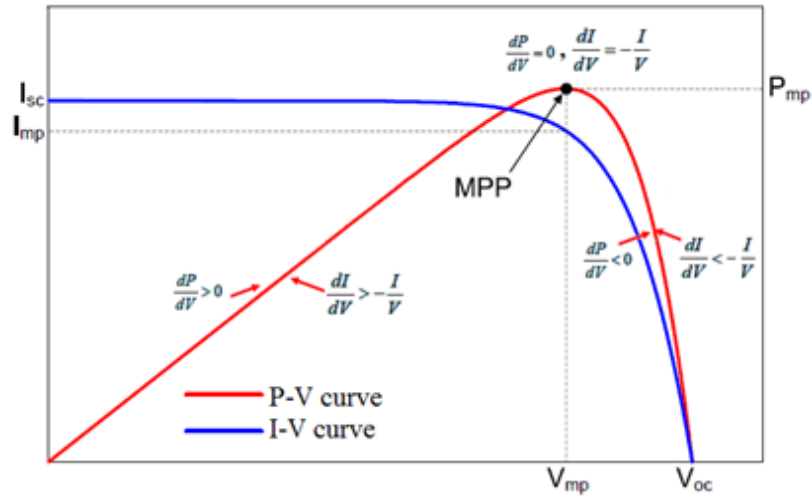
FIGURE 1.16: P-V and I-V curve characteristic of PV module

as shown in figure 1.16.

This technique has a serval drawback, it converges at MPP over serval perturbation, speed of convergence affected by the small or large step-size convergence variable step-size is used. It is never steady and hovering around MPP and struggles during rapidly changing atmospheric conditions [20].

1.9.4 Incremential Conductamce (Inc.Cond)

Incremental conductance (Inc.Cond) is direct method and also considered as a hill-climbing method. This technique is widely used in PV systems for MPP tracking. This technique uses the concept of conductance I/V, which is reciprocal of resistance. Instantaneous conductance I/V is compared with incremental conductance I/V to find the value of slope which is mentioned in figure 1.14. If $\Delta I/\Delta V$ is less than -I/V then the point of operation is on the left side of MPP, and if $\Delta I/\Delta V$ is greater than -I/V now operating point is on the right side of MPP. At MPP $\Delta I/\Delta V$ is equal to -I/V [21]. This method of MPP tracking is slightly complex then perturbation and observation technique and some extra computations are added. This technique can track changing weather conditions more quickly the perturb and observation method and have less oscillations in output power. Its modifications are explained in detail in coming chapter along with the flow chart and strength and weaknesses of each modified Inc.Cond methods.

1.9.5 Fuzzy Logic

Fuzzy logic is the AI based technique to execute on degrees of truth rather than the basic right and wrong or 0 and 1 which used in computer. The idea of FL was first represented by Lotfi Zadeh of the University of California at Berkeley in the 1960s and the applications of FL technique is automobiles, copy machines and more. Fuzzy logic is sufficient to control the technique used for the MPP tracking in the PV system because of its ability to handle non-linear systems and fast response time. No need for an accurate mathematical model of the PV module. The basic block of the fuzzy logic controller is shown in figure 1.17. The first stage is fuzzification, the second is a rule-based inference engine which is set by the user according to the requirement of the application and the last one is defuzzification. The input of the fuzzy model has varied some considered changes in voltage ΔV and power ΔP and some take a change in current ΔI and voltage ΔV of PV module as input. The output of the controller is a variation of the PV array voltage ΔV_{ref}. This ΔV_{ref} is converted into a PWM signal for converter by PWM generator [21].
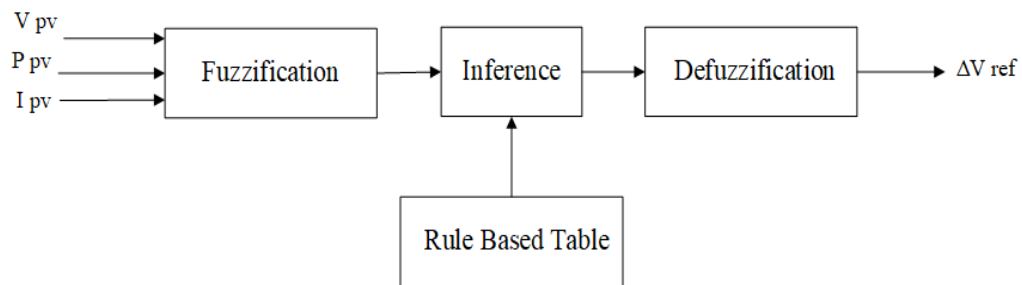
FIGURE 1.17: Fuzzy-logic Controller block diagram

In the fuzzification stage, numerical inputs are transformed into linguistic variables, like PS (Positive Small), PB (Positive Big), ZE (Zero), and NB (Negative Big), NS (Negative Small) are a subset of fuzzy functions. Now each of these, functions is the input of the inference engine where output is produced according to a rules-based table. Coming to the defuzzification stage, it converts the output linguistic variable again into numbers and ΔV_{ref} is get by adding the current V_{ref} into the previous value

1.9.6   Particle Swarm Optimization (PSO)

This is an advanced technique for MPP tracking and its behavior is like bevy. This technique uses the n-dimensional space of a swarm of particles and every particle represents a solution. These particles keep re-arrange themself in multi-dimension space to find the optimal location by using previous experience and neighbors. For finding the optimal location, the best particle $P_{best\ i}$ in the neighborhood holds each particle position. The particle at its best location is determined by increment or decrement in the initial velocity depending on the current value of the particle $G_{best\ i}$. If the current value of the location is less than the best location value then velocity needs to increase and vice versa [22]. The location X of the particle is adjusted based on the below equation.

$$X^{k+1} = X^K \ + \ V^{k+1} \tag{1.1}$$

$$V^{k+1} = WV^K \ + \ c_1 \ r_1 \{P_{best\ i} \ - X^k\} + \ c_2 \ r_2 \{G_{best\ i} \ - X^k\} \tag{1.2}$$

Where v is velocity, c_1, and c_2 are coefficients of acceleration, W represents the inertia weight, $P_{best\ i}$ is the present location of particle i, $G_{best\ i}$ represents the best location of a particle i and r_1,r_2, and $\in$ U.

1.9.7   Artificial Neural Network (ANN)

Artificial neural networks is like machine learning algorithm and its structure is approximately like human brain, they can solve problems using trial and error without being exact programmed with rules to obey. Its applications are Stock Market Prediction, Social Media, Aerospace, Defence and Healthcare. Artificial neural networks give the best estimation of a non-linear system. Generally, non-linear systems solved by multilevel neural networks and ANNs produce a satisfactory result as compared to other techniques. Basic neural networks have three

stages namely input, middle, and output stage. In the case of MPPT for the PV module, all PV module parameters like voltage, current, power, irradiance, and temperature may be considered as input of ANN. The first stage of ANN depends on the number of input parameters, the middle or hidden stage receives the raw information to process them. Then, this received value is sent to the output stage which will also process the information from the middle layer and generate the output.

ANN measured the voltage and current of the PV, the irradiance, and the temperature. The output is the reference voltage V_{ref}. ANNs system collects knowledge by detecting the patterns and relationships in data and learning through experience, not from programming, this data is used to train the ANN to find the optimal value of V_{ref} [23]. Figure 1.18 shows the ANN system image.
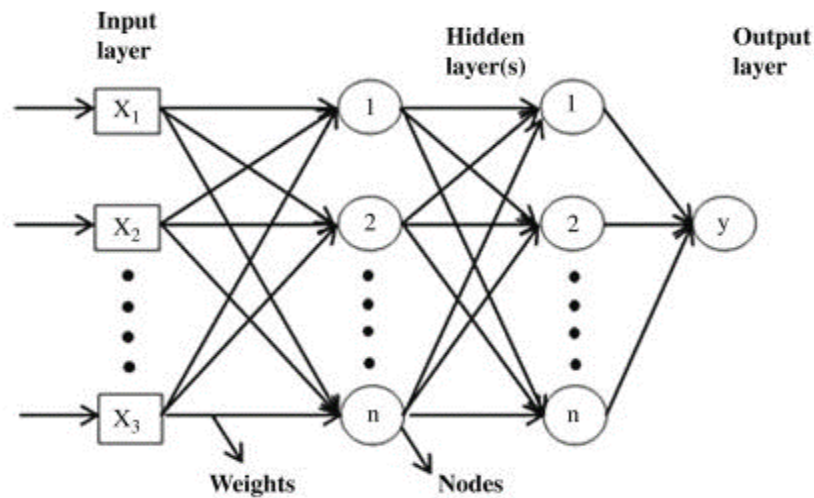
FIGURE 1.18: Artificial Neural Network ANN structure

1.10   Thesis Organization

The thesis comprises the following chapters.

Chapter 1: This chapter incorporates of introduction and working of the photovoltaic (PV) system. Detail explanation about the classification of the PV system along with the importance and basic function of its components is also explained.

Need and importance of maximum powerpoint tracking in PV systems, and different MPP tracking techniques are part of this chapter.

Chapter 2: This chapter is about a detailed literature survey of MPPT methods along with their strengths and weaknesses. The amount of solar energy used to meet the energy demands up till now is also mentioned. Distinct types of maximum powerpoint techniques including P&O, Inc.Cond, Fuzzy logic, and some control techniques are explained with their gains and losses. At the end of this chapter, motivation, research strategy, gap analysis, and problem declaration are also part of this chapter.

Chapter 3: This chapter deals with the complete modeling of a PV cell and PV array both in mathematical and in Matlab Simulink. Parameters that affect the generated power of the PV cell are also discussed. Modeling of the Solar car with MPPT controller is also the part of this chapter. Design calculation and Simulink modeling of the boost converter is also part of the chapter along with their electrical parameters.

Chapter 4: This chapter explains the detail of the basic Inc.Cond algorithm and its Variations using Direct Control along with the basic concept used in these variations for tracking the MPP point. This chapter also covers the flow chart diagram, equations used for tracking, and some drawbacks of the Inc.Cond techniques which are selected in this thesis work.

Chapter 5: In this chapter, a lot of simulations are done. Each modified version of the Inc.Cond technique is simulated against evaluation patterns to determine the effectiveness of the compared Inc.Cond technique and also discussion on the results is done in detail.

This chapter also includes the simulation results and information about the efficiency, tracking accuracy and simulation using different irradiance level with varying temperature of each mentioned Inc.Cond method with proposed tuning parameters. In the end, a comparison among five modified Inc.Cond techniques is conducted.

Chapter 6: This chapter is finally based on the conclusion and the discussion done throughout the complete thesis work and some future directions are also highlighted.

1.11 Chapter Summary

This chapter integrates with the basic concept of Solar Energy introduction and the history of the PV systems. Classification of the PV system along with the technologies and working of its components and performance parameters are also explained. The importance of maximum powerpoint tracking MPPT in PV systems and its benefits. The last section is about different MPPT techniques are explained.

Chapter 2

Literature Review and Problem Statement

This chapter is a combination of a detailed overview of the literature related to MPPT algorithms. Gap analysis, problem statement, and research methodology are also part of this chapter.

2.1   Introduction

With the depletion of the ozone layer, increase in global warming, and depletion of conventional sources for electricity generation, a simple renewable energy source Solar energy attracts more attention throughout the world. By 2030 the world energy needs reach up to 30TW, and the quantity of light energy reaches the earth is around 89,000 TW. Only 0.3% of that energy is enough to satisfy our load demands and without generating any kind of pollution. Dominating other renewable energy resources is still solar energy speaks for only 0.5% of total energy generation [24, 25].

With such advantages, the PV system also has some major weaknesses: (a) Non-linear electrical behavior, many control techniques are implemented to reduce the non-linearity of P-V and I-V curve (b) low efficiency of solar cells only reach up

to 19-20%, although a lot of research conduct in recent years and still going on to improve or escalate the effectiveness of solar cell material and (c) the efficiency depends on the intensity of solar irradiance and temperature when the weather is bad the conversion efficiency is even impoverished. Consequently, the PV system should be operated at max. power point (MPP) to attain the highest possible efficiency.

To ensure that, the PV array generates the highest possible power then a maximum powerpoint tracking (MPPT) is a paramount component of the PV system. MPPT is a programming algorithm that is implemented on an electronic device and becomes an electronic control system, which performs multiple tasks including measuring the PV terminal current/voltage and operating the PV system at MPP by controlling the duty cycle of a DC/DC converter [25, 26].

Traditional MPPT methods includes perturbation and observation, and incremental conductance methods [1, 27], modified incremental conductance methods [28–35], while intelligent control algorithms including fuzzy-logic [36–39] and advance fuzzy-logic [40–46], artificial neural networks [47].

The effectiveness of intelligent control algorithms has been tested by experiments but these algorithms still have the disadvantages of high complexity, cost, and enlarged size of technique. Controller-based MPPT technique including PID, sliding mode control, Back-setting control, and Non-linear adaptive control produce a better result with simple perturbation and observation but the cost of MPPT in hardware increase [48–51]. Conventional and widely used MPPT algorithms are known as Hill-climbing algorithms. The MPPT algorithms which are discussed in literature some are listed below:

1. Perturbation and Observation (P&O).

2. Incremental Conductance (Inc.Cond).

3. Fuzzy Logic.

4. Artificial Neural Network (ANN).

5. Particle Swarm Optimization (PSO).

2.2 Literature Survey of P and O and Modified Inc.Cond with Direct Control

In [1] a improved Perturb and Observe (P&O) technique is used to extract the maximum power from PV cells. During the fast change in irradiance, the conventional P&O fails to track MPP, because it just observes the power of photovoltaic and reference voltage leads to send the wrong signal to a controller. The modified P&O [27] deals with additional measurements of solar irradiance and move the solar module physically with help of a motor.

The algorithm split the whole P-V curve into three different areas, to reduce the search space for MPP points. Areas 1 and 3 are the left and right regions to the MPP respectively. Area 2 is the surrounding region of the MPP point on the power curve containing 10% area of the P-V curve and MPP lies in this area 2.

Now for a change in reference voltages (V_{ref})is based on these power and irradiance values, and than additional duty-cycle is calculated for solar tracker and MPP tracking. The drawback of this technique is that it is required to measure irradiance continuously which involves the light-dependent resistor (LDR) sensor and store its value for calculation of duty-cycle. Due involve of solar tracker motor is required for this purpose. These components are valid for a single PV module system only.

A fixed-step size incremental conductance Inc.Cond algorithm is presented in [28]. The algorithm uses the constant N to determine the suitable step-size, mostly N=0.001 which is multiplied with an absolute change in power and change in voltages (abs(ΔP/ΔV)). It tracks the MPP better as compared to conventional Inc.Cond method under a fast-change in irradiance.

The response time is large if step-size is small, but in case of large value of step-size it causes the power loss due to oscillations at MPP point. To overcome the oscillations and reduction of response time, serval varying step size Inc.Cond MPPT algorithms were proposed in [29, 30, 32].

Variable step size Inc.Cond MPPT algorithm based on changeable scaling factor is presented in [28]. This technique uses the analysis of slope $\Delta P/\Delta V$ to determine that which N is selected for the calculation of step size.

This technique starts with two different scaling factors N1=0.001 and N2=0.05 to multiply with the ratio of change in power and voltages (abs($\Delta P/\Delta V$)) to calculate the step size for delta. If the current value of slope is greater than the previous value, the algorithm considers that the operating point is faraway from the exact MPP point, as a result, a larger value of N is selected and vice versa. Figure 2.1 represent the working on fix and variable step-size on P-V curve.
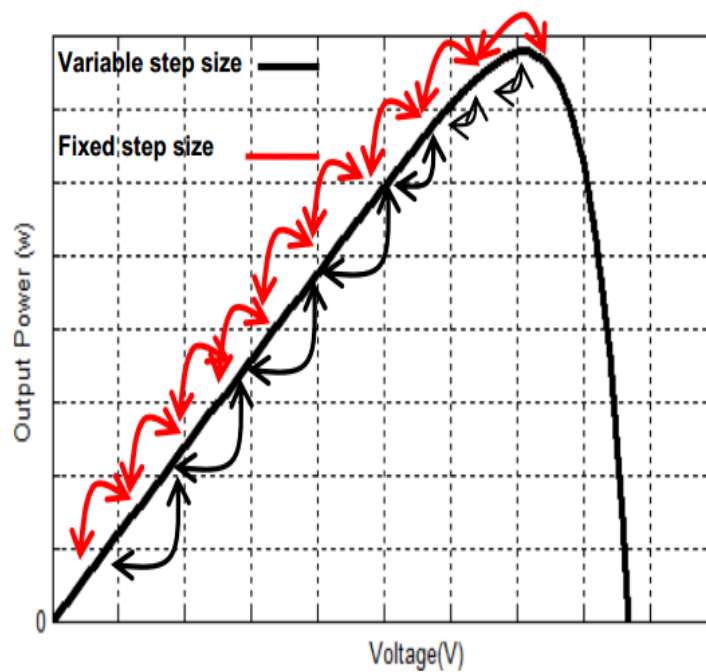
FIGURE 2.1: Hill climbing of Fix and Variable Step-size on P-V curve [29]

The snag in [28] is working on slope value and the remaining sequence is similar to conventional Inc.Cond. In reality, the zero slope condition is not achieved, the gradient is calculated by the algorithm is positive as the resulting algorithm makes the wrong decision to increase the PV module voltages and an inaccurate step-size is implemented when irradiance change from low to high [31].

A new advanced variable step-size Inc.Cond algorithm was proposed in [29] for better tracking accuracy, response time and reduce ripples during rapidly changing solar irradiance. The algorithm uses the basic parameters of PV cells, that are

affected by irradiance which are current and voltages. This technique uses $N *$ $(abs(\Delta P/\Delta V - \Delta I))$ instead of ratio of change in power and voltage to calculate the accurate step size, and N is the constant 0.05 value. The weakness of this method, it also works on the random absolute value of the expression $(\Delta P/\Delta V - \Delta I)$ chances of an error occurring are increased in case of continuously changing atmospheric conditions.

Another algorithm related to variable step-size called Dual scaled Adaptive step-size Inc.Cond method with direct control is proposed in [30] for MPP tracking. The technique uses the two different constants (N1=0.001, N2=0.005) instead of a single constant (N) for calculating step-size. Initially, the algorithm computes the absolute change of the current $abs(\Delta I)$ of the PV module with constant (e=0.04) and then selects the constant from N1 and N2.

After selecting the constant, it is multiplied with the change in power (ΔP) of the PV module, this gives the step-size for the algorithm to track the MPP. To mitigate the inaccurate response under a fast change in irradiance a modified Inc.Con algorithm is presented in [31].

This algorithm uses the variation of voltage and current of the PV module to track the increment in solar irradiance. A permitted error equation is applied to reduce the steady-state oscillations and accurately track the MPP point, the error is calculated by equation ($| I + V *(dI/dV) | < 0.06$), the number 0.06 is selected by comparing the errors produced from different step-size 0.001,0.005, and 0.01. This technique reduce the and steady-state error up to 0.7%.

In [32] enhanced auto-scaling Inc.Cond method is proposed with a new control strategy that divides the PV curve into two portions. These operating areas are reduced the main downside of traditional Inc.Cond algorithm which is the amount of perturbation step size and it also a swap between the speed of tracking and amount of oscillations at MPP point. Figure 2.2 show the division of the P-V curve. In [32] completely restructure the conventional Inc.Cond MPPT algorithm. This algorithm selects the value of the duty cycle, by computing the two expressions $(abs(\Delta P/\Delta V) <= z)$ and $((\Delta I/\Delta V) + (I/V) < e)$. It calculates the

$abs(\Delta P/\Delta V)$ and compares the power with power at MPP if the difference is large the algorithm uses LS=0.01 and if the difference is small it uses SS=0.001 for tracking the MPP of the PV module.
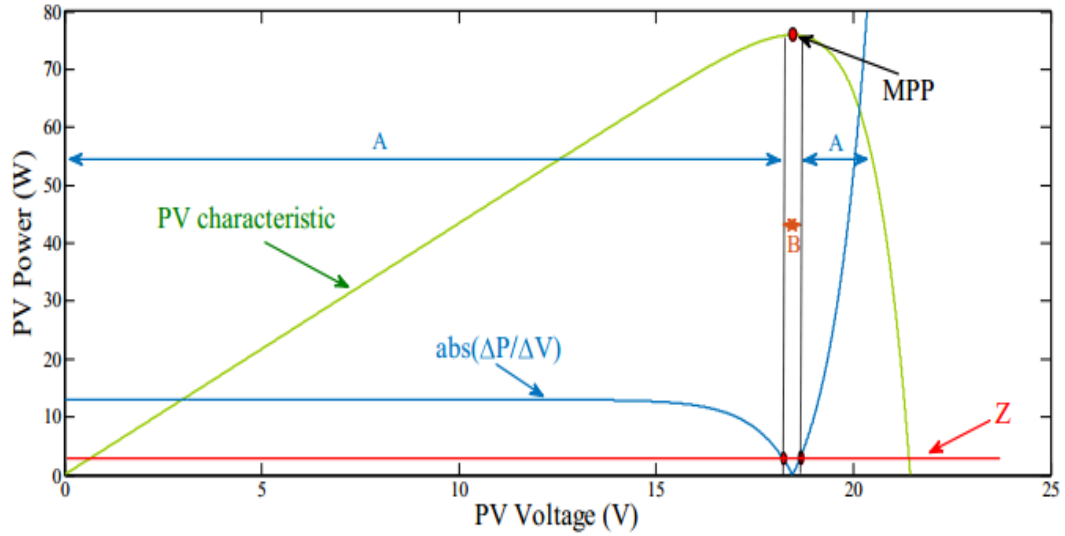
FIGURE 2.2: Two operating areas on P-V curve [31]

There are two main frameworks for the Inc.Cond algorithm are perturbation time and amount of step size. The drift occurs whenever solar irradiance increases or decreases suddenly within the perturbation in step size. To avoid drift occurrence in the PV curve a new modified Inc.Cond algorithm is proposed in [33].

This technique of Inc.Cond uses an extra condition $\Delta V > 0 \&\& \Delta I > 0$ to monitor the signs of change in current ΔI and voltage ΔV because whenever a change occurs in irradiance only these two parameters are affected. If both are positive then the duty cycle should be increased to reduce the PV module voltages to operate the system at the MPP point and vice versa.

A modified Inc.Cond algorithm is proposed in [34] which uses the same permitted error equation($|I + V*(dI/dV)| < 0.07$) a minimum error is accepted to admit that the slope is near to zero and the only difference is the value of an error. It also used the drift avoidance equation which is mentioned in [33].

When permitted error equation is satisfied then set the value of a variable (Var) to one and if not satisfied and Var=1, then this technique check the increment in current and voltages and increase the duty cycle.

To get high accuracy, stable tracking, and fast response of the PV module during fast-changing atmospheric conditions in [35] an improved Inc.Cond algorithm is presented. This algorithm works on the slope of the P-V curve and uses the condition ($| I + V * (dI/dV) | = 0$). If ΔV greater then 0 then the duty cycle will increase from the previous duty cycle value, and if ΔV less then 0 then we are on the right side of the P-V curve, and the duty cycle must be decreased to keep the system at MPP point..

2.3 Literature Survey of Simple PID Control based Inc Cond Algorithms

In [36] a modified Incremental conductance (Inc.Con) algorithm for the generation of constant power for fluctuated changes in solar irradiance. The presented technique performs two operating modes with the use of two different algorithms: the first is conventional Inc.Cond algorithm for MPP functioning depending on (P_{ref}) reference power and the second is for Constant Power Generation (CPG) operation.

Based on the reference power (P_{ref}) value the technique selects one algorithm for execution. If the Pref value is less than the floating power of the PV module then the MPPT algorithm is executed. If Pref value is greater than the floating power then the Constant Power Generation (CPG) algorithm is executed and the PV module does not force to operate at MPP point. Using the PID controller handle the proper operation of the CPG section of the technique and oscillations at the MPP point are reduced. The drawback of this technique, it is based on user-defined reference power values (P_{ref}) which may be not suitable for the better performance of the algorithm. Figure 2.3 represent the general blocks of PID based MPPT controller.

In [37] improved Incremental conductance (Inc.Cond) algorithm combined with a temperature controller is presented. This strategy is designed for in-door PV systems, concentrated sunlight is collected and transmitted into a room where

the PV system is installed with the help of Fresnel lenses and optical fibers. An intermediate optical stage called temperature controller is used to control the temperature of concentrated sunlight and MPP tracking a changeable step-size Inc.Cond algorithm is used.

This type of procedure is very helpful and produces more output power under (low irradiance) cloudy conditions. The drawback of this technique, it uses Fresnel lenses, optical fibers, and temperature sensor which are very expensive.
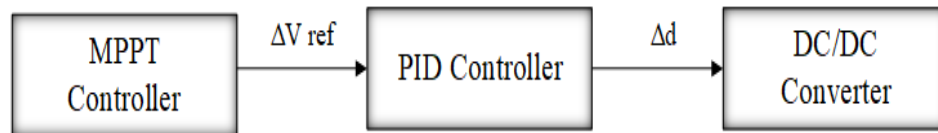
FIGURE 2.3: General diagram of PID based MPPT controller

In [38] variable step-size Inc.Con algorithm using a Genetic Algorithm (GA) based tuned PID controller is proposed. The presented technique uses online tuning of PID gains by GA which enhances the magnitude of step size for the duty cycle. This algorithm overcomes the shortcoming of P& O. It achieves a 56.4% quicker response, reduces ripple, and 49.2% of the overshoot are reduced as compared to P& O. The drawback of this technique its online calculation of step size by a Genetic Algorithm (GA) which required internet services for execution of the algorithm.

In [39] PID controller-based Inc.Con algorithm is purposed. This technique is based on a traditional incremental conductance algorithm and PID controller. This method uses the concept of the slope (dP/dV) to generate the error signal and the Grey Wolf Optimization (GOW) technique to tune the gains of the PID controller. Using the fitness function $J = \sum_{k=1}^{N} (|0 - (I/V + (dI/dV))|)$ in this paper the low tracking efficiency and steady-state oscillation problem of traditional Inc.Cond have been handled.

A PI controller-based charger with a FLC is proposed for maximum power point tracking in [42]. The FLC is used for MPP point tracking, and two inputs are used which are Error of system E(k) and change in error CE(k). These values are calculated using the ratio of change in power with voltage $\Delta P/\Delta V$.

2.4 Literature Survey of Fuzzy-Logic based Inc.Cond Algorithms

The researcher now moves towards intelligent control algorithms including fuzzy-logic, advanced fuzzy-logic, and artificial neural networks to track the MPP of the PV module. In fuzzy logic (FLC) an error equation is needed to produce the duty cycle and it does not require a complete mathematical model for tracking. Only one input is needed for the fuzzy controller includes three basic components fuzzification module, interference engine, and defuzzification module.

Fuzzification module takes an error as an input, interference engine contains membership function or rule table for the controller, the defuzzification produces duty cycle using PWM generation. For faster and accurate response with less oscillation at MPP point a fuzzy logic estimator using an incremental conductance algorithm presented in [40].

In this paper, a fuzzy estimator use an absolute error equation between instantaneous conductance and incremental conductance $e_{IC} = (dI/dV) + (I/V)$, is directly taken from the incremental conductance algorithm and feed to the fuzzy estimator. The next input is the ex-change in duty cycle which is taken from $\Delta d(k-1)$ the output of fuzzy estimator, $\Delta d(kT)$ is sent to incremental conductance algorithm, it determines the duty cycle of cuk converter.

For achieving more accurate and fast-tracking an extra calculation is considered called adapting calculation block is used with fuzzy logic controller block [41]. The reference voltages are calculated based on temperature and irradiance value for each MPP voltage. VMPP$_{ref}$ is compared with measure P-V voltage and their error Δe take as input to FLC. Adapting calculation block used different equations to find ref-voltage mention in [41]. The drawback of this technique is it involves the sensing of temperature and irradiance to start the adaptive calculation so a temperature sensor is required which increase the cost.

A fuzzy logic-based MPPT controller with a quadratic boost converter is purpose in [43]. For tracking the MPP point, the inputs of the FC change in PV module

power (dP/dt), and change in PV module voltages (dV/dt) and duty cycle as output. This procedure is similar to the Inc.Cond method which finds the derivative. The efficiency of this technique is 99.1% with very small oscillations at the output. The response of purpose technique is fast and converges the MPPT in 180ms for quickly changing weather conditions. The imperfection of this approach is the use of a quadratic boost converter which increases the number of components as a result cost will increase and second is the complexity of fuzzy logic in implementation.

In [45] optimization of fuzzy-based MPPT controller technique is presented to optimize the fuzzy membership function (MFs) and produce the proper duty cycle for MPPT. This study is about a comparison of different learning-based techniques includes: Teaching Learning Based Optimization (TLBO), Firefly Algorithm (FFA), Biogeography based optimization (BBP), and also Particle Swarm Optimization (PSO) are discussed.

In [46] optimization of a scaling factor of the fuzzy logic controller using particle swarm optimization, the technique is used for detecting the operating point. Numerical simulations are carried out for tuning the scaling factor of the duty cycle. Using the particle swarm optimization suitable scaling factor for the fuzzy controller is achieved by iteratively minimizing the error.

The algorithm takes two variables as input for the generation of error slope S(k) of P-V cure, and variation of the slope, and give the duty cycle for DC-DC Boost Converter respectively $S(k) = (\Delta P / \Delta V)$ and $\Delta S(k) = S(k) - S(k-1)$. The drawback of this method is it uses a sum of two techniques to find the MPP point.

Another intelligent and innovative control algorithm is presented in [47]. In this paper, the Neural Network Estimator (NNE) technique is the purpose for optimization of the P& O MPPT method.
Using the real-time data of weather and existing PV model to estimate the PV open-circuit voltage and voltage equivalent of maximum power to deduce its optimal duty cycle is determined for a switch of a DC-DC boost converter. Using the NNE-based controller MPPT is achieved almost 99% with accuracy.

2.5   Literature Survey of Control Techniques For MPP Tracking

For handling the non-linear behavior of solar cells and more accurate tracking of maximum power point, research purpose different control techniques using with conventional perturb and observe method and Inc.Cond method. In [48] Backstepping controller is applied to a boost converter to operate the PV module at the maximum powerpoint. In this paper, the global mathematical model of PV storage system which is non-linear is used to find the differential equation for the Backstepping controller. Error is introduced to reach the desired point, then defined the Lyapunov function (L-F) then take the derivative of the L-F.
After involving the system it checks the sign of the L-function if it is negative or less than zero then the error becomes zero at the PV system is operating at MPP. In the end, the final L-function was used to check the stability of the controller that is verified by Lyapunov stability analysis (LSA). Tracking error is reduced by selecting Lyapunov functions, which are the square of every stage of error.

In [50] for enhancing power production from PV module, a Sliding Mode Controller (SMC) is compared with the Inc.Cond method. The efficiency of the Inc.Cond method under rapidly changing climate conditions is not good accuracy, so that's why an SMC is purposed. To design the sliding mode controller it involves two steps: one is defining the sliding surface which is selected according to output force to zero in a limited time $\dot{\alpha} = -msign(\alpha)$, $-m|\alpha| < 0$.
The second step is the determine the control law, this control law forcing the output to zero in a limited time is composed of two terms Ueq and Ur, Where Ueq is the equivalent linear control which makes the system nominal state slide on sliding surface and Ur is the term, forcing the system remain on the sliding surface. Figure 2.4 show block diagram of MPPT algorithm with sliding mode controller.

In [51] Non-linear Adaptive Control is presented for MPPT of the PV system. The controller design is based on a non-linear model of PV arrays and boost converter,
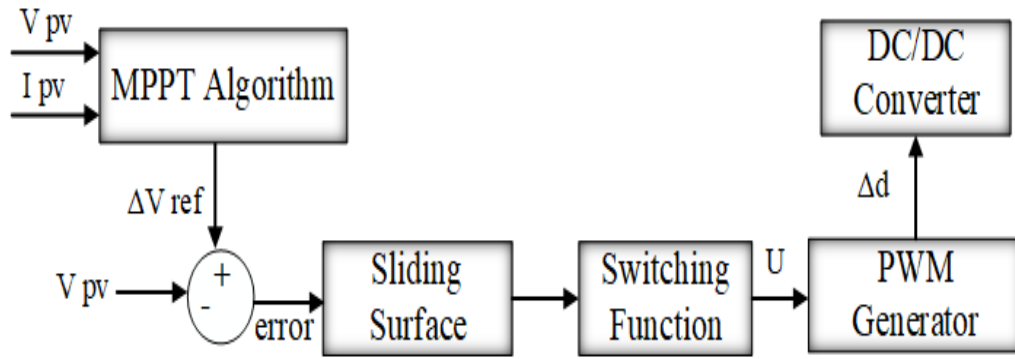
FIGURE 2.4: MPPT technique with sliding mode controller (SMC)

with the use of adaptive back-stepping control to achieve the desired output. The presented adaptive controller used online estimation of model uncertain parameters that change when change appears in irradiance and temperature. The adaptive controller meets the tracking requirement and reduces the steady-state error at MPP. The drawback with this technique is, increases the cost of the system and it required an internet connection for the online estimation of parameters.

In previous literature [28–35], the proposed IncCond algorithms were tested under standard testing conditions. The researchers use only change-in irradiance signal to determine the performance of their proposed algorithm. They provide only one comparison with basic IncCond MPPT algorithm. Also they do not mention any kind of comparative analysis among the tracking accuracy, efficiency and extracted power under rapidly changing weather conditions by using different modified IncCond algorithms.

In [36–39] PID based techniques uses the combinations of two algorithms to track the MPP point. This will increase the computational process to achieve the MPP point on P-V curve.

Fuzzy logic controller based IncCond technique increase the complexity of the algorithm [40–47]. They also use two or more AI-based algorithms to estimate the parameters of the fuzzy logic controller.

Control based technique including back-stepping, sliding mode and non-linear adaptive controller are used to achieve the MPP point with less oscillations [48–51]. By using these controller the cost of MPPT tracking will increases.

Every researcher proposed their MPPT technique and compared it with only basic Inc.Cond algorithm their target is to track MPP with faster response, good accuracy, and less oscillation at the point of convergence. Most of the MPP techniques do not consider a rapid change in irradiance and no simulations are given using varying temperature.

2.6   Motivation

As fuel prices are increasing almost on daily basis, now it is important to shift our convenient transportation system to electrify transportation. Max. power point tracking is one of the core parts of the PV system. A lot of methods are proposed for MPP point tracking in the literature to enhance the performance and the efficiency of solar energy systems. Among all of these methods, only the direct control technique can show a satisfactory result in tracking problems. This research has been conducted with the motivation to select the maximum power point technique among Inc.Cond algorithms which are simple and easy in implementation, small in length, better accuracy, better efficiency, detection of fast-change in irradiance, less response time, and able to extract maximum power from PV array both in constant and fast-changing irradiance and this kind of work is never be conducted before.

Proper data is given to the algorithm to improve tracking efficiency. In the case of achieving MPP point, tracking is must be done with a direct control technique, and proper operation of load controller is used on the load side. This will increase the overall productivity of the PV systems and reduce the carbon footprint created by Petroleum-based Vehicles (PBV) for a pollution-free future.

2.7   Gap Analysis

The MPP tracking can be achieved by using some set of instructions called an algorithm. For true detection of fast change in irradiance and to perform better

in every circumstance the algorithm should consider the change in current and voltage of the PV module. In the literature, most of the researchers compared their proposed technique with the traditional Inc.Cond algorithm and some researchers provide two comparisons of different Inc.Cond algorithms based-on direct control.

In [28] the researcher does not give any initial step-size value of N1 and N2. It only compares its proposed technique with conventional fixed step size IncCond algorithm. The parameter that is considered for testing the efficiency of the algorithm is only two: first is the time responses and second is the oscillations at MPP point. Previously, fast-changing irradiance input signal was not introduced for solar car applications which is the one of the novelties of this thesis.

In [29] with the addition of one more testing parameter which is the Tracking Accuracy of the algorithm. Decreasing irradiance signal was considered for simulations but exact value of irradiance is not given. Initial parameters are also not given and the power rating of the PV system is only 250 watts which is used to simulate the algorithm.

In [30] same testing parameters that are mentioned in [29] are used to test the proposed algorithm and only one comparison with the basic IncCond algorithm is given. Moreover, two sudden changes in solar irradiance signal are considered and tracking efficiency is also not given. So, user have no idea about the performance of the technique under different irradaince level.

Reducing system oscillation around the MPP point many MPPT techniques are proposed in [31–35]. The researchers do not provide the tracking error, tracking accuracy, convergence speed and consider the length of an algorithm to judge the exact efficiency of the algorithms. Furthermore, the PV system is implemented for against modified IncCond techniques are less than 100 watts. Only one comparison with the basic Inc.Cond algorithm is given. In addition, varying temperature signal is not considered to extract the voltage, current and power response of modified Inc.Cond algorithm.

Many researchers do not mention the input irradiance and temperature signals and most importantly they only compared their proposed technique with the basic

Inc.Cond algorithm. No simulations are taken using varying temperature and never mentioned the effect of temperature on their proposed algorithm.

In the literature, multiple algorithms of modified incremental conductance were proposed for maximum power point tracking (MPPT). These algorithms itself were not exhaustively tested against the range of performance testing parameters. For instance, rise time, settling time, tracking accuracy, efficiency, steady state oscillation, complexity and length of algorithm. Moreover, no comparison of these proposed modified incremental conductance algorithm was present [28, 34, 35].

2.8 Problem Statement

In the literature, multiple algorithms of modified incremental conductance were proposed for maximum power point tracking (MPPT). Firstly, these algorithms itself were not thoroughly tested against the range of performance testing parameters [28, 31, 32]. Like, rise time, settling time, tracking accuracy, efficiency, steady state oscillation, complexity and length of algorithm. Secondly, no comparison was present among these proposed modified incremental conductance algorithms [31–35].

Thus, after analyzing this gap, each modified incremental conductance algorithm is tested exhaustively, not only against the range of performance testing parameters but also against the fast-changing irradiance and varying temperature conditions. In addition, the best algorithm of modified incremental conductance is also suggested with the help of detail comparison of all the tested modified incremental conductance algorithms for solar cars applications.

2.9 Research Strategy

In this section of the thesis designing of a PV cell model, PV module, software tool and recommendations and future work related to this work are discussed and a flow chart diagram of strategy is shown in figure 2.5.

2.9.1   Software Tool

A selection of software is an important part of research and is easy to use for a researcher. It must offer a complete interface that permits modeling of the PV system. The software checked for suitability of the system in MATLAB 2020b. In MATLAB 2020b Sim scape Power Systems provides a large variety of examples and analysis tools for modeling and simulation for electrical power system modeling.

2.9.2   Designing of System

This study is about to select the tracking algorithm that accurately tracks the max. power point of PV array during fast-changing solar irradiance with good efficiency. An algorithm is selected by comparison among different step-size direct control based Inc.Cond algorithm. Therefore, engrossing all parameters of performance of the selected algorithm, a complete PV system integrated with DC/DC boost converter and DC bus as the load has been modeled in Matlab 2020b.

2.9.3   Research Conclusion

The PV system model simulations have been run at various irradiance conditions with a constant and varing temperature. This study is the comparative analysis of direct control step size-based Inc.Cond techniques. All of these techniques are tested included constant irradiance and temperature and rapidly changing irradiance and temperature is also constant but its value is high. Serval simulations take place to compare their results.

Based on the results and testing parameters includes Simplexity and Ease sin implementation, Small in length, Finer accuracy, Superior efficiency, Detection of fast-change in irradiance, Less response time, and able to extract maximum power from PV array both in constant and fast-changing irradiance, one or more direct control based Inc.Cond algorithm are suggested of implement in the solar-charging station.
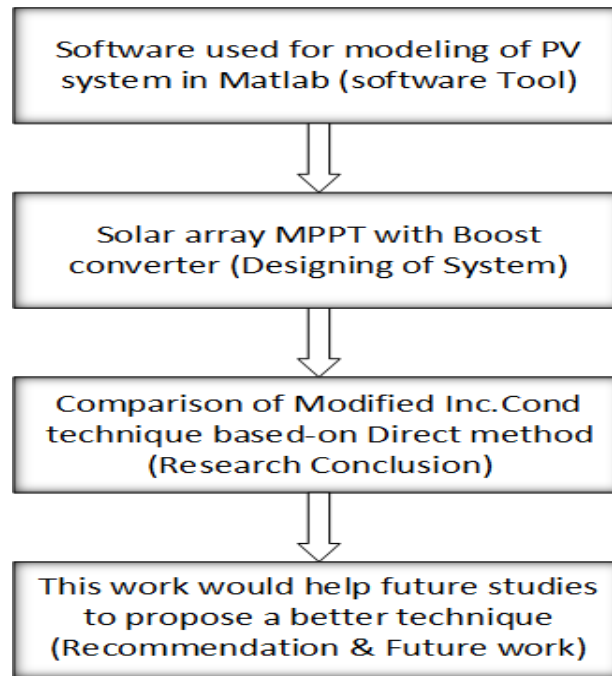
FIGURE 2.5: Flow chart of Research Strategy / Methodology

2.10 Chapter Summary

In this chapter, world power requirements and the contribution of solar energy by 2030 have been discussed. Literature Survey of different MPPT techniques including Conventional, Modified Conventional methods, Advanced tracking, and Control strategy of load are discussed in this chapter along with their pros and cons. Motivation, gap analysis, problem statement, and research strategy is also the portion of this chapter.

Chapter 3

System Modeling

To simulate the system model and to extract all performance parameters, this chapter is about complete modeling of the PV system that is implemented in Simulink/Matlab.

3.1   Introduction

Photovoltaic cell is the fundamental or core of the PV module and without understanding this we cannot acknowledge the whole PV system. In 1839, French scientist Edmund Becquerel discovered that certain materials would give off a spark of electricity when place in sunlight. The amount of power generated by PV cells depends on many aspects, such as solar irradiance, temperature, shaded condition, dirt, and output voltage of the PV cell.

The equivalent PV module can be modeled as a current source in parallel with a diode, and two resistance Rsh, and Rs. To increase the output power of PV systems, PV modules are generally construct using serval PV cells connected in series and parallel [29]. In this chapter mathematical model od PV array, modeling of solar car and MPPT controller and Matlab modeling of the boost converter. The main components of a PV system including PV panels, a DC-DC converter,

MPPT controller, and the load. The general diagram of complete PV system is shown in figure 3.1. On the other side, a DC load and AC inverter act as loads.
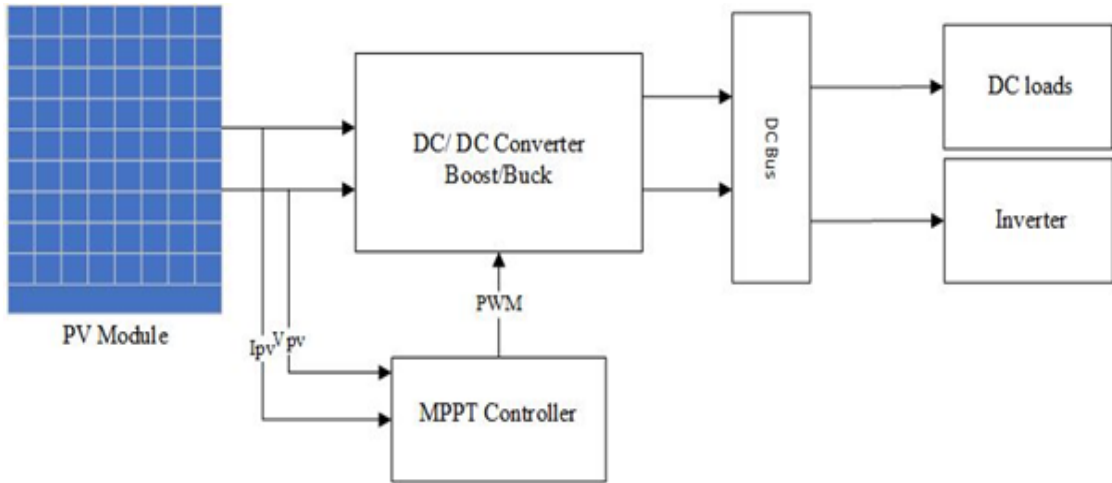
FIGURE 3.1: General block diagram of a PV system [29]

3.2 PV Cell Model

The fundamental and smallest section of the PV module or array is a solar cell. On account of this, it is obligatory to model the solar cell before modeling the PV module and array for constant and rapidly changing atmospheric conditions. There are two representations of a PV cell in literature single diode and double diode-based models. A solar cell can be classified as a semiconductor device, and flow direct current through it when solar irradiation penetrates to the photovoltaic cell surface [42].

In this study, a single diode model is picked for its simplicity, precision, and ease of implementation. Figure 3.2 represents the corresponding circuit of the PV cell. It comprises photo-current source I_{ph}, which is parallel to a non-linear single-diode, a shunt resistance R_p, and series resistance R_S.

Modeling equations are given below [45], to get the total current of the equivalent circuit Kirchhoff's Current Law is applied to compute the output solar cell current.

$$I = I_{ph} - I_o - I_{sh} \tag{3.1}$$

Where I is the total current of a solar cell, I_{sh} is current through a shunt resistor, I_{hp} is photo-current and I_o is current through a diode.
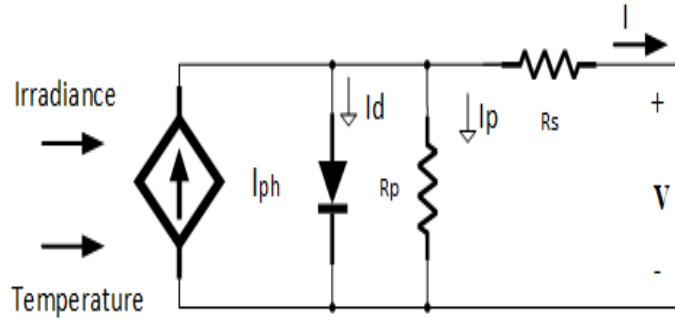
FIGURE 3.2: Equivalent circuit model of Photovoltaic cell

For total output voltage V, Kirchoff's Voltage Law is applied

$$V = V_d + (R_s \times I) \tag{3.2}$$

Where V_d is diode voltage and R_s is the series resistor.

$$V_d = I_{sh} \times R_{sh} \tag{3.3}$$

By substituting eq 3.2 and 3.3, we get I_{sh}

$$I_{sh} = \frac{V_d}{R_{sh}} = \frac{V + I \times R_s}{R_{sh}} \tag{3.4}$$

$$I_{ph} = \frac{E}{E_n} \ (I_{sC} + \ (K_I \times \Delta\text{T})) \tag{3.5}$$

The above eq 3.5 shows that, I_{ph} depends on irradiance value E and E_n is standard irradiance value which is 1000 W/m^2, and I_{sC} is short circuit current.

ΔT is the difference between standard and operating temperature.

K_I is the temperature coefficient of the Solar cell.

$$V_{th} = \frac{N \times K \times T}{q} \tag{3.6}$$

V$_{th}$ is the terminal voltage

K represents the Boltzmann constant

q is the amount of electron charge

T is the temperature of the p-n junction

$$I_o = I_{on} \times \left(\frac{T}{T_n}\right)^2 \times exp\left[\left(\frac{q \times E_g}{n \times K}\right) \times \left(\frac{1}{T_n} - \frac{1}{T}\right)\right] \tag{3.7}$$

$$0 = I_{ph} - I_d - I - \frac{(V + R_s I_{pv})}{R_p} \tag{3.8}$$

$$I_{pv} = I_{ph} - I_o \left\{ exp\left[\frac{(V + R_s I_{pv})}{V_{th} \times n}\right] - 1 \right\} - \frac{(V + R_s I_{pv})}{R_p} \tag{3.9}$$

Where:

I_{ph} the generated current of solar cell under a given insolation

I_{pv} an output current of a cell

I_o diode reverse saturation current

I_d diode current

I_{on} nominal saturation current

R$_p$ is the series resistor

n identity factor for p-n junction

T_n cell temperature at a reference condition

E_g bandgap energy ($\approx 1.1eV$)

3.3 Effects of several parameters on Solar cell Efficiency and Output Power

Photovoltaic cell power and efficiency effected and limited by many losses, few of them are manageable/controllable but few of them are uncontrollable due to their nature. PV cell operates on its maximum efficiency under standard temperature and irradiance value which is the ideal case. In reality these conditions are never achieved.

Parameters which are effect the efficiency of solar cell includes irradiance, temperature, tilt, and orientation, converter and cable loss, shading effect, dust, cooling of the cells, heat transfer, and humidity on PV cells [53]. To observe the effect of the above mention parameters an experimental study is conducted in [52].

3.3.1 Effects of Irradiance on PV cell

Solar light intensity has a remarkable effect on PV module cell temperature and output power. The amount the current is generated by the PV cell is depending on only irradiance value, not on temperature value. PV cell output power is increase with solar irradiance intensity and decrease with low irradiance.

3.3.2 Effects of Temperature on PV cell

The operating temperature of the PV module is an essential factor for PV conversion action. The increment of working temperature acts as a censorious aspect that causes the efficiency and generated output power of the PV module will decrease. The bandgap will shrink with the increase in temperature because of this substantial reduction of V_{OC} will appear.

At high irradiance, the flow of electric charge rises from the valence band to the conduction band. Due to this only 15 to 20 percent of solar irradiance is turned into electric power. The remaining of the irradiance is permute into the heat on

the PV module [53]. The temperature effect differently on solar cell technologies including mono-crystalline, thin-film, and polycrystalline.

3.3.3 Effects of Cooling on PV cell

Cooling of PV module can be done by water flow and use heat exchanger mounted to the backside of the PV module. The temperature of the PV module decrease as the flow rate of water increase and the output power increase slightly. For achieving a large increment in the output of the PV cell. The flow rate must be double but the pump needs to devour twice the power to flow the water rapidly through the PV panel. Solar cell temperature can also be reduced through the heat exchanger mounted to the back side of the PV module. Reducing the temperature of the PV module will increase the electrical efficiency up to 0.64%.

3.3.4 Effects of Tilt and Orientation on PV cell

The PV module efficiency increase as the maximum solar insolation is absorbed by PV cells, for this purpose, the module surface is perpendicular to the direct sunlight. The higher direct irradiance on a perpendicular to the solar radiation can increase energy yield. To enlarge the amount of sunlight strick the surface of the PV module it is important to place the orientation of the PV module concerning the direction of the sun [53]. Figure 3.3 shows the proper angle placement and direction of the PV module under sunlight.
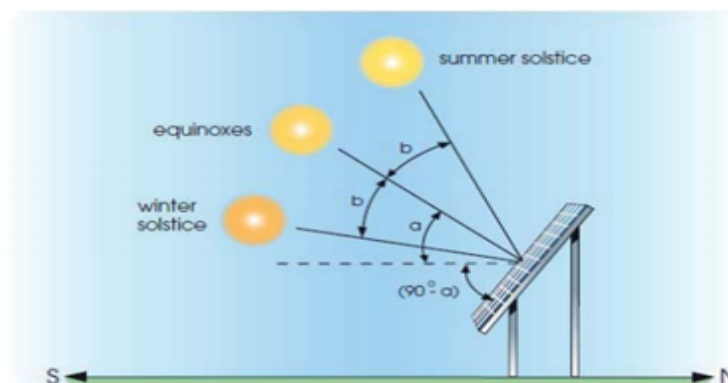
FIGURE 3.3: Insolation on PV module concerning in sun angles [53]

3.3.5   Effects of Shading or Partial Shading on PV cell

A PV solar module is very sensitive to shading. Shading is a phenomenon in which the PV module is fully or maybe some part of it is covered and less amount of irradiance is absorbed by that portion. The efficiency and power loss now depend on that section which is shaded. There are two kind of shading sources fully or soft shading, and the other one is partial or hard shading. A soft shading is due to those objects or things that are far away from the PV module and diffuses the solar irradiance fall on the module.

The partial shading includes the tree leaves, bird dropping, snow, and thick dust layer at the surface of the PV module which stops the sunlight reach to the solar cell [53]. Those cells which are half-shaded will produce less current as compared to other cells. So the power is reduced to 50% of its total generation. Now, these cells act as load and consume the power across it.

To mitigate this problem, the shaded cells must be bypassed using the bypass diode. The bypass diode is connected parallel to the group of the solar cell which is in series as shown in figure 3.4. The current is flowing through the bypass diode, not from the shaded cell.
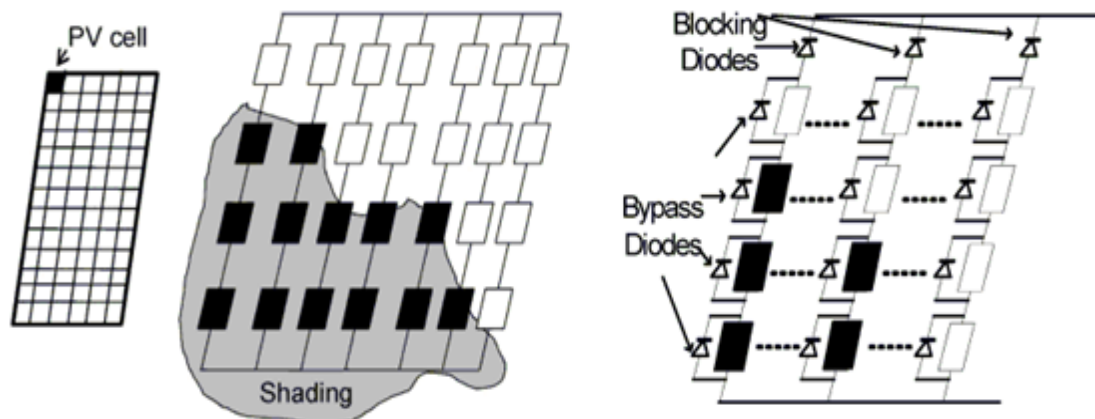
FIGURE 3.4: PV array with Bypass. The dark section represents shaded cells
[53]

To operate the PV module at a maximum point during the shading effect on PV cells many algorithms are presented. P&O and Inc.Cond are the maximum powr

point techniques which are widely used to mitigate partial shading problem of a PV cell. The modified versions of these two techniques are perform better in normal and shaded cases.

3.3.6 Effects of Dust on PV cell

PV module is placed in an open environment, the factor that has the worst effect on the PV efficiency is dust. Dust may resist the solar radiation to reach the PV module. The efficiency drops to 1.47% and the dust on the upper side of the module reduced the performance by 30.43% as compared to the clean surface of the PV module.

The study in [52] describes the efficiency and output power with and without dust on the module. To achieve better efficiency and performance, the surface of the module must be clean. Cleaning may be done manually or automatically by retrofitting a spry nozzle at the top, to remove the dust from the PV module surface one time per week.

3.4 Mathematical Model of PV Module and Array

After describing and expressing the mathematical model equations and equivalent circuit, now we can model the complete PV module and PV array. Based on the above analysis and the parameters that effect the performance of the PV module. The output equation is the function of different variables like irradiance E, temperature T, current Ipv, voltage Vpv. So, due to this eq 3.9 also change for the PV module [29, 32]. A module is made of several cells connected in series and parallel to have reasonable voltage and current.

N_s and R_s are the number of series and parallel connected cells.

$$F(I_{pv}, V_{pv}, E_n, T) = I_{pv} - I_{ph} - I_o \left\{ exp \left[\frac{(V + R_s I_{pv})}{N_s \times V_{th} \times n} \right] - 1 \right\} - \frac{(V + R_s I_{pv})}{N_s \times R_p} \quad (3.10)$$

For modeling the PV system, one PV module is connected in series and three modules in parallel. The current of each PV module is added and the voltage is the same in all of the modules. Figure 3.5 shows the equivalent circuit single diode-based model of three modules connected in parallel.
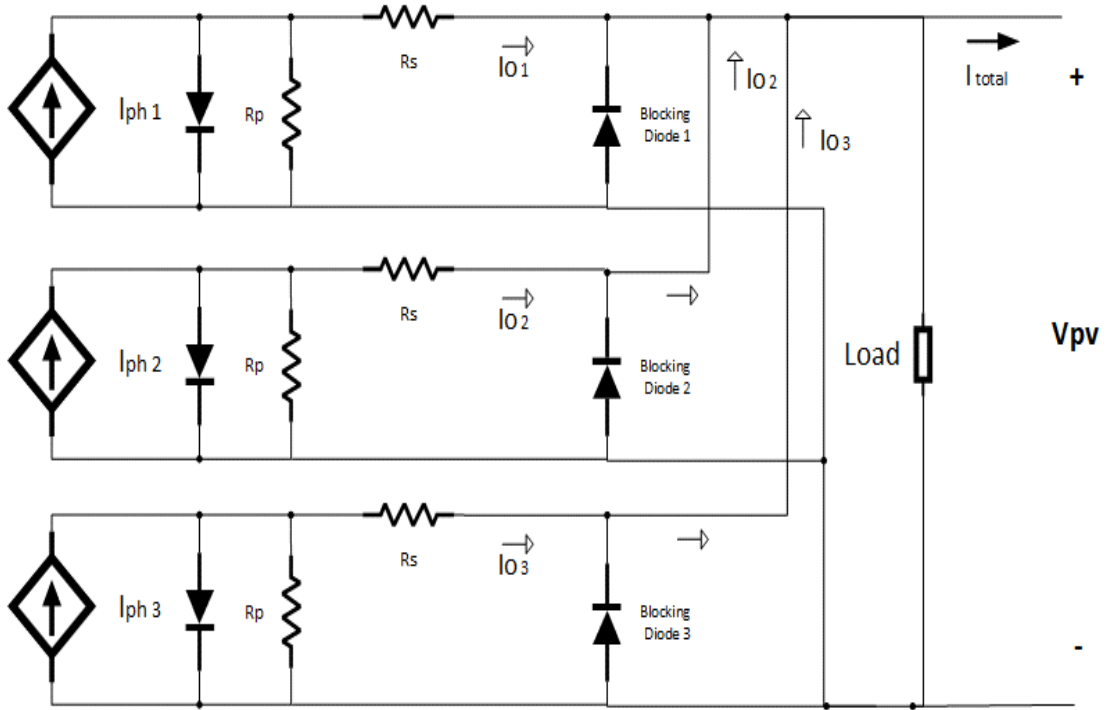
FIGURE 3.5: Equivalent Circuit of three PV modules Connected

For calculating the Mathematical equation as we have done in a single PV cell. Now the mathematical model of four PV modules becomes;

$$I_{pv1} = I_{ph} - I_o \left\{ exp \left[\frac{(V_{pv1} + R_s I_{pv})}{V_{th} \times n} \right] - 1 \right\} - \frac{(V_{pv1} + R_s I_{pv})}{R_p} \tag{3.11}$$

$$I_{pv2} = I_{ph} - I_o \left\{ exp \left[\frac{(V_{pv2} + R_s I_{pv})}{V_{th} \times n} \right] - 1 \right\} - \frac{(V_{pv2} + R_s I_{pv})}{R_p} \tag{3.12}$$

$$I_{pv3} = I_{ph} - I_o \left\{ exp \left[\frac{(V_{pv3} + R_s I_{pv})}{V_{th} \times n} \right] - 1 \right\} - \frac{(V_{pv3} + R_s I_{pv})}{R_p} \tag{3.13}$$

Where I_{pv1}, I_{pv2}, and I_{pv3} are the added to each other and V_{pv} of PV module is the same. Total I_{pv} of the whole PV array can be expressed by the equation 3.14

$$I_{pv} = I_{pv1} + I_{pv2} + I_{pv3} \tag{3.14}$$

For the PV array, all PV modules in an array are considered to have the same characteristics and the equivalent circuit of the PV cell is represented in figure 3.6. The voltage and current relationship of the PV array can be by the below equation in [47]. Where N_p and R_s is the number of panels in parallel and series-connected respectively.

$$I_{pv} = N_p \times I_{ph} - N_p \times I_o \left\{ exp \left[\frac{(V + R_s I_{pv})}{V_{th} \times n} \right] - 1 \right\} - \frac{(V + R_s I_{pv})}{R_p} \tag{3.15}$$
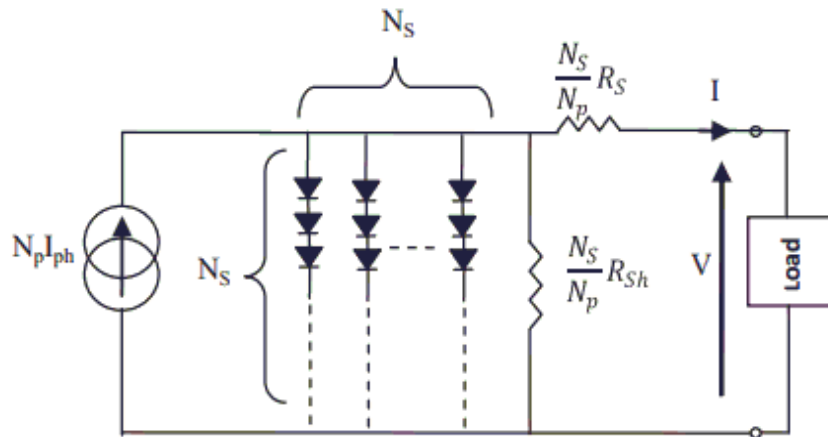
FIGURE 3.6: Single Diode model of Nth no. of PV Array [47]

At ambient conditions, the voltage of the PV array V_{pv} is the same for three PV modules and the current flow through each module is added. V_{pv} is adjusted like that the PV array must operate at max. power point by utilizing a DC-DC converter with MPPT technique.

With the fast change in irradiance value, the voltage of the PV array is change simultaneously and the MPP point also shifts. As irradiance drops down from 1000 watts per meter square and continuously drops up to its lowest value. In this case, voltages V_{MPP} of the PV module reduce very quickly but the current is

slightly reduced. To detect the change in irradiance, the algorithm must measure the change in voltage ΔV_{PV} along with the change in current ΔI_{PV}. After this, the algorithm check the change in ΔP_{MPP} power to take the final decision.

3.5 Modeling of a Solar Car and MPPT Controller

Solar vehicle is an electric car which has PV cells mounted on its roof. These cells increase the range of the vehicle up to 12 km and also regulates the charging of the battery. The key components of a solar car is: solar cell roof, battery, charger controller and motor. Figure 3.7 represent the block diagram of a solar car. First the power is extract from solar car and then it will charge the battery or also give directly to inverter to drive the motor. Some components rating is taken from [55]: including battery capacity 72V/100Ah, AC-motor 7.5 kw, solar module 300w and charger is 2kw.
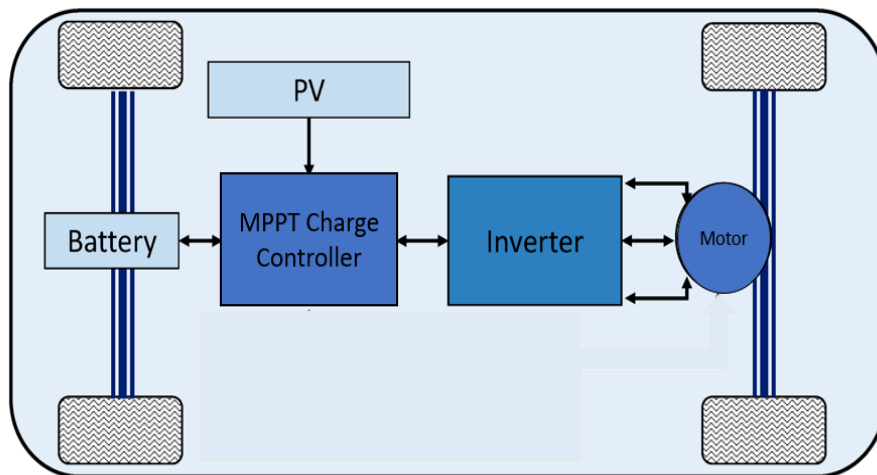
FIGURE 3.7: General block diagram of a Solar car

The main focus in this work is the MPPT technique in charge controller which is one of the key part of a solar car. Now the system includes: PV cells or module, DC-DC converter, MPPT algorithm and the load or a dc-bus. Figure 3.8

represent all components involve in extraction of power from PV cell for the solar car operation. First component is the PV cell, second is the switching converters which always required for the proper operation of PV systems.

These converters are required to adjust the output voltage to operate the load or charge a battery. To make the MPP point tracking inexpensive the Boost converter is the better option among other DC-DC converters.

The next component is the core of the PV system which is the max. power point tracking controller. This controller generate optimum duty cycle by using the MPPT technique to operates the system on maximum power point all the time.

This work focuses on only extracting the max. power from solar cells of a solar electric car using modified IncCond algorithms. Some assumptions are considered related to load and the battery of a solar car. The load is not varying and consume constant power. The solar cells produce enough power to operate the motor of the solar car. The MPPT tracking process continuously take place to increase the power production of the solar cells and enhance the overall efficiency of the system.

The battery is fully charged and the power flow is only towards the load through an inverter. The input of the inverter is the variable DC and then the inverter convert this variable dc power into constant AC power to operate the load.

3.6   Designing of Boost Converter

In this system Mosfet is used as a switch, it has two states on and off state. D is defined as the duty ratio for a converter. During $0 < t < DT$, the Mosfet is in on state and the diode is reverse biased. Input supply V_{IN} are now parallel to an inductor, voltage across an inductor is $V_L = V_{IN}$. During $DT < t < T$, the Mosfet is in an off state, and the diode becomes forward bias [42, 53]. Inductor's voltage is equal to $V_L = V_{IN} - V_{Out}$.

The total change of current in the inductor must be zero in a period of switching
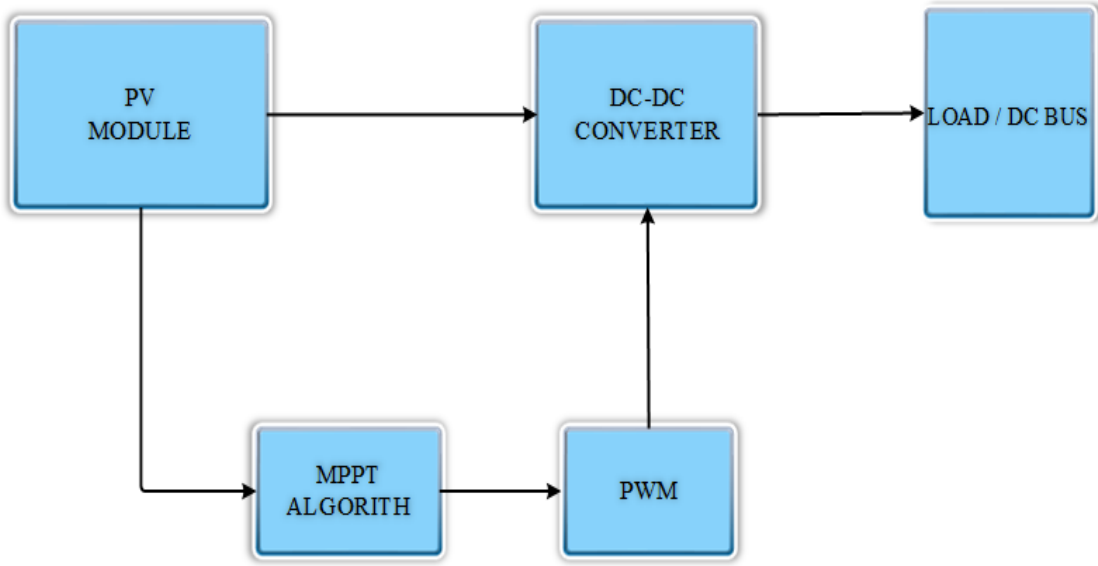
FIGURE 3.8: A general overview of a PV module and its components with an MPPT controller

[53]. The equations which are used in the designing of the boost converter for the solar electric car is taken from Power Electronic: circuits, devices and applications [54]. The design parameter of boost converter using the following eq's is mentioned in Table 3.1.

$$V_{in} = V_{out} \times (1 - D) \tag{3.16}$$

$$\frac{V_{in}}{V_{out}} = \frac{1}{1 - D} \tag{3.17}$$

$$\Delta I_L = \frac{V_{in} \times D}{F_s - L} \tag{3.18}$$

Where: ΔIL is a change in inductor current V_{in} is input side voltage. D is the duty ratio. L is the required inductor value. F_s is Switching Frequency of the boost converter used to extract the simulations results of IncCond algorithms.

$$L = \frac{V_{in} \times V_{out} - V_{in}}{\Delta I_L \times F_s \times V_{out}} \tag{3.19}$$
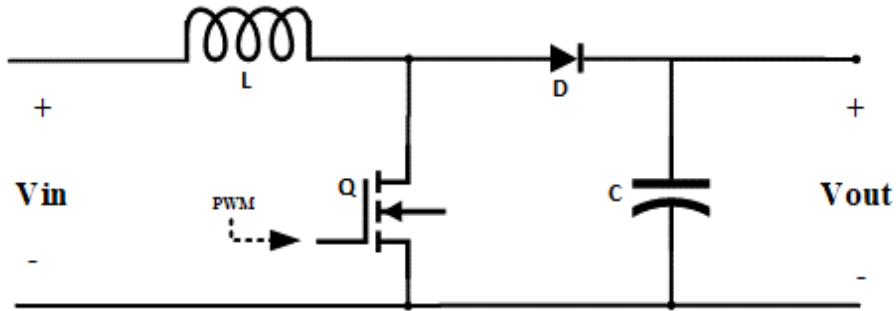
FIGURE 3.9: Circuit representation of Boost Converter

L is the required value of the inductor. ΔIL is ripple current of the inductor. V_{in} and V_{out} are input and output voltages respectively [42].

$$C = \frac{I_{out} \times D}{\Delta V_{out} \times F_s} \tag{3.20}$$

C is the required Capacitor value, used in boost converter. ΔV_{out} is output ripple voltage. I_{out} is output current. F_s is switching frequency. Figure 3.9 shows the circuit representation of the boost converter.

3.7 Matlab/Simulink Representation of PV System with a Boost Converter and MPPT Controller

In this section complete system implementation with MPPT algorithms is done. The PV array, boost converter and MPPT controller are implemented in Matlab/Simulink 2020b. The different modified Inc.Cond algorithms are presented in [28–35] are implemented on the same matlab model of a PV system. These algorithms are simulated and results are shown in coming chapter.

Figure 3.10 shows the Simulink model of a PV with a boost converter and MPPT Controller. The PV module of Lifeline energy (Trina Solar) is select for the construction of the PV array. The Voc and Isc of the single module is 49.9V and 9A respectively. With Vmpp and Impp is 41.5V and 8.07A and total power rating

of one module is 334.95 watt. Three PV modules are connected in parallel to meet the current requirements. The total PV array power rating is equal to 1005 watt. By clicking on the block of PV array, parameters of PV module are adjusted according to requirements. Table 3.2 shows the parameter of solar PV array and single module.
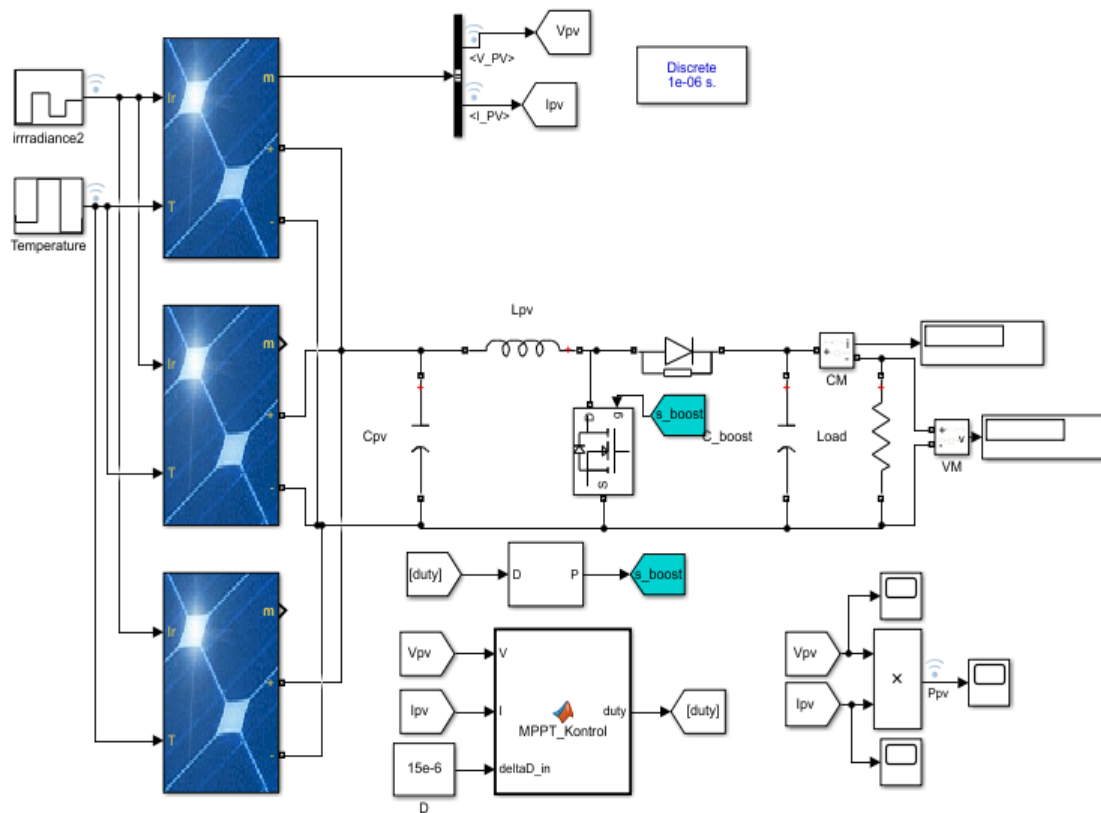
FIGURE 3.10: Overall Simulink representation of a PV system with MPPT Controller

Second section of the matlab simulink model is the boost converter. The inductor value of the boost converter is 1.2 mH and switch is the IGBT and schottky diode is used in boost converter construction. The voltage and current rating of the IGBT and diode is high. Switching frequency is 10kHz and IGBT used as a switch. Boost converter is used to adjust the voltage of PV array to operate the PV system at its max. efficiency. Parameters of boost converter which are select in this work is given in Table 3.1.

The controller block in which MPPT algorithm is implemented is used for the execution of each algorithm. But programming is according to the flow chart of
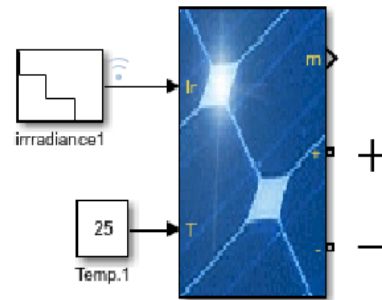
FIGURE 3.11: Matlab/Simulink representation of Solar PV Array

the Inc.Cond algorithm. As this work is focused on extracting max. power from solar cells a resistive load of 20 ohm is used to extract the voltage, current and power response of each Inc.Cond algorithm.

This work is only related to the MPPT operation of the PV array at its efficiency using Inc.Cond technique. So, thats why resistive load is used in simulation result of modified Inc.Cond techniques. The comparison of each modified Inc.Cond MPPT algorithms are discussed in detail in the next chapter.

In figure 3.11 a user define its on PV array by selecting the no. of PV module in parallel and in series. On the right side of the PV array block, irradiance and temperature are the input of the PV array and on the other side connection for a Boost converter are present in order to operate the load, and " **m** " is for measurement of the PV voltage and current in order to examine the PV array operation at MPP point.

TABLE 3.1: Calculated Parameters of a Boost Converter

Parameters	Value & Units
Inductor	1.2mH
Input PV Capacitor	1000μF
Output Filter Capacitor	3300μF
Switch Type	IGBT
Diode Type	Schottky diode
Switching Frequency	10KHz
Resistive load	20Ω

TABLE 3.2: Electrical Parameters of PV array at STC: irradiance 1000W/m2 at 25 ℃

Parameters	Value & Units
Maximum Power P_{MPP}	1005 W
Voltage at max. Power V_{MPP}	41.5 V
Current at max. Power I_{MPP}	24.21 A
Open circuit voltage V_{OC}	49.9 V
Short circuit current I_{SC}	27A
Single module max. Power P_{MPP}	334.95 W
Single module voltage at max. Power V_{MPP}	41.5 V
Single module current at max. Power I_{MPP}	9 A
Single open circuit voltage V_{OC}	49.9 V
Single short circuit current I_{SC}	8.07A
Max. Input Irradaince	1000 W/m^2
Min. Input Irradaince	300 W/m^2
Max. Input Temperature	65 ℃
Min. Input Temperature	28 ℃
Series Resistance R_S	0.26 Ω
Shunt Resistance R_{Sh}	77.6 Ω
No. of cells in PV array	248

3.8   Chapter Summary

At the start of this chapter, modeling of a PV cell is done along with the parameters that can affect the efficiency and output power. After that, complete mathematical modeling of a PV module and a PV array is conducted. Modeling of a Solar car with Pv module and MPPT controller is also include in this chapter. Electrical parameters of a PV array, design calculation, and Matlab/Simulink modeling of the Boost converter are also included in this chapter.

Chapter 4

Incremental Conductance MPPT Algorithm and its Variations using Direct Control

4.1 Introduction

In this chapter, a detailed explanation of the Inc.Cond algorithm and its variations are conducted. Five modified Inc.Cond algorithms are compared. First the basic Inc.Cond is explained with its limitations and then its modifications are discuss. Each algorithm discussed in detail with its major modification. Equations which are used in these algorithms are also the part of this chapter. Furthermore, the flow chart of each modified Inc.Cond technique is also given. To determine the transient response of the each algorithm a irradiance signal is applied to the matlab simulink which is mention in previous chapter. The modified Inc.Cond algorithms which are going to compared in this work are listed below:

1. Basic Inc.Cond algorithm.

2. Variable step-size with variable scaling-factor (VSS-VSF) Inc.Cond.

3. New advance Variable step-size (NAVSS) Inc.Cond.

4. Modified Inc.Cond for dynamic irradiance.

5. Modified Inc.Cond for changing solar irradiance.

6. An improved control-strategy based on Inc.Cond.

With the help of transient response of current, voltage and power of each Inc.Cond algorithm, the strengths and limitations are explain in this section. Based on their simulation results, a detail comparative analysis is explain in the next chapter.

4.2 Traditional Inc.Cond MPPT Algorithm

Incremental Conductance (Inc.Cond) is a widely used MPPT technique which is works on the detection of the slope of the P-V curve given in figure 4.1. This method is often considered, because of its better performance like fast-tracking speed, ease of implementation, and high efficiency. The instantaneous conductance value $\frac{I}{V}$ and the incremental conductance $\frac{\Delta I}{\Delta V}$ value is compared to determine the position of the MPP point on the P-V curve.

If eq 4.1 is satisfied then the PV module operates at its maximum point. If $\frac{I}{V}$ is less then $\frac{\Delta I}{\Delta V}$ value then the PV module operates at the left side of MPP which means MPP point is not achieved yet and if $\frac{I}{V}$ is greater then $\frac{\Delta I}{\Delta V}$ value, than the PV module operates at the right side of the MPP in the P-V curve [29, 31]. Figure 4.2 represents the flow chart of the conventional Inc.Cond MPPT technique. Here V and I is the voltage and current of the PV module.

$$\frac{dI}{dV} = -\frac{I}{V} \tag{4.1}$$

$$\frac{dI}{dV} > -\frac{I}{V} \tag{4.2}$$

$$\frac{dI}{dV} < -\frac{I}{V} \tag{4.3}$$
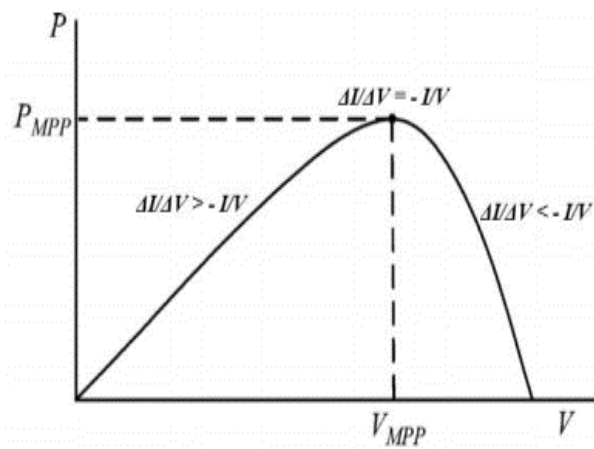
FIGURE 4.1: P-V curve related to Inc.Cond MPPT Algorithm
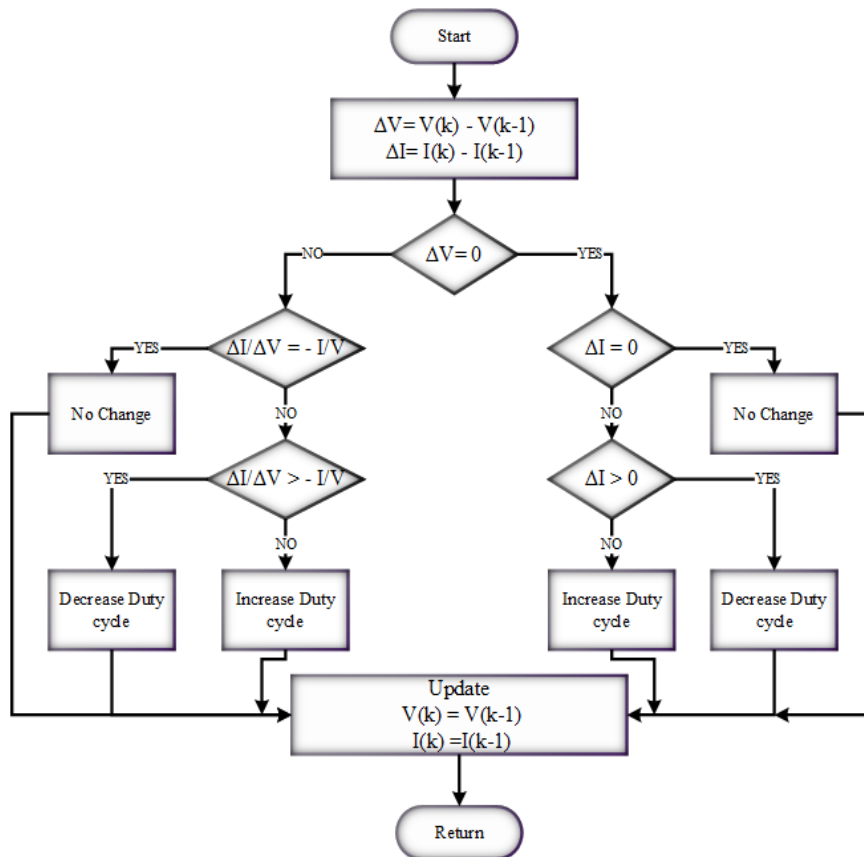
FIGURE 4.2: Flow chart of the Conventional Inc.Cond technique[21]

If eq 4.1 is fulfill, then the controller keep the reference voltage unchange and fixed the duty cycle untill the condition is not true. When eq 4.2 is achieve, then the duty cycle must be increase in order to reach at MPP point and operate the PV module at its max. effectiveness. But when eq 4.3 is satisfied, then opposite step is taken. Here duty cycle is reduced to get the MPP point at P-V curve.

A irradiance signal is used to determine the transient response against high and low irradiance level which is shown in figure 4.3. The irradaince signal is change from 1000 W/m² to 400 W/m² and temperature is fix at 25 ℃. Using this kind of siganl it is easy to observe the behaviour of the each modified Inc.Cond algorithm under two sudden change in irradaince level. The rise and settling time against 1000 W/m² and 400 W/m² for Inc.Cond techniques is extracting using the irradiance signal presented in figure 4.3. This irradaince signal is given to each modified Inc.Cond algorithm to test their transient response against to different irradaince levels.
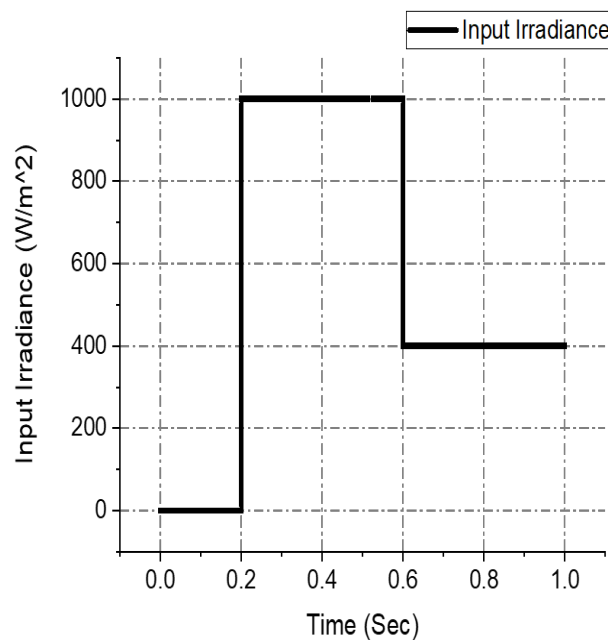
FIGURE 4.3: Input irradiance siganl level at 1000 W/m² and 400 W/m²

The above irradiance signal is given to traditional Inc.Cond MPPT algorithm. Figure 4.4 shows the response of the traditional Inc.Cond MPPT algorithm. The time is taken by this technique to achieve the MPP point is 0.03 sec with a settling time of 0.098 sec.

However, the oscillations around MPP are zero. But as the irradiance value reduces to 400 W/m², the basic Inc.Cond method is not able to extract the max. power and stable at 348.16-watt value with rising and settling time equal to 0.046 sec. The over-shoots are occur when irradiance shift its level.
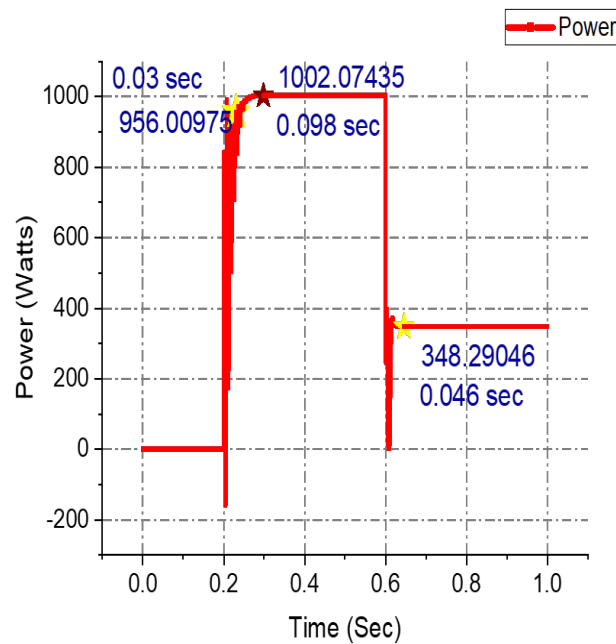
FIGURE 4.4: Transient response of traditional Inc.Cond against 1000 W/m^2 and 400 W/m^2 irradiance level

It can be observe from figure 4.4 that basic Inc.Cond MPPT can work better under the constant value of irradiance with better tracking efficiency. Detail discussion and result related to basic Inc.Cond algorithm is mention in next coming chapter.. So that is why we need to make improvements in the basic Inc.Cond algorithm to perform better under rapidly changing irradiance.

4.2.1 Drawback of Conventional Inc.Cond Algorithm

The main disadvantage of this technique is it can lose its path from true MPP point during the rapid change in sun irradiance. In the case of constant irradiance, the step-change generated by the method can track the MPP accurately due to the change being only instantaneous.

But when irradiance change continuously, the P-V curve also change with irradiance value and the technique is not able to determine the swap in power. It occcurs due to its own perturb in reference voltage. The zero slope condition rarely reached, and the traditional Inc.Cond got confused during the increasing sun irradiance level[25, 29].

4.3 Variable Step-size Based-on Variable Scaling Factor (VSS-VSF) Inc.Cond MPPT Algorithm

4.3.1 Varying Step-Size (VSS) Inc.Cond Algorithm

Step size affects the performance of the MPPT in two ways oscillations and response time. If larger the step size then faster the response time. if the step size is small then the response time is slow. The second is the oscillation around the MPP point, oscillations are occur due to the value of the step size. A Varying-Step size Inc.Cond method is compared with the Varying Step size based on Variable Scaling Factor (VSS-VSF) Inc.Cond technique in [28]. The step size and duty cycle is calculated for varying step-size by the following equations:

$$Step = \ N \times abs\left(\frac{\Delta \text{P}}{\Delta \text{V}}\right) \qquad (4.4)$$

$$D_K = \ D_{(K-1)} \pm \ step \qquad (4.5)$$

Where, D_K and $D_{(K-1)}$ are current and previous duty cycle of the converter respectively. N is the fixed scaling factor and ΔP is a change in power and ΔV is a change in voltage.

4.3.2 Drawback of Fixed Scaling Factor

N=0.005 is a constant which is used the form a reasonable step size because the ratio of the ΔP/ΔV may be very small. If the step size is small then the response time of the algorithm is slow with less no. of oscillation. If "N" is large the response time is fast but it leads towards the unwanted oscillations at the MPP point [31].
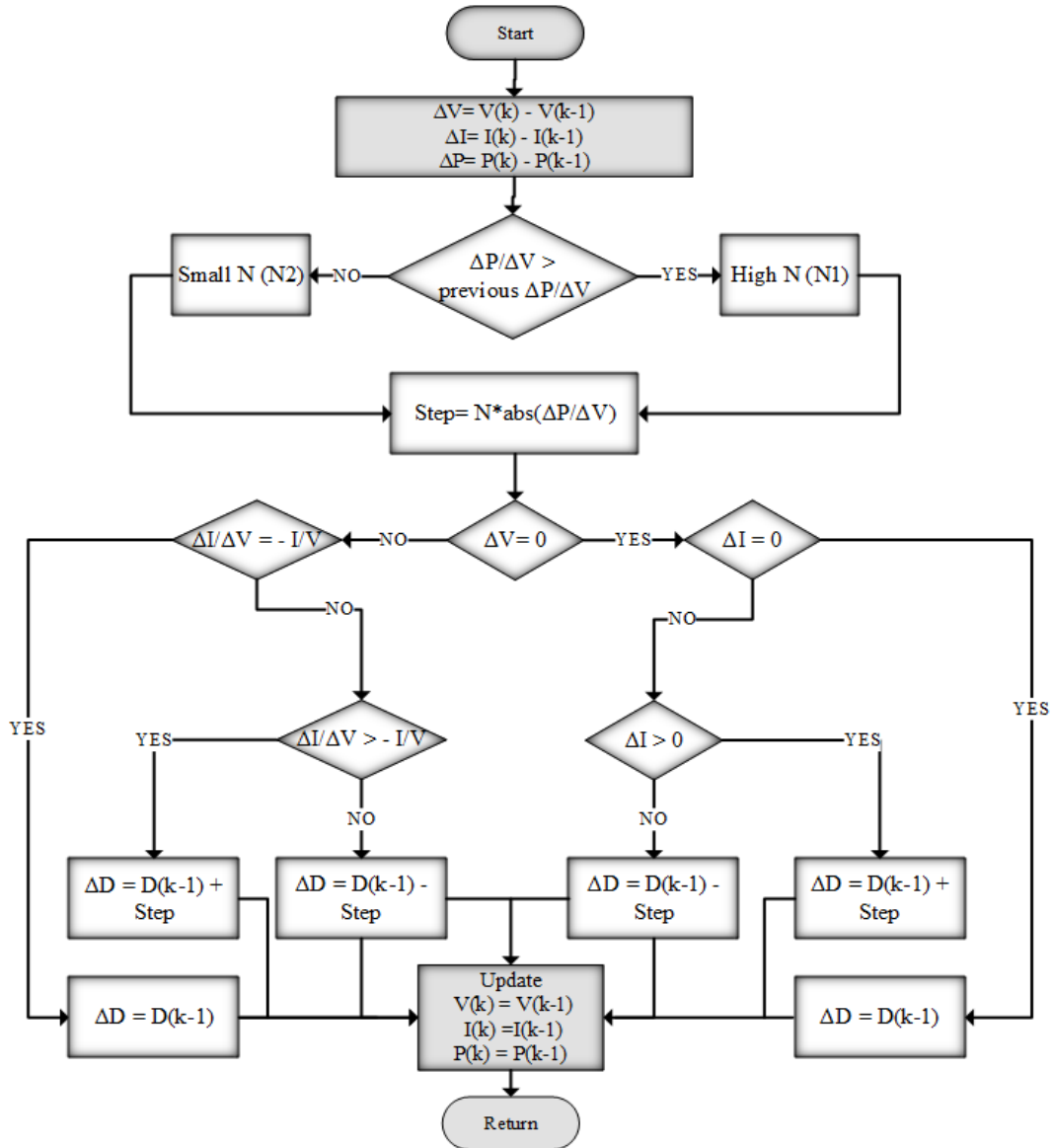
FIGURE 4.5: Flow process diagram of the VSS-VSF Inc.Cond technique [28]

4.3.3   VSS-VSF Inc.Cond MPPT Algorithm

To reduce the trade-off between steady-state oscillation and response time, instead of a fixed scaling factor, a step size based on a varying scaling factor is proposed in [28]. The only difference is the selection of the "N" scaling factor for calculating the step size. Now the step size is calculated by the same eq 4.5, but the scaling factor is variable which is chosen by the analysis of the $\Delta P/\Delta V$ slope value.

If the value $\Delta P/\Delta V$ is greater than the previous $\Delta P/\Delta V$ then, the algorithm assumes that the MPP point is far away. Thus the higher value of "N1=0.01" is
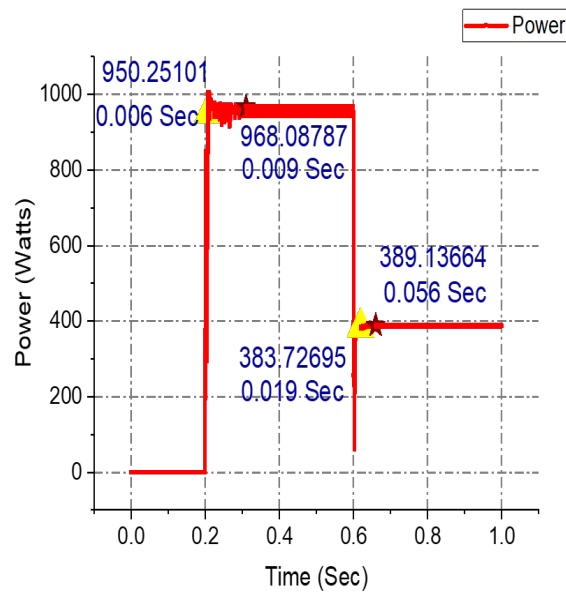
FIGURE 4.6: Power response of the Variable Step size based on Variable Scaling Factor Inc.Cond at 1000 W/m^2 and 400 W/m^2

selected and if not then the algorithm considered that MPP point is near so small value of "N2=0.005" is chosen. Figure 4.5 shows the diagram of the VSS-VSF Inc.Cond algorithm.

The basic difference between VSS and VSS-VSF MPPT techniques is that VSS uses a fixed "N" value while VSS-VSF adopted a combination of a large and small value of "N" which is also called the multiple. This varying value of "N" is high at the start and small when the slope is reduced. The purpose of this is to increase the efficiency by reducing the oscillations at a steady-state point.

A irradiance signal is used to determine the transient response against high and low irradiance level which is shown in figure 4.3. With the use of the proper tuning parameter N1=0.01 and N2=0.06 for the VSS-VSF Inc.Cond algorithm. It reduces the oscillations against 1000 W/m^2 and the power capture is about 965 watts. For the 400 W/m^2, the oscillations are fewer and the power is about 386 Watts.

The transient time response is 0.006 sec and 0.0198 sec and the settling time is 0.109 sec and 0.056 sec as shown in figure 4.6 against the 1000 W/m^2 and 400 W/m^2 irradiance value. The thing worth mentioning is that, if the value of N1 and N2 is large, the oscillations are large and the rising time is slightly increased.

Also, the optimal value of N1 and N2 has some trade-offs between oscillations, rise time, and the power execration against 1000 W/m² and 400 W/m². So, to avoid the oscillations proper values of N1 and N2 are used in this thesis work.

4.4 New Advanced Variable Step-Size Based (NAVSS) Inc.Cond MPPT Algorithm

The solar irradiance is not constant throughout the day so every MPPT technique must be able to track accurately during a rapid change in solar irradiance. As mentioned in [28] the fixed step has slow response time and oscillations at MPP point, and struggle during under fast-changing irradiance.

To mitigate the above problem, a new advanced variable step (NAVSS) size Inc.Cond algorithm is presented in [29]. The NAVSS Inc.Cond introduced the new strategy to detect the change in solar irradiance. It uses the change of current ΔI with a change of voltage ΔV of the PV module, instead of slope $\Delta P/\Delta V$ of the P-V curve.Because when irradiance is change, then both the voltage and current of the PV array is change.

Using the eq 4.6 the step size is calculated by NAVSS Inc.Cond. The NAVSS MPPT method is executed with a Flyback DC-DC converter to improve the efficiency of the PV system. This topology of the converter deliver isolation between output side and input side and operates over a wide range of input voltage variations.

$$D_K = D_{(K-1)} \pm N \times |\frac{\Delta P}{\Delta V - \Delta I}| \tag{4.6}$$

Where D_K and D_{k-1} are the converter duty-cycle at time K and previous instant K − 1 respectively. N is the scaling factor which is adjusted manually, and it is equal to 0.001. This constant may be adjust according to the requirements or by hit and trial method. After computing the absolute of $\frac{\Delta P}{\Delta V - \Delta I}$ finally, the step size

FIGURE 4.7: Flowchart of the NAVSS Inc.Cond MPPT Algorithm [29]

is determined. ΔP, ΔV, and ΔI are the change in power, voltage, and current respectively. Eq 4.6 is the only instruction that is additional in the conventional Inc.Cond algorithm and the rest of the algorithm is the same. Figure 4.7 shows the implemented MPPT technique in [29].

A irradiance signal is used to determine the transient response against high and low irradiance level which is shown in figure 4.3. Figure 4.8 shows the transient time response of the new advance variable step size (NAVSS) Inc.Cond algorithm. This algorithm produce the oscillations against the high irradaince level 1000 W/m^2 with response time of 0.0068 sec. These oscillations occurs due to random value of absolute of $\frac{\Delta P}{\Delta V - \Delta I}$. As irradiance level is reduce to 400 W/m^2 the oscillations are minimum between 7 to 10 watts. The response time against low irradaince level is 0.0062 sec. It stable at 390 watts in 0.066 sec. The proper selection of scaling

FIGURE 4.8: Transient time and Power response of the new advance variable step size (NAVSS) Inc.Cond algorithm

factor N is 0.011, and duty-max is 0.49 to keep the duty cycle in limit. By using these parameters the oscillations generated against high and low irradaince level are minimum.

The program starts with the initial setting of step size and notice the swap in current and voltage. If it determine any change the step size is updated by eq 4.6. All previous Inc.Cond algorithms work on the same procedure but the difference is the calculation of step size for the converters duty cycle.

The drawback of this method is that it may have oscillations due to random value result of ΔV - ΔI in computation of the setp size. Second is the use of flyback converter which increase the number of components used in hardward as result the cost of the MPPT controller is increased.

4.5 Modified Inc.Cond Algorithm during Fast-changing Solar Irradiance

When solar irradiance changes it affects the output power of the Solar cell. Current and voltage both are change when solar irradiance increases or decrease. Due to

this MPP point drifting away if the wrong step size added or subtracted from the duty cycle. To handle this issue, with some variation in conventional Inc.Cond a new enhanced Inc.Cond MPPT method for fast-varying weather conditions was presented in [33]. In this paper, two major parameters for the Inc.Cond algorithm are explained and how they affect the tracking efficiency of the algorithm (a) Perturbation time and (b) step size.

For drift avoidance in maximum power-point tracking, the algorithm uses the below equation;

$$(\Delta V > 0)\&\&(\Delta I > 0) \tag{4.7}$$

Where ΔV and ΔI are the change in voltage and current of the PV array respectively.

Figure 4.9 shows the step involved in the modified Inc.Cond algorithm [33]. As irradiance change suddenly the ratio of the derivative of the current and voltage $\Delta I \Delta V$ become positive value. This happened in the conventional Inc.Cond algorithm. And it reduces the duty cycle of the converter to increase the PV array voltage. As result the operating point drifts away from the MPP point.

The execution of eq 4.7 with conventional Inc.Cond algorithm continuously checks the sign of ΔV and ΔI wherever solar irradiance changes its value. If the ΔV and ΔI both are positive then the algorithm should increase the duty cycle for the reduction of the PV array voltage for operating the PV array at MPP. Both ΔV and ΔI is monitor at the same time for identify the change in irradiance level.

For this technique, only perturbation step size 0.04 is given. In this thesis work, using give step size with other tuning parameters is selected for the proper working of the algorithm. The parameters are delta-in, step size, and duty-max, they are equal to 225e^{-6}, 0.04, and 0.48 respectively. In figure 4.10 when the irradiance level reaches 1000 W/m^2 then, the transient response is 0.0077 sec, and the settling time is 0.0593 sec with zero oscillations at 1004 watts. With the drop in irradiance level
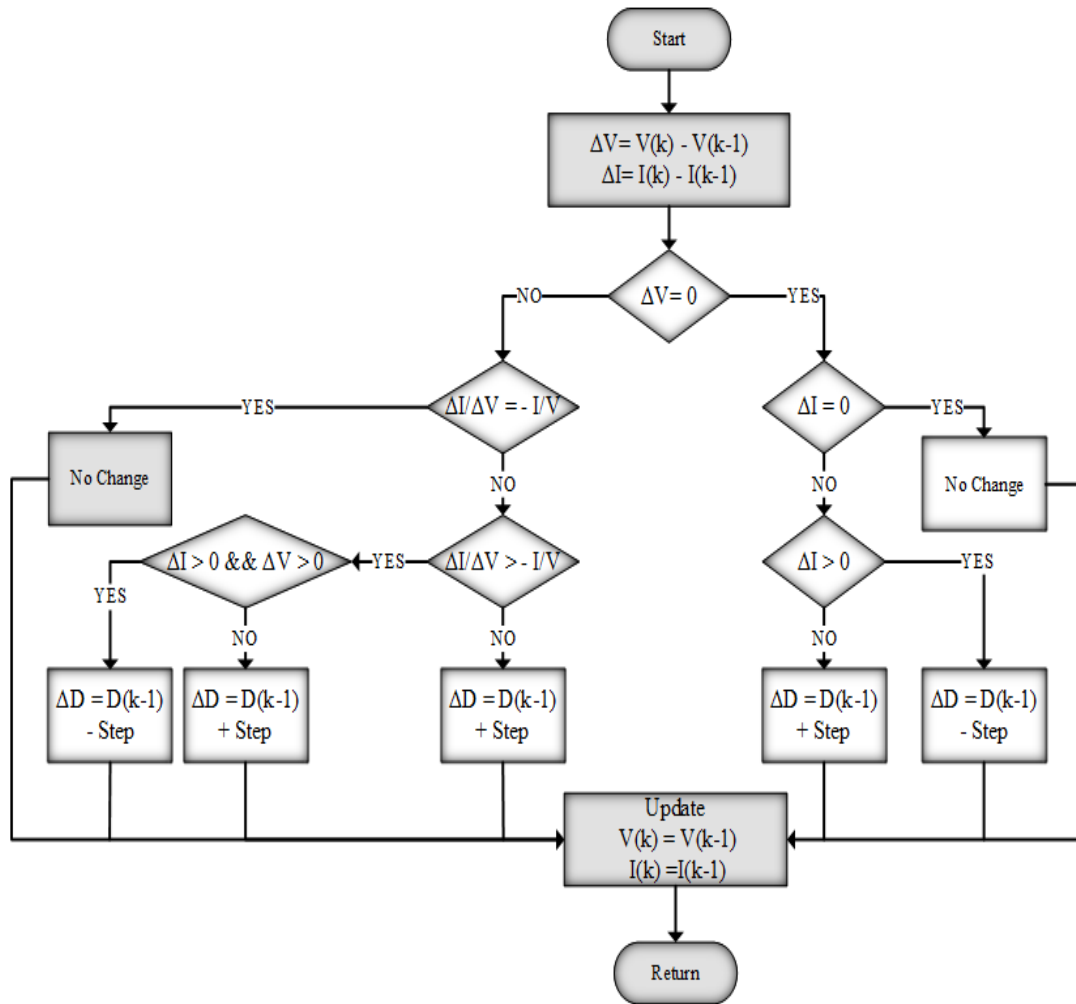
FIGURE 4.9: Step involved in Modified Inc.Cond algorithm [33]

to 400 W/m^2, the rising and settling time is 0.037 sec and 0.099 sec respectively, and it is stable at 384.1 watts value. So, it can be observe from figure 4.10, this algorithm is perform better in both high and low irradance level. Due to no oscillations at steady state the efficiency of this technique is better from others.

4.6 Modified Inc.Cond Algorithm for Fast Varying Solar Irradiance

New tracking instructions are presented for the identification of changes in solar radiations in [34]. This technique is the same as mentioned in [31], the only difference is the permitted error. It uses the derivatives of current ΔI and voltage
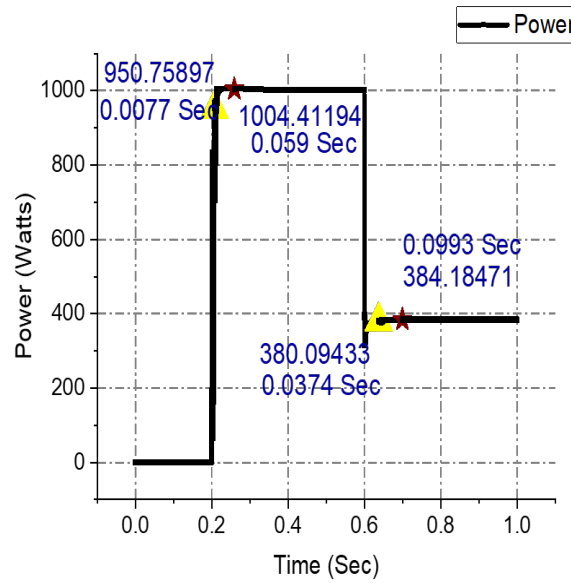
FIGURE 4.10: MPPT response of Modified Inc.Cond algorithm for fast-changing irradiance levels

ΔV value of the PV array to find the increment in solar irradiance instead of the slope ΔP/ΔV of the P-V curve. The same permitted error equation is given below but the constant value of error is change:

$$|\frac{I}{V} + \frac{\Delta I}{\Delta V}| < 0.07 \tag{4.8}$$

Where ΔI and ΔV are the change in current and voltage respectively. I and V are the instantaneous value of the current and voltage of the PV module.

The algorithm assumes that the permitted error is equal to 0.07. With the use of the permitted error equation, this technique also used another instruction set to identify any variation in current and voltage of the PV module by checking ΔI and ΔV at the same instant.

$$(\Delta V > 0)\&\&(\Delta I > 0) \tag{4.9}$$

Where ΔI and ΔV are the derivatives of current and voltage respectively. Figure 4.11 shows the steps of the modified Inc.Cond mentioned in [34].
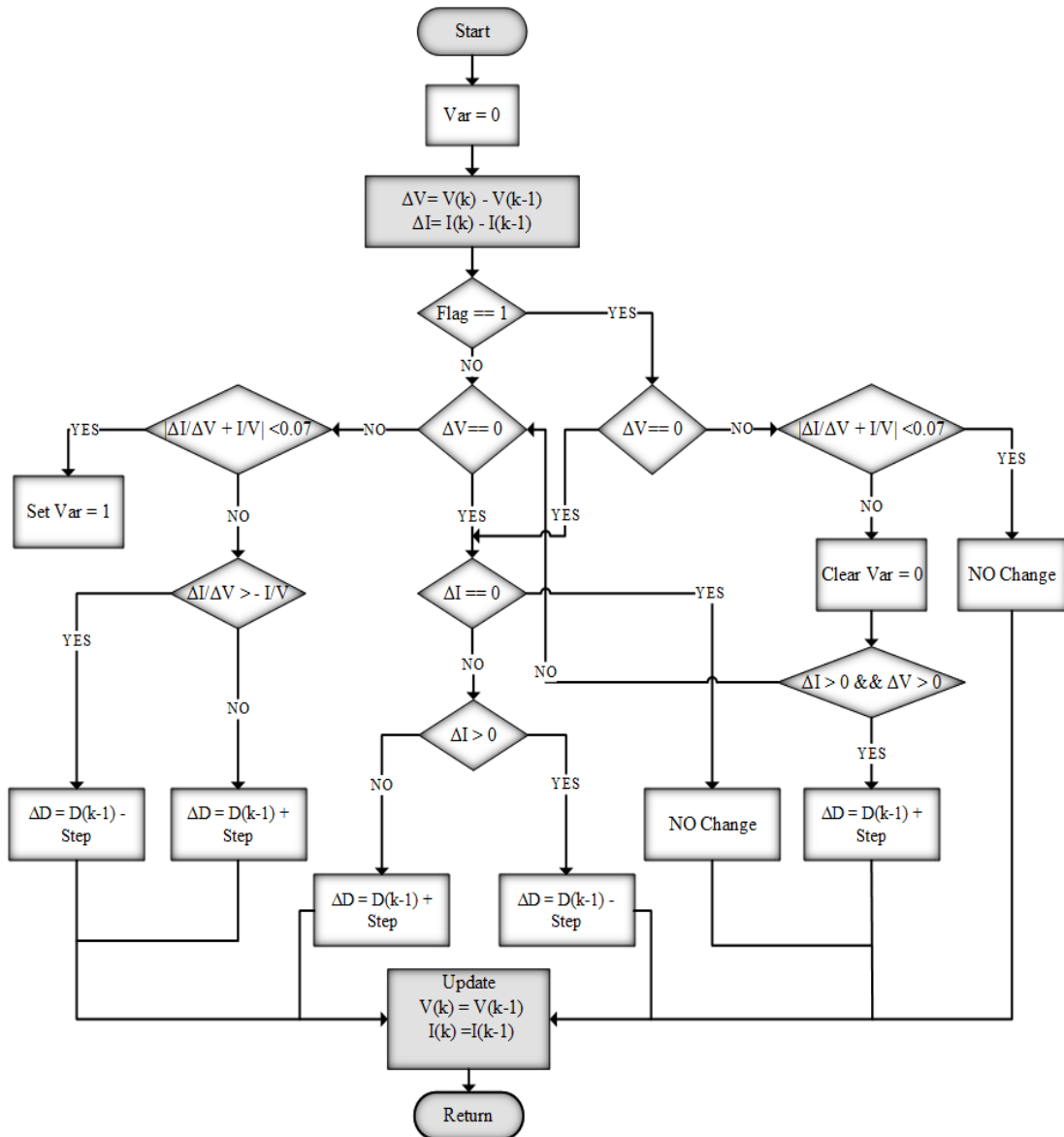
FIGURE 4.11: Flowchart diagram of modified Inc.Cond algorithm [34]

The presented [34] algorithm works on the same steps which are used in [31], to pin out the location of the MPP at the P-V curve this algorithm used the "Var" variable. Here If the MPP point was achieved by executing eq 4.8, then 1 is assigned to Var variable. This technique use the "Var" instead of "Flag" variable and the remaining instructions are the same as given in [31].

For the simulations of the technique, a suitable factor α must be selected. This factor represents the duty cycle value at which the MPP point is achieved. Figure 4.12 shows the power response of the modified Inc.Cond for fast-dynamic of irradiance. By using the α equal to 0.42 and the other parameters include the delta-in
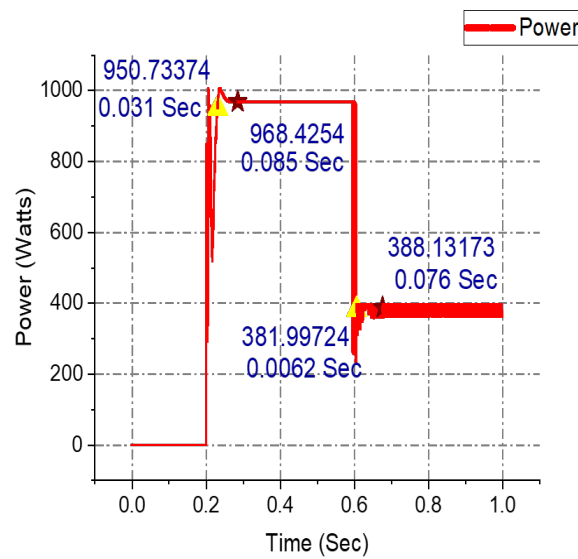
FIGURE 4.12: MPPT response of Modified Inc.Cond for fast-dynamic irradiance

and initial step size or delta-initial are $15e^{-6}$ and 0.008 respectively. The rise time against 1000 W/m^2 is the 0.031 sec, but the settling time at MPP is 0.0855 sec. The power extracted against 1000 W/m^2 is 968.4 watts with few oscillations of 3 watts only at the start but after settling the oscillations are zero.

However, in the case of 400 W/m^2 irradiance level, the power response is fast 0.0062 sec as it can be observed in figure 4.12. The oscillations are occur with peak to peak amplitude of 20 watts.

The thing worth mentioning here is that, by reducing the α value, the oscillations can be reduced when irradiance is increasing. And with more reducing the value of α cause wrong calculation of the duty cycle for the converter which leads to oscillations and causes large power loss. So, this algorithm performs better when solar irradiance is increasing and struggles when the irradiance is decreasing.

4.6.1 Drawback of Modified Inc.Cond Algorithm

The main drawback of this technique instructions is dependent on two or more other instructions as result, the complexity of understanding the algorithm is increased. Due to more instructions are used in this method the computational process is also increased.

4.7 An improved MPPT Control Strategy Based On Inc.Cond Algorithm

An improved control strategy based on the Inc.Cond MPPT algorithm is proposed in [35]. The conventional Inc.Cond algorithm struggle when solar irradiance increase. It calculates the gradient between two local MPP points of two different P-V curves at different irradiance values. When irradiance changes it produces the negative value of the gradient. As irradiance changes the voltage and current of the PV array will be affected correspondingly. So, the presented improved Inc.Cond in [35] use the below equation to calculate the instantaneous change of current and voltage.

$$[(\frac{\Delta V}{\Delta I}) \times (I + V)] = 0 \qquad (4.10)$$

$$[(\frac{\Delta V}{\Delta I}) \times (I + V)] > 0 \qquad (4.11)$$

Where ΔV and ΔI are the derivatives of the current and voltage respectively and I and V are the present value of the current and voltage of the PV module respectively. Figure 4.13 shows the flowchart diagram of an updated MPPT control strategy based on the Inc.Cond method.

The conventional Inc.Cond algorithm decides based on the current location of the system point of operation. But the improved control strategy based Inc.Cond algorithm makes decision-based on the direction of the Power, voltage, and current of the PV module.
If the system operates on the left side of the MPP and $\Delta V > 0$ then the duty cycle will increase in a positive direction of the previous step. And if $\Delta V < 0$ variations in voltage is negative then the duty cycle will decrease in the opposite direction of the previous step. Similarly, if the system is at the right side of the P-V curve, here if $\Delta V > 0$ is achieved the duty cycle is decreases in the direction

of the previous step and vice versa. This algorithm only judges the disturbance direction of the next point of working. Using this technique the tracking speed is increased by 20% - 30% as compared to the traditional Inc.Cond algorithm.
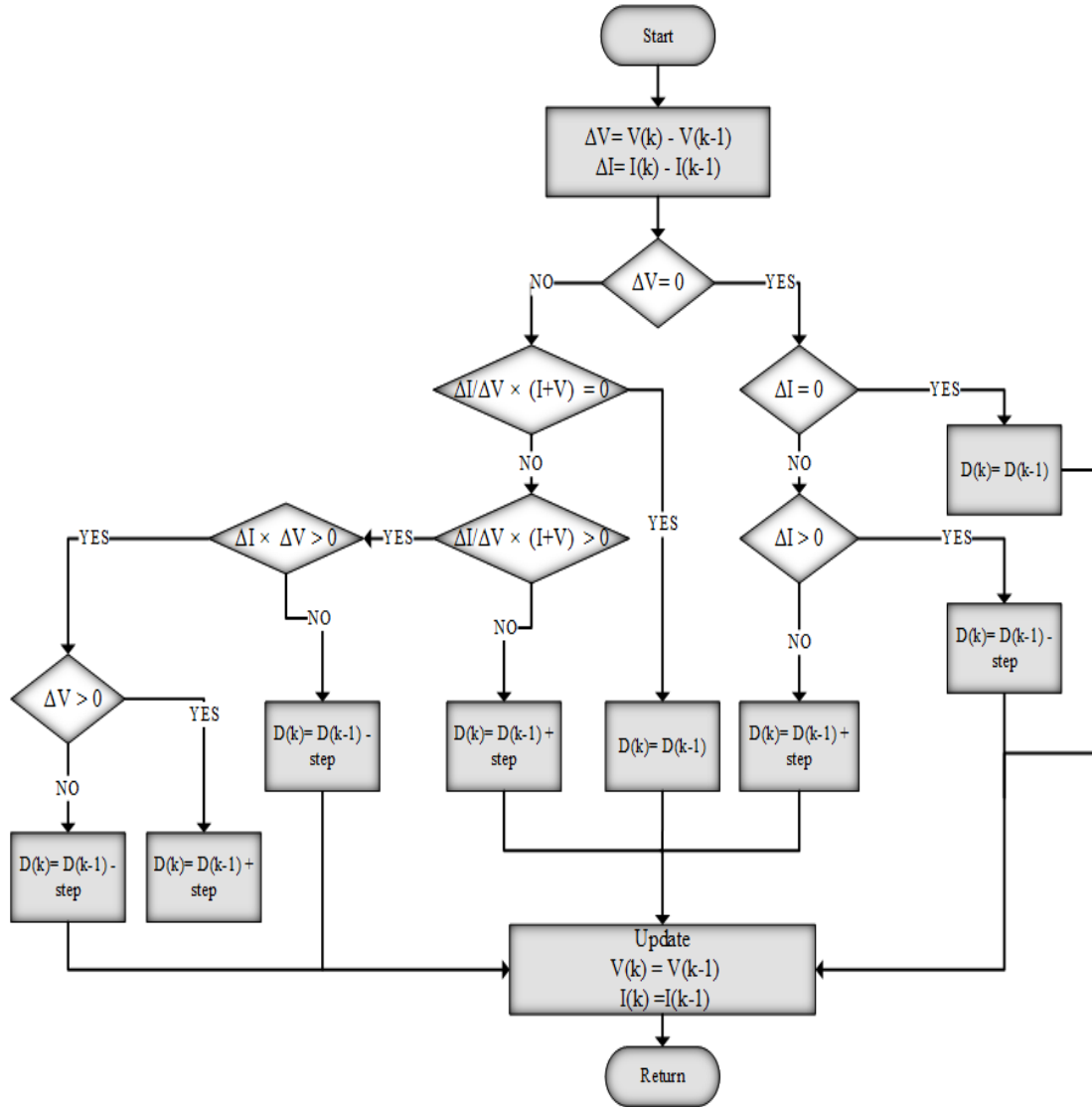
FIGURE 4.13: Flowchart diagram of an Improve MPPT Control Strategy based on Inc.Cond algorithm [35]

Figure 4.14 shows the MPPT response of an improved MPPT control strategy based on the Inc.Cond algorithm. No initial tuning parameters are given in [35]. So, the algorithm is simulated parameters including: duty-initial, duty-max, and delta-in and they are equal to 0.008, 0.52, and $225e^{-6}$ respectively.

The rising time against the 1000 W/m^2 is 0.043 sec, with settling time is about 0.0981 sec at 1001 watts. When the irradiance level drops to 400 W/m^2 the method
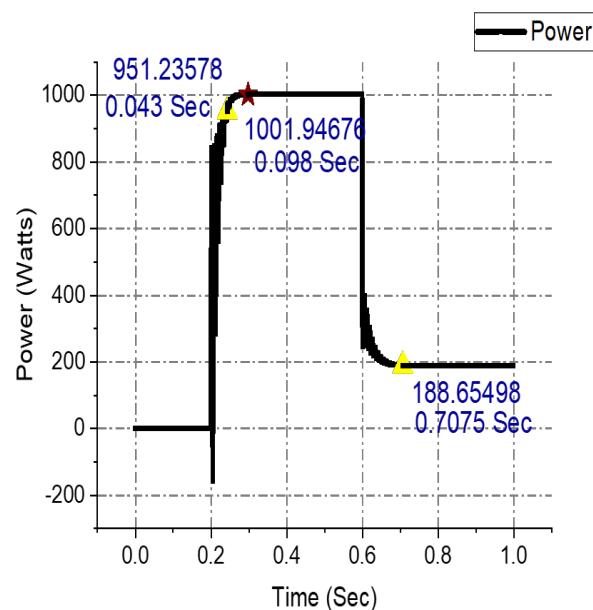
FIGURE 4.14: MPPT response of an Improved control strategy based on Inc.Cond under two different irradiance levels

is not able to extract max. power and settle at 188.5 watts in 0.0075 sec. So, this algorithm perform better during high irradiance level, but it struggle against low irradiance level.

4.7.1 Drawbacks of Improved MPPT Control Strategy Based On Inc.Cond Algorithm

The main drawback of this technique is that it takes a decision based on the only change in voltage ΔV of the PV module during the fluctuating solar irradiance. But when irradiance change it effect both current and voltage of the PV array.

The algorithms which are discussed above is simulated on the same Matlab-Simulink module which is mentioned in figure 4.15. Only controller programming block is different and each technique is simulated against mention parameter of the PV array and the boost converter to extract the result.
To determine the performance of each modified Inc.Cond technique, the performance criteria with input irradiance signal will be provided in the coming chapter. Details analysis and discussion on results are also given in next cahpter.
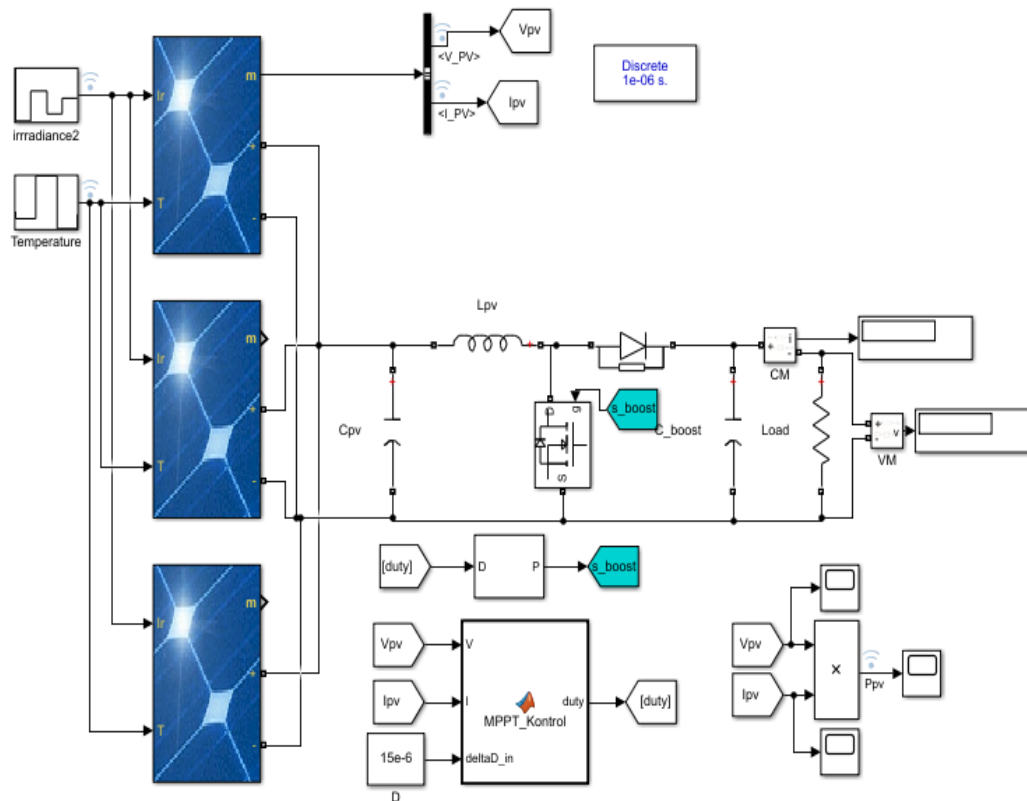
FIGURE 4.15: Overall Simulink Model of a PV System with PV array and MPPT Controller

4.8 Chapter Summary

This chapter comprises the explanation of the Conventional Inc.Cond algorithm and its variations using the Direct Control strategy with transient response of each algorithm. These transient response extracted against two different irradiance level 1000 W/m^2 and 400 W/m^2. At the start of this chapter, basic working of the Conventional Inc.Cond algorithm are explained and after that, all available variations in the literature of Inc.Cond using Direct Control strategy are explained in detail along with their flow chart diagram, main working concept, and equations that are used in tracking, and drawback of some techniques is also the part of this chapter. At the end of this chapter, the overall Matlab-Simulink model of the system that is used for comparing simulation results of all those techniques which are selected in this thesis work.

Chapter 5

Simulation Results and Discussion

This chapter contains the simulation result of basic and modified Inc.Cond MPPT algorithms based-on direct control. A matlab/simulink model is develop to extract the simulation results of modified Inc.Cond algorithm against the evaluation pattern. This chapter also include the test case which cover all condition of operations including the fast-changing solar irradiance at constant temperature. Five different irradiance level with varying temperature values are aslo use to check the response of each modified Inc.Cond technique.

Furthermore, a complete comparison analysis of five modified Inc.Cond techniques is also presented in this chapter. To make the comparison more authentic and close to realistic condition a fast dynamic irradaince signal is used to extract the voltage, current and power response for each Inc.Cond algorithm. To judge the performance under normal and fast changing irradaince level, eight performance testing parameters (PTP) are used in this thesis work [16, 22]. Simulation parameters are given in Table 5.1 which are used in this thesis work. Eight performance indices are listed below:

1. Rising time is extracted for the PV output power to reach 0% to 95% of the max. power value.

2. Settling time is required for the PV output power to settle within 1% of the reached power value.

3. Tracking accuracy is calculated by $(Pavg)/(Preal)$ at MPP dividing average simulated power with real MPP power against fast-changing irradiance.

4. Exact fast MPP detection during a continuous change in irradiance.

5. Oscillation at the steady-state point.

6. Efficiency is calculated by $(Preal)/(Pavg)$ at MPP real MPP power value is divided by average simulated power against fast-changing irradiance.

7. Complexity.

8. Length of the proposed algorithm compared to basic Inc.Cond

Parameters which are used to extract the simulation results of each modified Inc-Cond algorithms are given in Table 5.1.

TABLE 5.1: Simulated tuning parameters for modified Inc.Cond MPPT algorithms

Sr.no	Description	Parameters				Note
		Delta-in	Delta-initial/step-size	Duty-max	Step-size	
1	VSS-VSF	225e-6	0.08	0.48	N1=0.02, N2=0.09	Denoted as method 1
2	NAVSS	115e-6	0.08	0.49	N=0.011	Denoted as method 2
3	Modified - 1	325e-6	0.08	0.51	N/A	Denoted as method 3
4	Modified - 2	15e-6	0.008	α=0.42	N/A	Denoted as method 4
5	Improved	225e-6	0.008 or 0.08	0.52 or 0.38	N/A	Denoted as method 5

5.1 Simulation Model

The matlab/Simulink platform is used to simulation each modified Inc.Cond technique. The matlab PV system model is develop by using three the PV modules in parallel. These PV modules connected in parallel to meet the current requirements and generate the specific value of voltage. The total power of the PV array is 1005 watts. The PV array input is irradiance and temperature signal. The

second main element of the simulink model is the DC/DC boost converter which energized the DC-bus or load. load rating is 20 ohm's which is used for extracting the simulation results. The third section is MPPT controller. The controller section has an MPPT algorithm implemented in it. The input of the controller is voltage and current of the PV array and its output is the optimal duty cycle. Using this optimum duty cycle the system works at the its maximum efficiency point all the time.
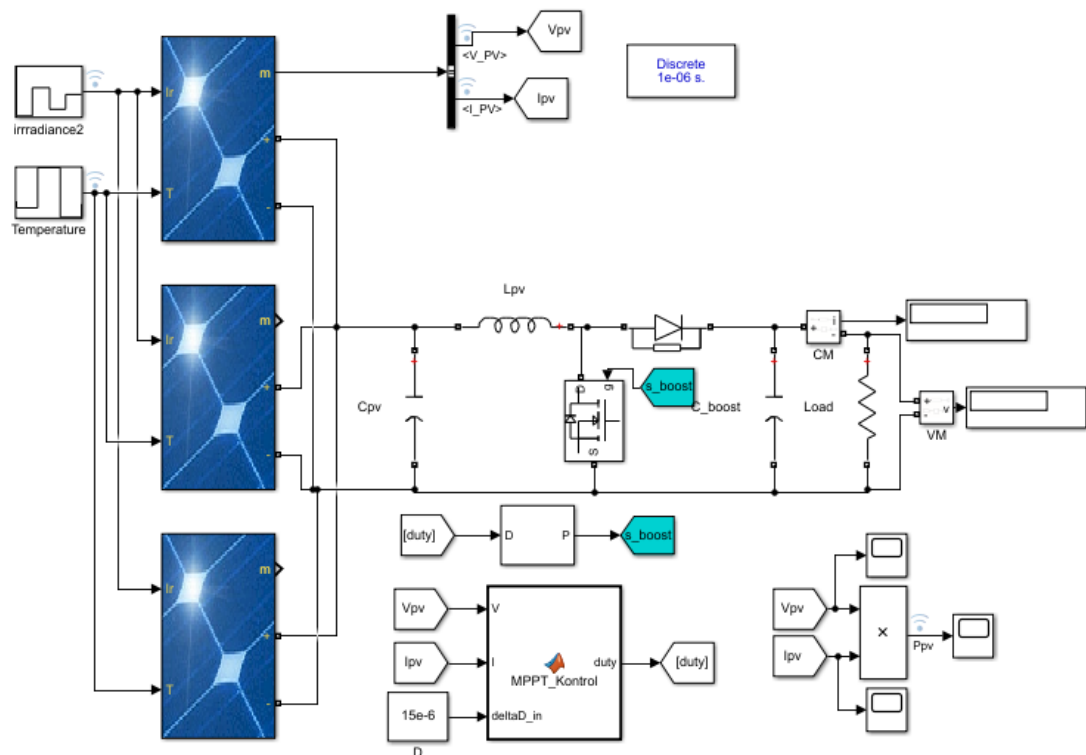
FIGURE 5.1: Matlab/Simulink model of a PV System used for simulations

All five modified Inc.Cond algorithms are simulates on the same matlab/simulink model which is presented in figure 5.1. Each technique is simulated against the evaluation pattern. The evaluation pattern have two cases, first one is the rapidly-changing irradiance signal with constant temperature values.

Second case is varying temperature value with five different irradiance levels signal. Second case is only used to examine the behaviour of the modified IncCond under high temperature with high and low irradiance levels. Complete design parameters of a boost converter and a PV system are mentioned in Table 3.1 and 3.2 in chapter 3.

5.2 Simulation using Evaluation Pattern

The evaluations pattern is selected to examine the performance of different modified Inc.Cond algorithm under more realistic weather conditions. In this evaluation pattern solar panels are subjected to extreme fluctuating irradiance signal. Because using this kind of signal no simulation results are extracted with modified Inc.Cond technique.

There are two cases of this evaluation pattern: first case is using fast dynamic irradiance signal at constant temperature and second case is varying temperature with five different irradiance levels signal.

Case 1:

In case 1 of evaluation pattern, a rapid fluctuating irradaince signal at constant temperature value is given to the matlab/simulink model of the PV system. This signal is selected to determine the behaviour of current, voltage and power of the PV array using modified Inc.Cond techniques implemented in MPPT controller as a algorithm. The fast fluctuation irradiance signal with constant temperature is shown is figure figure 5.2.
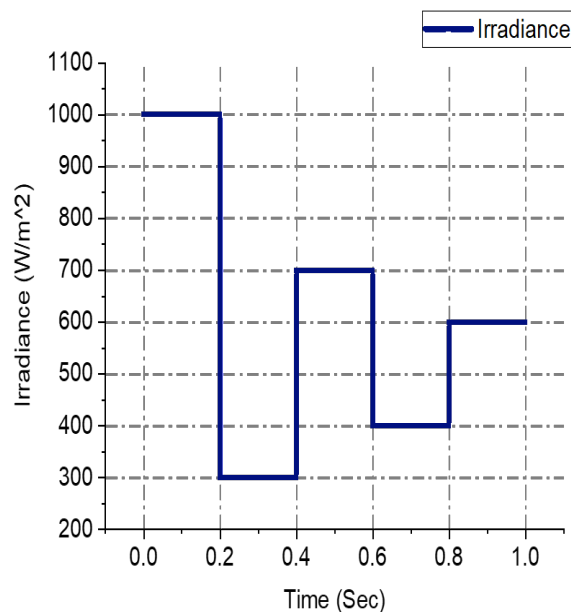
FIGURE 5.2: Input Irradiance response for PV system at 25 ℃ in case 1
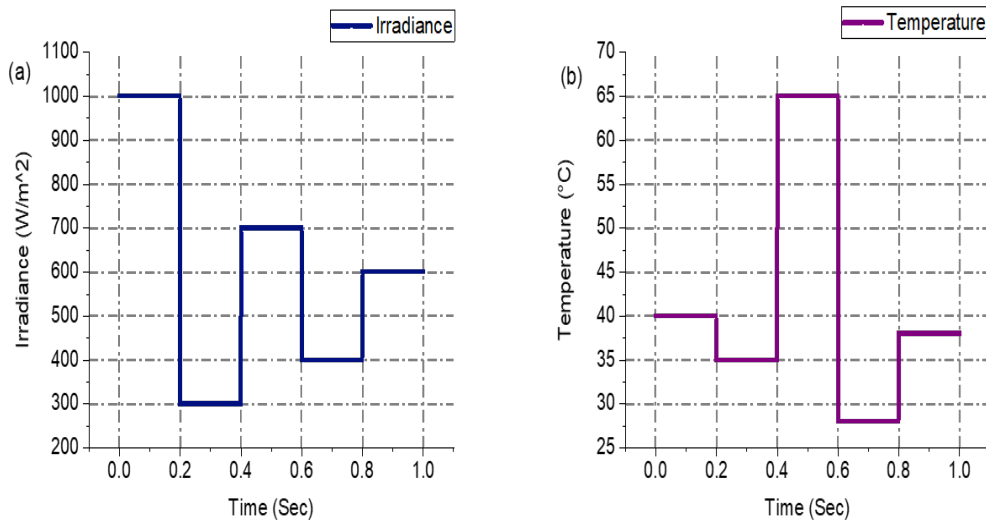
FIGURE 5.3: Five different Irradaince and varying Temperature levels for PV system in case 2

The input irradiance signal is change from low to high and high to low irraadiance level. The irradiance value is the starts from 1000 W/m² and then change to 300 W/m², 700 W/m², 400 W/m² and 600 W/m² in zero to one sec time and temperature is fixed at 25 ℃ for the first simulation case. Same irradaince signal is give to each modified Inc.Cond technique to examine their response power, current and voltage under fast dynamic irradiance.

Case 2:

In this case a varying temperature signal is used to examine the performance of each modified Inc.Cond under normal and high temperature. Because tempera-ture effect the generated power of the PV array. The purpose of using varying temperature value is just observe the response of the PV array current, voltage and power. To keep the simulation results synchronize same irradiance signal is used. In reality temperature is not change rapidly but in this thesis work just to examine the effect of different temperature value on PV array output.

The irradiance signal and varying temperature signal is shown in figure 5.3. For this case, we assume that simulations time is divided in to five time intervals in which irradaince and temperature value is constant. Figure 5.3a show the five different irradaince levels and in each time interval irradaince is constant and not

related to fast chnaging irradaince level. Figure 5.3b represent the five different temperature levels.

The temperature values varying from 25 ℃ to 65 ℃. The irradiance signal is same and the variations in temperature starts from 40 ℃ to 35 ℃ consider as high temperature. 65 ℃ is the highest temperature which a PV cell can reach and 28 ℃ is the normal temperature for a PV cell, and then 38 ℃ is the lest temperature level used in this case.

5.2.1   Traditional Inc.Cond MPPT Algorithm

The basic Inc.Cond is simulated against the two different cases which are explain in previous heading. The result against these two cases are discuss below.

Case 1:

In this case, the irradiance signal in figure 5.2 is given to the whole PV array, and the temperature is constant at 25 ℃. The V_{MPP} is changing between 41.5 V to 40.4 V. The fixed irradiance starts from 0 to 0.2 sec, after some fluctuations the V_{pv} reaches the Vmpp 41.5V. It can be observed from figure 5.4a that as fast-dynamic irradiance occurs from 0.2 to 1 sec, the V_{pv} starts decreasing.

For low irradiance the V_{pv} is 13 V which is far away from V_{MPP} and for high irradiance it almost near to 31 V. Oscillations against dynamic irradiances is large at the start but oscillations are zero when V_{pv} is settled to its maximum value against each irradiance levels.

From figure 5.4b during the constant irradiance or at the start the current of the PV Array is fluctuating almost at 27.5A. It settles at I_{MPP} which is 24.21 A with no oscillations. With the start of dynamic irradiance from 0.2 sec, the current of PV Array is also decreasing but near to its I_{MPP} value in each irradiance level. From 0.2 to 0.4 sec the current is decreasing and it reaches the 6.2A.

As irradiance increase from 0.4sec to 0.6sec the current is increasing and settle at 18 A. From 0.6 sec to 0.8 sec the current is again decreasing and reaches at 10.1

FIGURE 5.4: PV array output response of (a) voltage, (b) current and (c) power of the basic Inc.Cond technique against rapidly changing irradaince for case 1

A due to low irradaince. At the end, 0.8 sec to 1 sec the current is increasing and constant at 16.1 A.

At the start from 0 to 0.2sec, the Array Power P_{PV} is increasing and it reaches the Pmpp around 1002W which is noticed from figure 5.4c. During constant irradiance, no oscillations are occurs. As the dynamic irradiance form 0.2 sec, the power of the PV Array is also decreasing almost around 108W. From 0.4 to 0.6 sec the Ppv is increasing and it reaches the 547W and then from 0.6sec to 0.8sec the power P_{PV} is decreasing due to voltage value V_{PV}. Here PV array power

settles at almost 195W. From 0.8 sec to 1 sec the power is now increasing because the voltages are also increasing and the power is constant at 410W. Traditional Inc.Cond method perform better in gradually increasing and decreasing irradiance due to the step-size of 0.02. But when solar irradiance swap quickly between high and low level, it struggle to extract the max. power from PV Array.

Case 2:

In this case, the same irradiance signal is given to the whole PV array, but the temperature is now varying shown in figure 5.3. The dynamic irradiance starts from 0.2 sec to 1 sec with a temperature of 45 ℃ at the start. The voltage of the PV system V_{PV} is not at V_{MPP} point against each irradiance level.

For high irradiance at high temperature, the V_{PV} is greater than its V_{MPP} value almost around 45V to 43V. When irradiance level is low and also the temperature is low the V_{PV} of the PV Array is 1V or 2V less the Vmpp voltage of the PV Array. Oscillations are occurring at the time when irradiance changes its value. Figure 5.5a shows the voltage response of the PV Array at varying temperatures with fast-dynamic irradiance.

The temperature will affect the performance of the PV Array. From figure 5.5b it can be observed that temperature values limit the output current of the PV Array. At high irradiance with a temperature value between 40 ℃ to 45 ℃ the current is between 8A to 7.1A which is very less than the I_{MPP} of the PV Array. For low irradiance with temperature between 28 ℃ to 36 ℃ the current Ipv is between 7.3A to 7.8A.

A high temperature that a PV cell can reach is 65 ℃ at this temperature with irradiance level is 700W/m^2 the I_{PV} is 7.11A. Fewer oscillations occur when the irradiance level is shifted. Over-shoot occurs in the current I_{PV} of the PV Array when both irradiance and temperature change their values. So, high temperatures have a negative effect on the current of the PV Array.

Power is the combination of the voltage and current value. The power P_{PV} of the PV Array is shown in figure 5.5c. The Ppv value is low against each irradiance
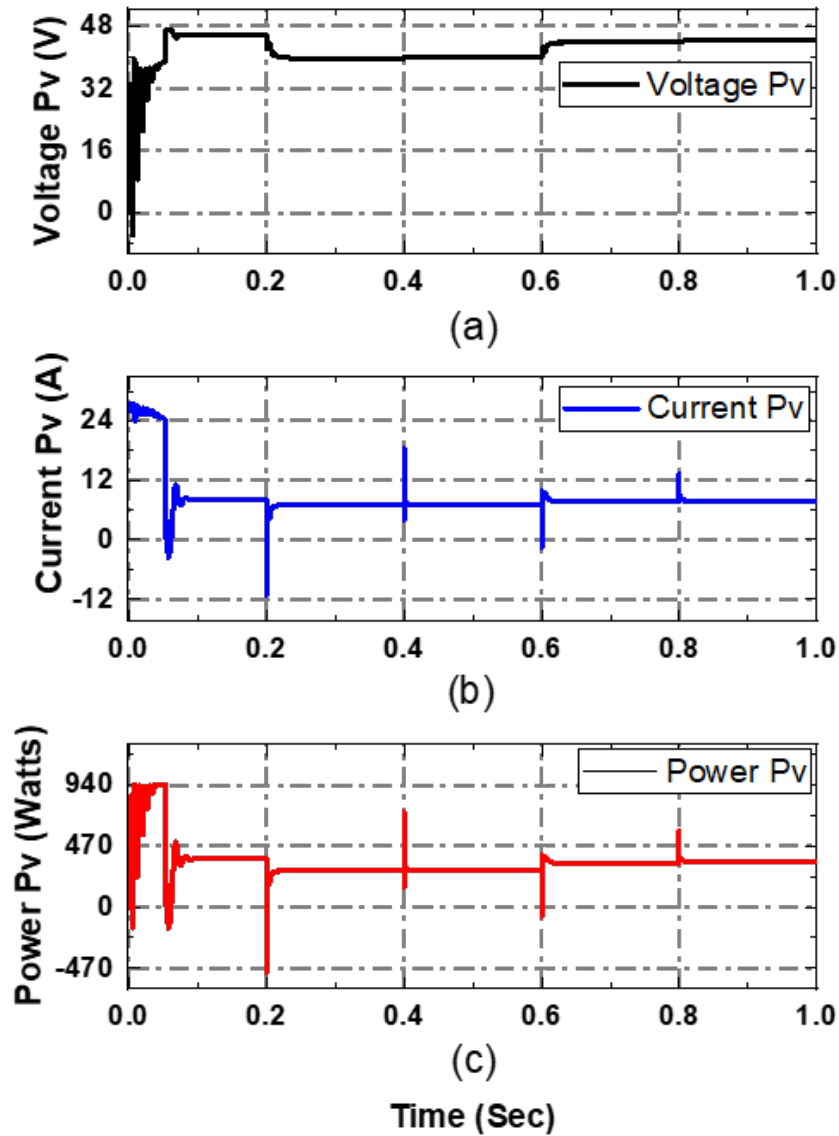
FIGURE 5.5: Tracking waveform of PV array (a) voltage, (b) current and (c) power of the basic Inc.Cond technique against varying temperature for case 2

value due to the high-temperature level. For high irradiance and temperature is around 40 ℃ to 45 ℃ the Ppv is between 285W to 375W. With the decrease in irradiance level and the temperature is 28 ℃ to 36 ℃ the P_{PV} is increasing and its value is between 280W to 345W.

Over-shoot occurs in P_{PV} of the PV Array due to fixed stepsize of 0.02 with delta-max is 0.40, when both irradiance and temperature change their values. The power P_{PV} is less due to the less generation of the current Ipv in each irradiance level caused by the high value of the temperature.

5.2.2 VSS-VSF Inc.Cond MPPT Algorithm

This technique work on two scaling factor N1 and N2 which is explain in detail along with its pros and cons in previous chapter.

Case 1:

In this case, the irradiance signal in figure 5.2 is given to the whole PV array, and the temperature is constant at 25 ℃. The Vpv is changing between 44V to 45.5V. The fixed irradiance starts from 0 to 0.2 sec, after some fluctuations the V_{PV} settles at 44V. But it can be observed from figure 5.6a that as fast-dynamic irradiance occurs from 0.2 to 1 sec, the V_{PV} starts increasing and limit between 44V to 40V.

For low irradiance, the V_{PV} is near to V_{MPP}, which is between 40.1V to 42.7V. For high irradiance, the V_{PV} of the PV Array is around 43.5V to 44V. Oscillations are large against the first low irradiance value but oscillations are fewer for the next coming irradiances level.

From figure 5.6b during the constant irradiance or at the start the current of the PV Array is fluctuating between 21.6A to 23A and it settles at 21.7A with oscillations. With the start of dynamic irradiance from 0.2 sec, the current of PV Array is decreasing but not near to I_{MPP} value in each irradiance level.

From 0.2 to 0.4 sec the current is decreasing and it reaches the 6.2 A. From 0.4sec to 0.6sec the current is increasing and settle at 15.5 A with oscillations. As irradiance decreasing from 0.6 sec to 0.8 sec the current is again decreasing and reaches at 9.23 A with fewer oscillations. From 0.8 sec to 1 sec the current is now increasing and constant at 13.2A.

At the start from 0 to 0.2sec, the array power Ppv is increasing and it reach at 971W. But with oscillations which is clearly observed from figure 5.6c. As the dynamic irradiance form 0.2 sec, the power of the PV Array is also decreasing almost around 294W and fewer oscillations dips are generated. From 0.4 to 0.6 sec the P_{PV} is increasing and it reaches the 677W. From 0.6sec to 0.8sec the power
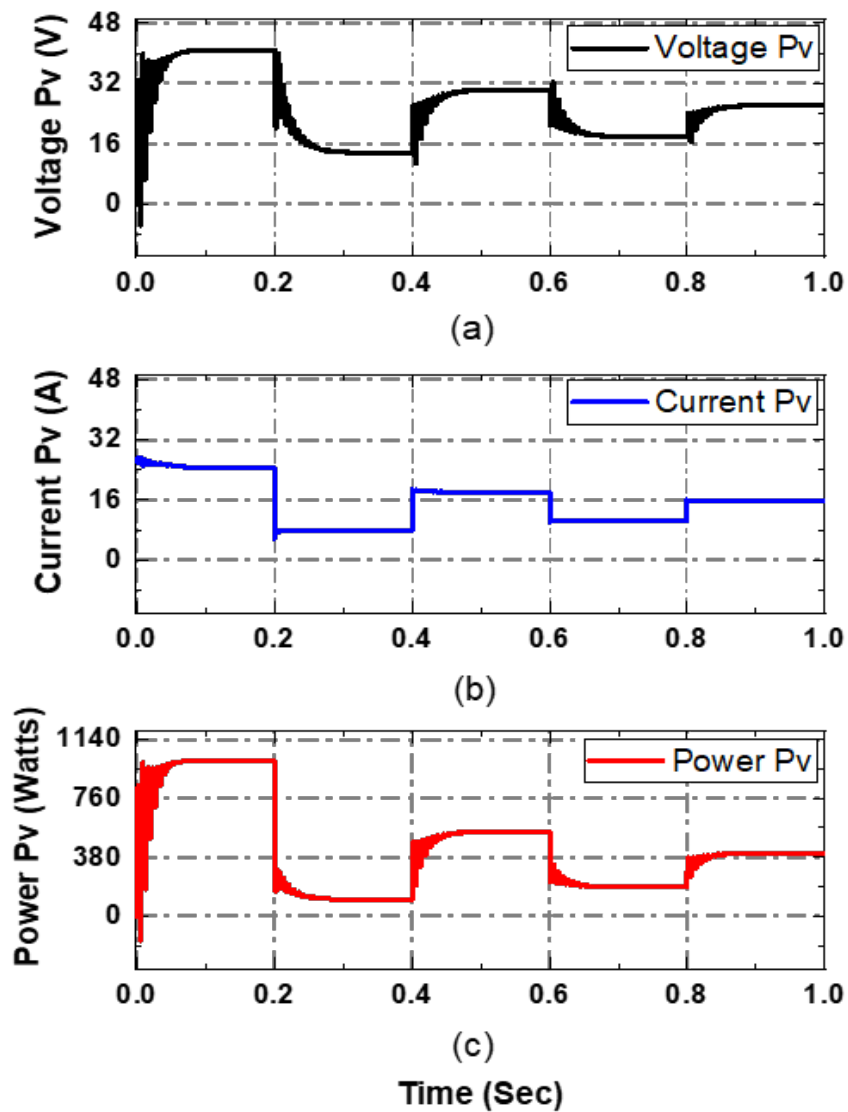
FIGURE 5.6: PV array output response of (a) voltage, (b) current and (c) power of VSS-VSF Inc.Cond technique against against fast-changing irradaince for case 1

P_{PV} is decreasing due to decrease in irradiance level, and at settle at almost 389W with zero oscillations. When irradiance change from 0.8 sec to 1 sec the power is now increasing with initial fewer oscillations and power is constant at 578W. The thing worth mentioning here is that the algorithm performs better, extraction available power is almost 90% with step-size is 0.08 with duty-max 0.48, and has fewer oscillations during low irradiance levels.

Case 2:

In this case, the same irradiance signal is given to the whole PV array, but the
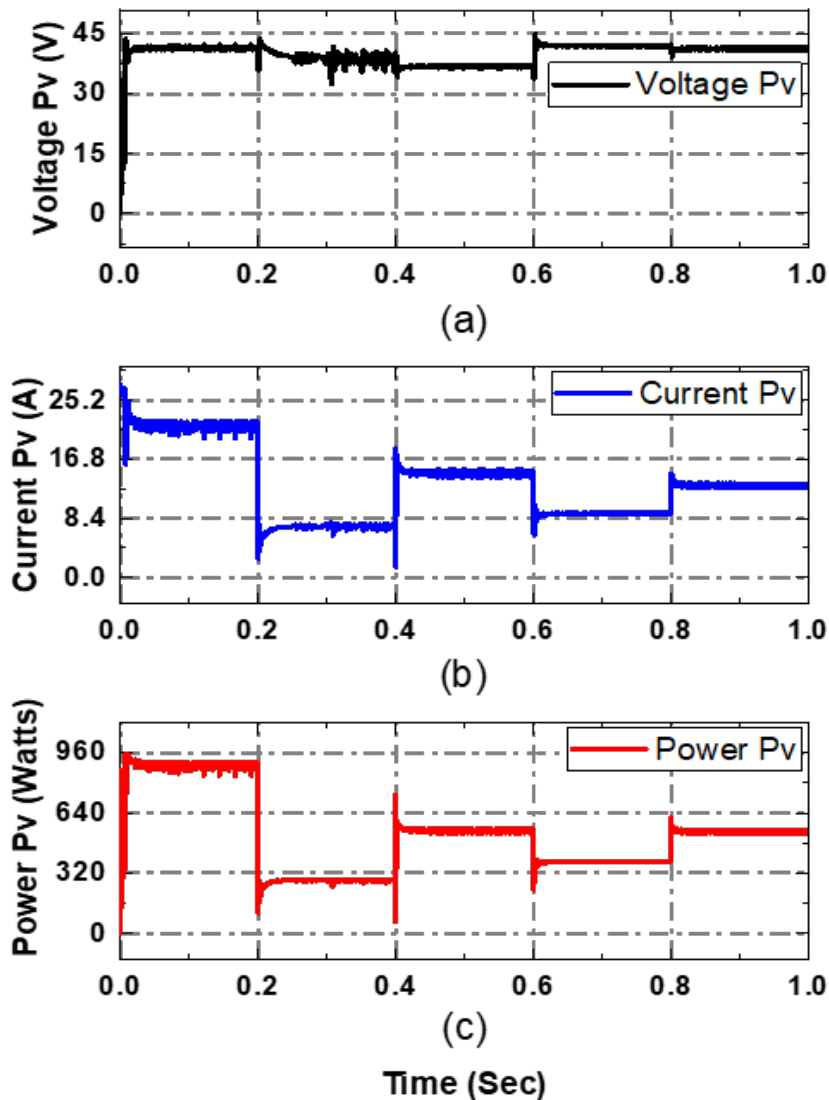
FIGURE 5.7: Tracking waveform of PV array (a) voltage, (b) current and (c) power of VSS-VSF Inc.Cond technique against varying temperature for case 2

temperature is now varying shown in figure 5.3. The constant irradiance starts from 0.2 sec to 1 sec with a temperature of 45 ℃ at the start. The Vpv voltage of the PV Array is at V_{MPP} point against 1000W/m^2 irradiance level. But for high irradiance at high temperature, the V_{PV} is around V_{MPP} value 41.02V to 41.6V. When irradiance level is high and the temperature is 65 ℃ the V_{PV} of the PV Array is 36.5V, which very less than the V_{MPP} value.

For low irradiance between 300 to 400 W/m^2 with low temperature between 25 ℃ to 35 ℃ the voltage V_{PV} fluctuates from 36V to 42V. Oscillations are high when

irradiance and temperature are high but oscillations are less against low irradiance and temperature. Figure 5.7a represents the voltage response of the PV Array at varying temperatures with five different irradiance levels.

The temperature will affect the performance of the PV Array. From figure 5.7b it can be observed that temperature limits the output current of the PV Array. At high irradiance with a temperature of 40 ℃ the current is between 20A to 22A which is near to the Impp of the PV Array. For low irradiance with temperature between 28 ℃ to 36 ℃ the current I_{PV} is between 7A to 9.17A with less oscillations.

A high temperature that a PV cell can reach is 65 ℃. At this temperature with irradiance level is 700W/m^2 the I_{PV} is fluctuating between 14A to 15.6A. Fewer oscillations occur against the irradiance from 400W/m^2 to 600W/m^2 and the temperature is 28 ℃ to 36 ℃. Over-shoots occur in the current I_{PV} of the PV Array when both irradiance and temperature are increasing. So, high temperatures have a negative effect on the current of the PV Array.

Power is the combination of the voltage and current value. The power Ppv of the PV Array is shown in figure 5.7c. The P_{PV} value is different against each irradiance level is due to the high temperature compared to the extracted power at a constant temperature. For high irradiance with temperature is around 40 ℃ to 45 ℃ the P_{PV} is 887.5W with oscillations. With the decrease in irradiance level and the temperature is 28 ℃ to 36 ℃ the Ppv is between 281W to 385W. Over-shoot occurs in Ppv of the PV Array when both irradiance and temperature change their values from low to high.

At temperature 65 ℃ and irradiance is 700W/m^2, the P_{PV} is settled at 542W with oscillations. When irradiance shifted towards 600 W/m^2 and temperature is around 30 ℃ to 35 ℃ the algorithm manages to reduce the over-shoot and almost zero oscillations at 550W. The P_{PV} shows an almost similar response to I_{PV} of the PV Array in the VSS-VSF Inc.Cond technique under varying temperature and five different irradiance levels. The worth thing mention here is , VSS-VSF IncCond perform quite well under high temperature with low irradiance level. But it has oscillations against high irradiance with high temperature. The overall extracted

power is less compared to case 1. This is because of high temperature variations are involved in input signal of the PV array.

5.2.3 NAVSS Inc.Cond MPPT Algorithm

Step involve in NAVSS Inc.Cond technique explain in previous chapter along with the initial simulation. This technique work on the slope value which is calculated by power and voltage.

Case 1:

In this case, the irradiance signal in figure 5.2 is given to the whole PV array, and the temperature is constant at 25 ℃ and the V_{PV} is changing between 35V to 44V. The fixed irradiance starts from 0 to 0.2 sec, the V_{PV} settles at 42.6V with oscillations. It can be observed from figure 5.8a that as fast-dynamic irradiance occurs from 0.2 to 1 sec, the V_{PV} oscillates around V_{MPP}. For high irradiance, the V_{PV} is fluctuating between 40.5V to 43V which are acceptable oscillations. For low irradiance, the V_{PV} of the PV Array is between 35V to 41.1V. Oscillations against the first low irradiance value which is around 5V but oscillations are fewer for the next coming irradiances level.

From figure 5.8b during the constant irradiance or at the start the current of the PV array is fluctuating between 22A to 24A and it settles at 22A with oscillations. With the start of dynamic irradiance from 0.2 sec, the current of PV array is decreasing due to low irradiance level. I_{PV} at this time is 7.8A which is almost near to I_{MPP} with fewer oscillations.

From 0.4sec to 0.6sec the current is increasing and settle at 16.2A with oscillations. From 0.6 sec to 0.8 sec the current is again decreasing and reaches 9.5 A which is almost near to I_{MPP} at the available irradiance and with oscillations of 0.5A. From 0.8 sec to 1 sec the current is increasing and reached the I_{MPP} at the available irradiance. Here fluctuation in current is between 13A to 14A value. The thing worth mentioning here is that this method is achieving its I_{MPP} during low irradiance levels with minimum oscillations.
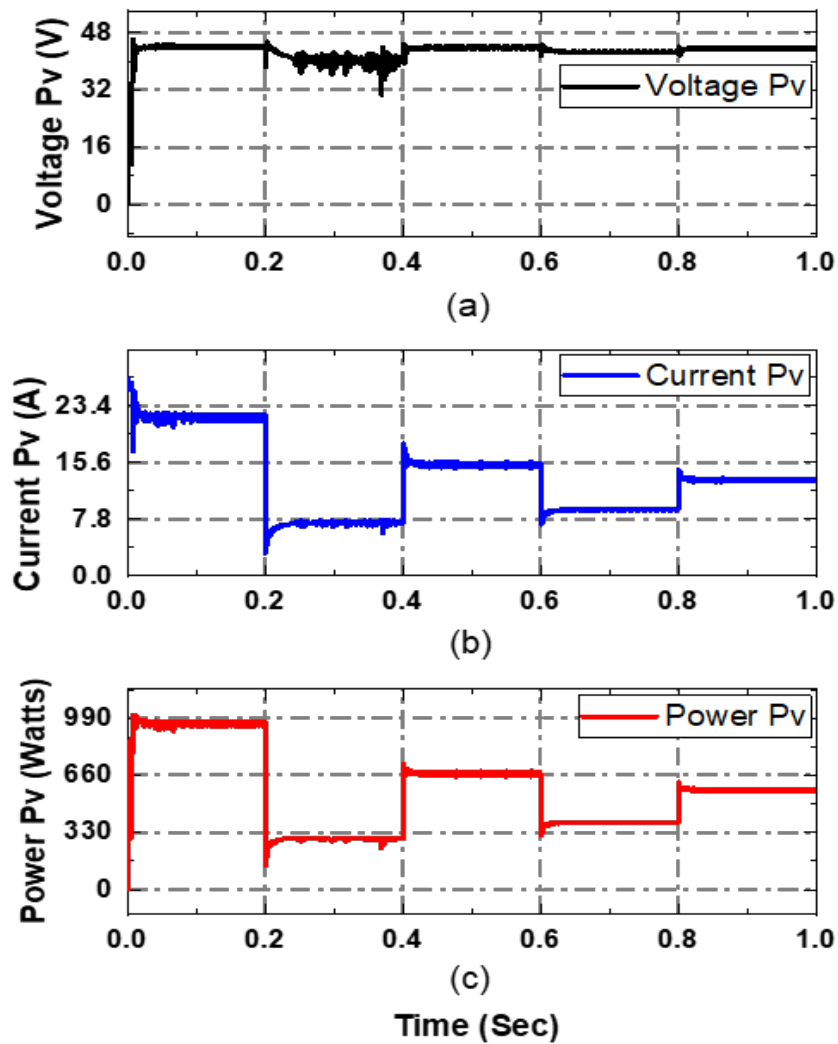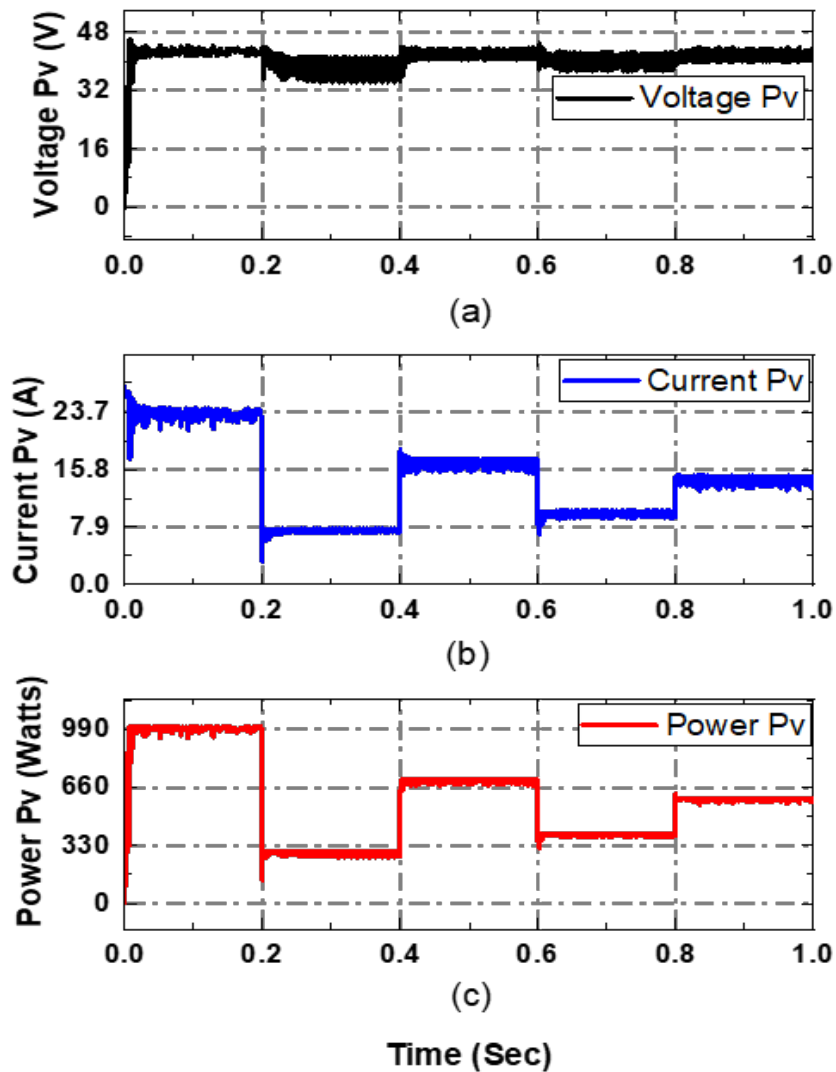
FIGURE 5.8: PV array output response of (a) voltage, (b) current & (c) power of NAVSS Inc.Cond technique against against fast-dynamic irradaince for case 1

At the start from 0 to 0.2sec, the Array Power P_{PV} is increasing and it reaches P_{MPP} 1004W but with oscillations and dips which is clearly observed from figure 5.8c. As the dynamic irradiance form 0.2 sec, the power of the PV Array is decreasing and achieves 292W and oscillations are also generated. From 0.4 to 0.6 sec the P_{PV} is increasing and it reaches the 694W with oscillations.

During 0.6sec to 0.8sec the power P_{PV} is decreasing due to decrease in irradiance level. Here P_{PV} is settle at 379W with minimum oscillations. As irradiance is increase during 0.8 sec to 1 sec the power is now increasing and extracts 581W

power but with oscillations. The thing worth mentioning here is that the algorithm performs better and extraction of available power is almost 90% using the setp size of 0.08 with duty-max 0.49. But fewer oscillations are occur during low irradiance levels. Using suitable tuning parameters the oscillations are reduced which increase the efficiency of the NAVSS Inc.Cond method against fast varying high to low and low to high irradiance level.

Case 2:

In this case, the same irradiance signal is given to the whole PV array, but the temperature is now varying shown in figure 5.3. The dynamic irradiance starts from 0.2 sec to 1 sec with a temperature of 45 ℃ at the start. The V_{PV} voltage of the PV Array is near to the V_{MPP} point against 1000 W/m^2 irradiance level with 1V peak-to-peak oscillations. For the whole irradiance and temperature signal, the V_{PV} is between 34V to 42V.

When the irradiance level is high and the temperature is 65 ℃, the V_{PV} of the PV Array is away from its V_{MPP} value and oscillates around 34V to 36V. During this time the algorithm performance efficiency is very low.
For low irradiance between 300 to 400W/m^2 with low temperature between 25 ℃ to 35 ℃, the voltage V_{PV} fluctuates from 33V to 41V. During the 600W/m^2 irradiance at 38 ℃, the oscillations are 1V to 2V and the algorithm manages to achieve the nearest point of the V_{MPP}. Oscillations in voltage values are high when irradiance is low and temperature is greater than 30 ℃. Figure 5.9a shows the voltage output of the PV Array at varying temperatures with five different irradiance levels.

The temperature will affect the performance of the PV Array. From figure 5.9b it can be observed that temperature limits the output current of the PV Array. At high irradiance with a temperature of 40 ℃, the current is between 18 to 23A and here current oscillations are quite high.
For low irradiance with temperature between 28 ℃ to 36 ℃ the current I_{PV} is between 7A to 7.3A and 9.7A to 10A. It is similar to the current response during constant temperature but the current oscillations are less in this scenario.

FIGURE 5.9: Tracking waveform of PV array (a) voltage, (b) current and (c) power of NAVSS Inc.Cond technique against varying temperature for case 2

A high temperature that a PV cell can reach is 65 ℃. At this temperature with irradiance level is 700W/m^2 the I$_{PV}$ is fluctuating between 15A to 17.6A, here current oscillations are also large. When irradiance changes from 400 W/m^2 to 600 W/m^2 and the temperature also shifts from 28 ℃ to 36 ℃, again I$_{PV}$ shows a similar response compared to the fixed temperature response.

Over-shoots occur in the current I$_{PV}$ of the PV Array when both irradiance and temperature are increasing. So, high temperatures have a negative effect on the current of the PV Array.

Power is the combination of the voltage and current value. The power P_{PV} of the PV Array is shown in figure 5.9c. The P_{PV} value is different against each irradiance level is due to the high temperature compared to the extracted power at a constant temperature. For high irradiance with temperature is around 40 ℃ to 45 ℃ the P_{PV} is 787.5W and oscillations are large. With the decrease in irradiance level (300 W/m² and 400 W/m²) and the temperature is 28 ℃ to 36 ℃ the P_{PV} is between 255W to283W and 378W to 389W respectively. Over-shoot occurs in P_{PV} of the PV Array when both irradiance and temperature change their values from low to high.

At temperature 65 ℃ and irradiance is 700W/m², the P_{PV} is settled at 562W with oscillations. When irradiance shifted towards 600W/m² and the temperature is around 30 ℃ to 35 ℃, the algorithm manages to reduce the overshoot and oscillations to the acceptable level. The extracted power P_{PV} against 700 W/m² is reache to 555W. The thing worth mentioning is that the P_{PV} shows an almost similar response to I_{PV} of the PV Array in the NAVSS Inc.Cond technique under varying temperature and fast-dynamic irradiance levels. The algorithm performs better and has acceptable efficiency under low irradiance levels and the temperature is between 28 ℃ to 36 ℃. But as temperature and irradiance both increase instantly the algorithm generates large oscillations.

5.2.4 Modified Inc.Cond Algorithm for Fast-varying Solar Irradiance

This modified Inc.Cond technique is simulated against the two different cases which are explain above. The result against these two cases are discuss below.

Case 1:

In this case, the irradiance signal in figure 5.2 is given to the whole PV array, and the temperature is constant at 25 ℃ and the V_{PV} is changing between 37.1V to 41.9V. The fixed irradiance starts from 0 to 0.2 sec, at the start oscillations are occur and then V_{PV} settles at 40.7V which is near to V_{MPP} value and the

oscillations are zero after settling. It can be observed from figure 5.10a that as fast-dynamic irradiance occurs from 0.2 to 1 sec. For high irradiance, the V_{PV} is reached 40.7V which is near to the V_{MPP} value. For low irradiance 300W/m^2 and 400W/m^2, the V_{PV} is 37.1V and 40.3V respectively. During high irradiance for 600 W/m^2 and 700 W/m^2, the V_{PV} is 41.9V and 39.5 which is again near to V_{MPP}. Oscillations are less at the start and after settling these oscillations are zero but overshoots are generated only when irradiance is decreasing.
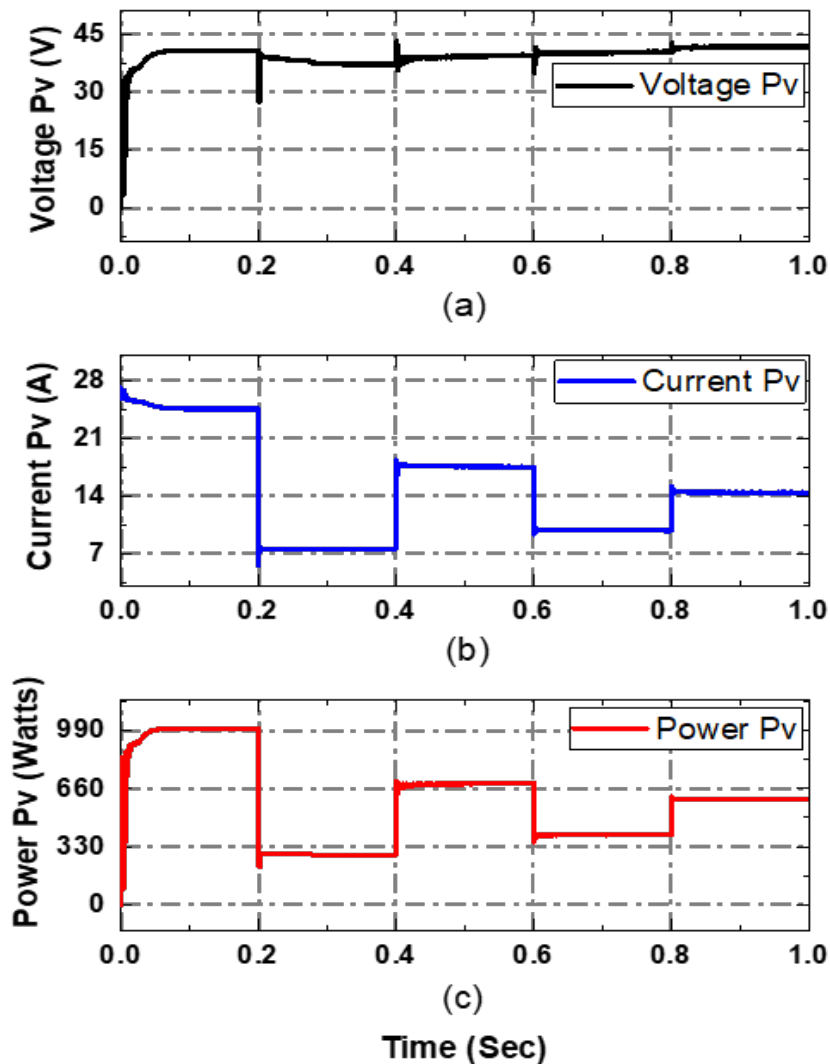
FIGURE 5.10: PV array output response of (a) voltage, (b) current & (c) power of Modified-1 Inc.Cond technique against against fast-dynamic irradaince for case 1

From figure 5.10b during the constant irradiance the current of the PV Array has

some oscillations and it settles at I_{MPP} value 24.5 with zero oscillations. With the start of dynamic irradiance from 0.2 sec, the current of PV Array is decreasing due to low irradiance level and I_{PV} is 7.64A which is almost equal to I_{MPP} value. From 0.4sec to 0.6sec the current is increasing and settling at 17.6A and then from 0.6 sec to 0.8 sec the current is again decreasing and reaches I_{MPP} value 9.9A.

From 0.8 sec to 1 sec the current is increasing and reached the 14.4A value which is two amps less to I_{MPP} at that available irradiance. The thing worth mentioning here is that this method is achieving its I_{MPP} against each irradiance level with zero oscillations after settling and overshoot occurs only during irradiance is shifted from high to low level.

This power response is extracted using proper tuning parameters. At the start from 0 to 0.2sec, the array power P_{PV} is increasing and reach at 1003W which is clearly observed from figure 5.10c. As the dynamic irradiance decrease form 0.2 sec, the power of the PV array is decreasing and settlt at 286W with zero oscillations. From 0.4 to 0.6 sec the P_{PV} is increasing and reach at 692W which is almost equal to Pmpp value. During 0.6sec to 0.8sec the power P_{PV} is decreasing due to decrease in irradiance level, but extracted power is 395.5W which is equal to Pmpp value. From 0.8 sec to 1 sec the power is now increasing due to high irradaince and Ppv is 599.6W which is equal to P_{MPP} value. The thing worth mentioning oscillations are occur when irradiance shifts from or high to low. But the technique performs better and extracts maximum power during all irradiance levels with almost zero oscillations. Over shoots are occur only when irradaince level shift from high to low. So, this technique achieves maximum power efficiency under fast-dynamic irradiance.

Case 2:

In this case, the same irradiance signal is given to the whole PV array, but the temperature is now varying shown in figure 5.3. The dynamic irradiance starts from 0.2 sec to 1 sec with a temperature of 45 ℃ at the start. The Vpv voltage of the PV Array is at V_{MPP} point against 1000 W/m^2 irradiance level the V_{PV} is 39.6V with oscillations at the start. For the whole irradiance and temperature
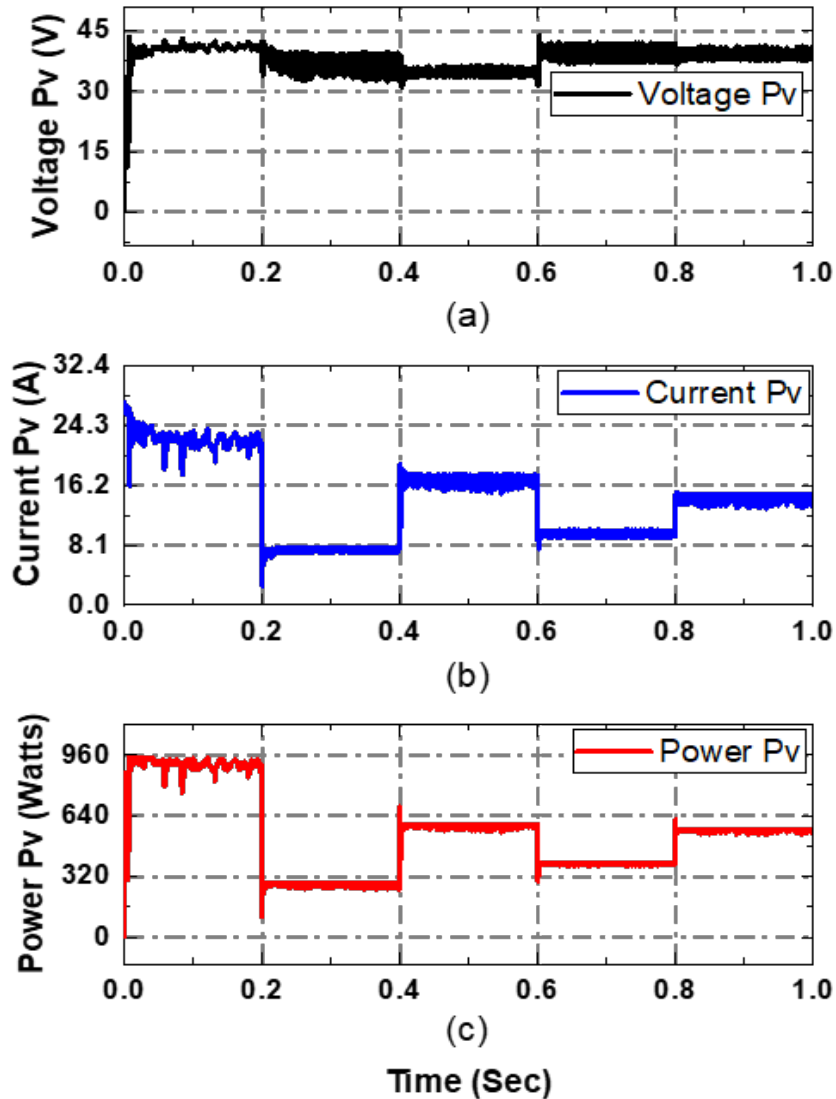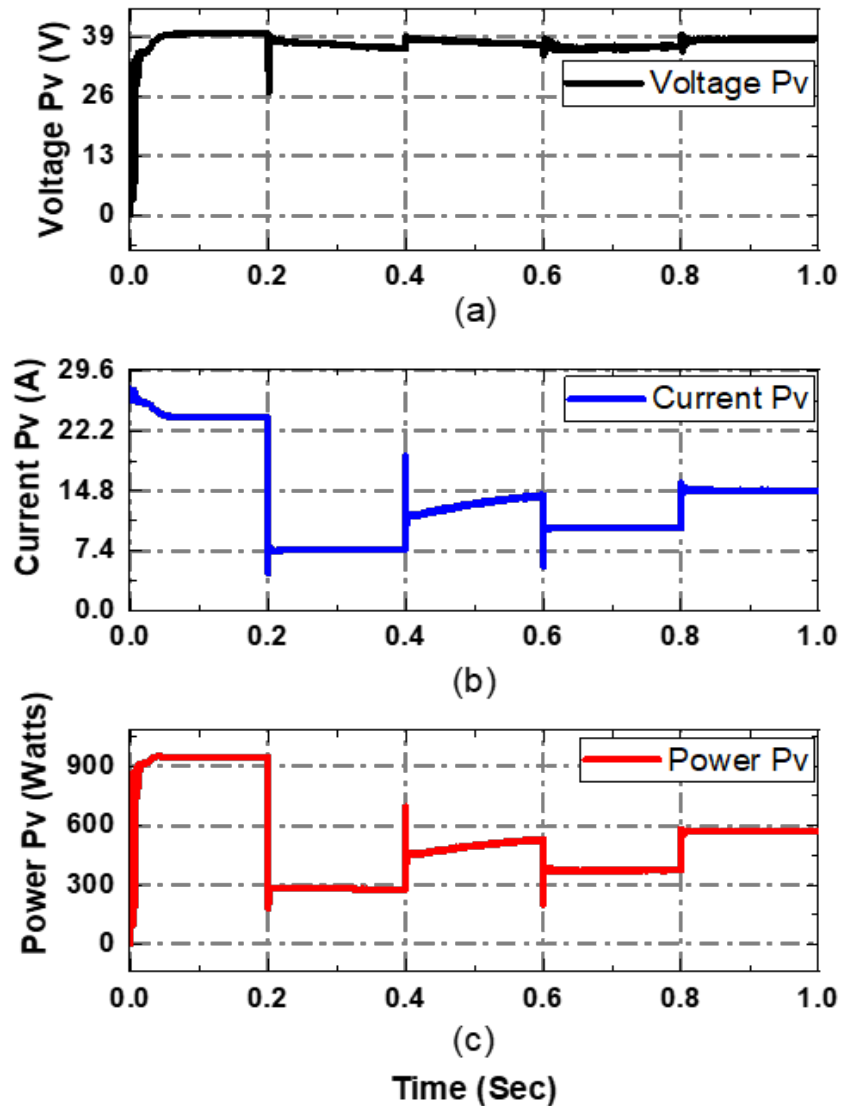
FIGURE 5.11: Tracking waveform of PV array (a) voltage, (b) current and (c) power of Modified-1 Inc.Cond technique against varying temperature for case 2

signal, the V_{PV} is between 36.4V to 39.6V. When the irradiance level is high and the temperature is 65 ℃, the V_{PV} of the PV Array is oscillating between 37.2V to 38V. Under this condition the algorithm's performance and efficiency is quite good.

For low irradiance between 300 to 400 W/m^2 with low temperature between 25 ℃ to 35 ℃, the voltage V_{PV} fluctuates from 36.4V to 37V which away from V_{MPP}. During the 600W/m^2 irradiance at 38 ℃, the oscillations are negligible and the algorithm manages to settle at 38.3V. Oscillations in voltage values only occur

when irradiance and temperature value are shifted from high to low. Figure 5.11a shows the voltage response of the PV Array at varying temperatures with fast-dynamic irradiance. Here the voltage V_{PV} is not up to the mark against the low irradiance at a low-temperature level.

The temperature will affect the performance of the PV Array. From figure 5.11b it can be observed that temperature limits the output current of the PV Array. At high irradiance with a temperature of 40 ℃, the current is 23.8A and here current oscillations are present at the start but after settling, oscillations are zero. For low irradiance with temperature between 28 ℃ to 36 ℃ the current I_{PV} is between 7.5A and 10A, which is similar to the current response during constant temperature.
A high temperature, a PV cell can reach is 65 ℃ at this temperature with irradiance level is 700W/m² the I_{PV} is increasing from 11A to 14A. When irradiance changes from 400W/m² to 600W/m² and the temperature also shifts from 28 ℃ to 40 ℃ again I_{PV} shows a similar response compared to the fixed temperature response and I_{PV} is between 10.1A to 14.8A. Over-shoots occur in the current I_{PV} of the PV Array when both irradiance and temperature are decreasing.

So, high temperatures have a negative effect on the current of the PV Array. Over-shoot occurs in the I_{PV} of the PV Array when both irradiance and temperature change their values from high to low.

Power is the combination of the voltage and current value. The power P_{PV} of the PV Array is shown in figure 5.11c. The P_{PV} value is different against each irradiance level is due to the high temperature compared to the extracted power at a constant temperature. For high irradiance with temperature is around 40 ℃ to 45 ℃ the P_{PV} is 943.6W which is less as compared to power extracted during fixed temperature and oscillations are occur at the start.

With the decrease in irradiance level (300 W/m² and 400 W/m²) and the temperature is 28 ℃ to 36 ℃ the P_{PV} is 281W and 371W respectively. Over-shoot occurs in P_{PV} of the PV Array when both irradiance and temperature change their values from high to low.

At temperature 65 ℃ and irradiance is 700 W/m^2, the P$_{PV}$ is increasing at the start and fluctuates between 463W to 523W. This power response reduces the overall performance efficiency of the algorithm. When irradiance shifted towards 600 W/m^2 and the temperature is around 30 ℃ to 38 ℃, the algorithm manages smoothly to reach 570W with zero oscillations. The duty-max is 0.51 is used to get the MPP point. The thing worth mentioning is that the P$_{PV}$ shows leading performance in power extraction during high temperatures compared to the other. The algorithm performs better and has acceptable efficiency under both high and low irradiance levels. The overall power extraction is reduced due to high temperature level. Because of temperature the PV Array current Ipv and voltage Vpv are affected which causes the reduction in the power of the PV Array.

5.2.5 Modified Inc.Cond Algorithm for Fast-changes of Irradiance

This modified Inc.Cond technique works on two major equations which are discuss in chapter 4. Here this technique is simulated against the two different cases which are explain above. The result against these two cases are discuss below.

Case 1:

In this case, the irradiance signal in figure 5.2 is given to the whole PV array, and the temperature is constant at 25 ℃ and the V$_{PV}$ is changing between 37V to 44V. The fixed irradiance starts from 0 to 0.2 sec, V$_{PV}$ settles at 43.6V after some time, it can be observed from figure 5.12a, as fast-dynamic irradiance occurs from 0.2 to 1 sec, the V$_{PV}$ oscillates throughout the whole signal whenever irradiance level shifts. For high irradiance 700 W/m^2 and 600 W/m^2, the V$_{PV}$ is between 38V to 44V and oscillates continuously. During low irradiance at 300 W/m2 voltage oscillations are less than 400 W/m^2, the V$_{PV}$ is between 37.6V to 42.6V. The V$_{PV}$ of the PV Array is 3V peak-to-peak away from the V$_{MPP}$ value. Against the 1000 W/m^2 irradiance level, the algorithm shows better performance compared to other irradiance levels. Oscillations in V$_{PV}$ are zero at 1000 W/m^2 irradiance level.
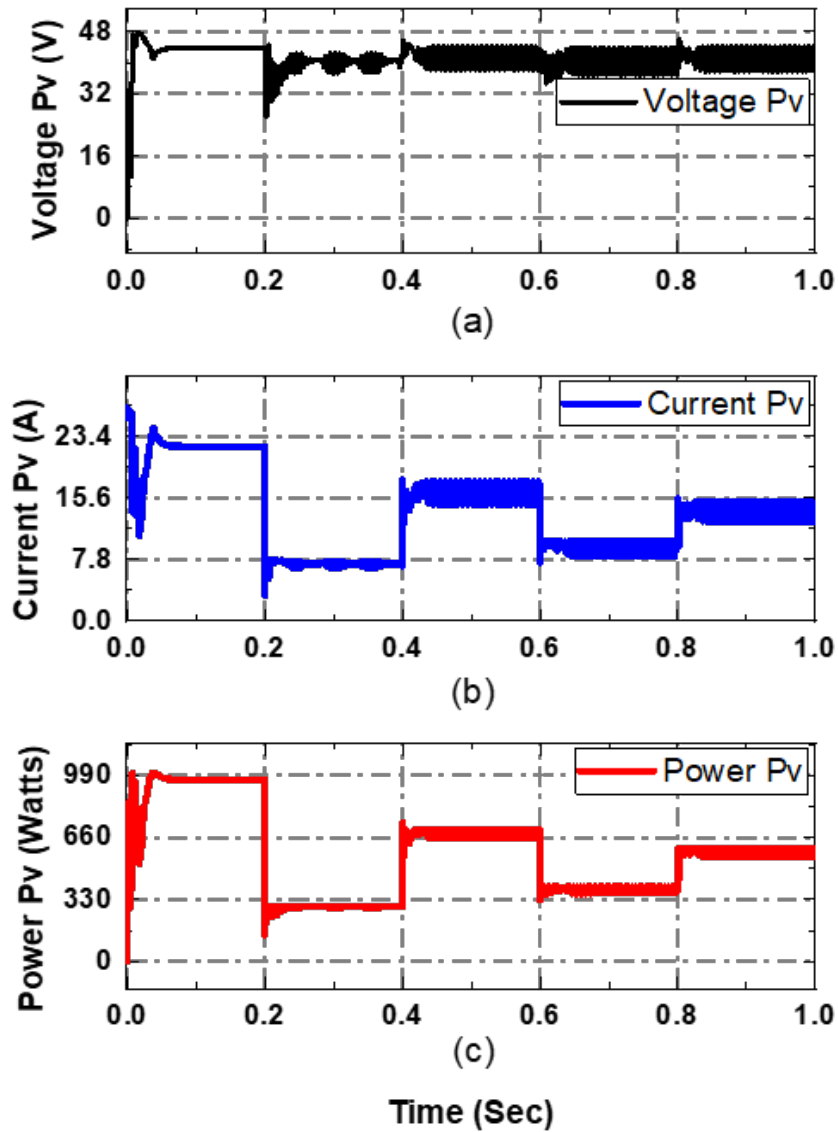
FIGURE 5.12: PV array output response of (a) voltage, (b) current & (c) power of Modified-2 Inc.Cond technique against against fast-dynamic irradaince for case 1

From figure 5.12b during the constant irradiance or at the start the I_{PV} current of the PV Array is fluctuating and it settles at 22.1A with zero oscillations. With the start of dynamic irradiance from 0.2 sec, the current of PV Array is decreasing due to low irradiance level and I_{PV} is 6.7A to 7.6A which is almost near to I_{MPP}. But here oscillations are present. From 0.4sec to 0.6sec the current is increasing and oscillates between 15A to 17A and then from 0.6 sec to 0.8 sec the current is again decreasing and value between 8.2A to 9.9A. At this stage this I_{PV} is almost

near to I_{MPP} at the available maximum current.

From 0.8 sec to 1 sec irradaince is high and the current is now increasing and also the oscillations, the I_{PV} at the available irradiance is fluctuating between 12.7A to 15A value. The thing worth mentioning here is that this method performs better at the start but has oscillations against the remaining irradiance signal.

This power response is extracted using proper tuning parameter. At the start from 0 to 0.2sec, the array power P_{PV} is increasing because irradaince is high the Ppv is reache at 968W with zero oscillations which is clearly observed from figure 5.12c. As the dynamic irradiance form 0.2 sec, the power of the PV array is decreasing as irradiance is decreasing. At this stage the achieved power is 294W with minimum oscillations. From 0.4 to 0.6 sec the P_{PV} is increasing and it start fluctuating between 652W to 700W.

From 0.6sec to 0.8sec the power P_{PV} is decreasing due to decrease in irradiance level. Here power oscillations are between 370W to 396W. During 0.8 sec to 1 sec the power is increasing and extracted power is fluctuating between 555W to 600W. The oscillations are quite large against the 600W/m². The thing worth mentioning here is that the algorithm performs better against the first two irradiance changes. The extracted available power is almost 97%. The technique produces large oscillations against low irradiance level. This is the same power response compared to the algorithm mentioned in heading of modified Inc.Cond to mitigate the response during fast-varying irradiance.

Case 2:

In this case, the same irradiance signal is given to the whole PV array, but the temperature is now varying shown in figure 5.3. The dynamic irradiance starts from 0.2 sec to 1 sec with a temperature of 45 ℃ at the start. The voltage of the PV array V_{PV} is 41.6V against 1000 W/m² irradiance level with zero oscillations. This V_{PV} is equal to V_{MPP}. For the complete input irradiance and temperature signal, the V_{PV} is between 34.2V to 43V. When the irradiance level is high and the temperature is 65 ℃, the V_{PV} of the PV Array is 34.2V. During this time the algorithm performance efficiency is quite good and oscillations are almost
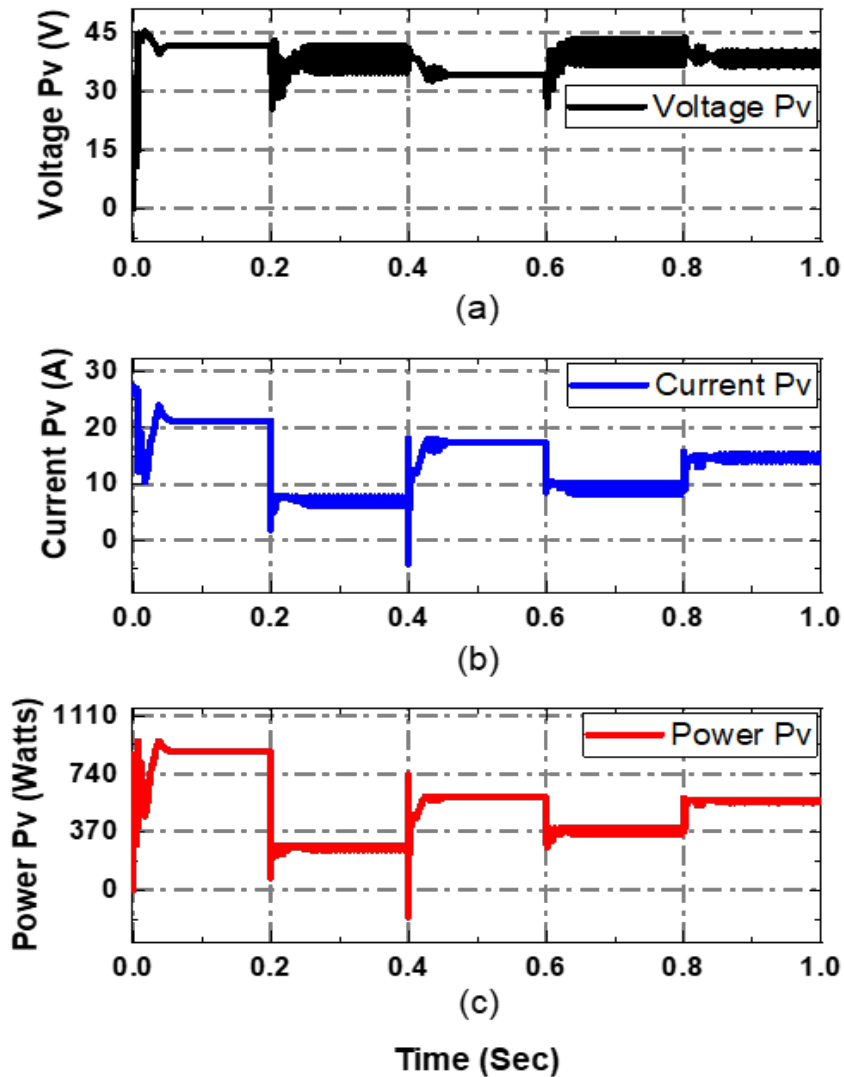
FIGURE 5.13: Tracking waveform of PV array (a) voltage, (b) current and (c) power of the Modified-2 Inc.Cond technique against varying temperature for case 2

negligible. For low irradiance between 300 to 400 W/m² with low temperature between 25 ℃ to 35 ℃, the voltage V$_{PV}$ fluctuates from 34.6V to 41.5V and 37V to 43V but voltage oscillations are quite large.

During the 600 W/m² irradiance at 38 ℃, the voltage oscillations are 4V at the start and the algorithm manages to settle at 39V with minimum oscillations. Over shoots occurs only when irradiance is changed from high to low level. Figure 5.13a shows the voltage response of the PV Array at varying temperatures with dynamic irradiance. Here the voltage response of the technique is satisfactory also

the oscillations against the high irradiance at the high-temperature level are very minimum as compared to voltage response at a constant temperature.

The temperature will affect the performance of the PV Array. From figure 5.13b it can be observed that temperature limits the output current of the PV Array. At high irradiance with a temperature of 40 ℃, the current Ipv is 21.1A which is near to Impp and here current oscillations are zero overshoot occur at the start. For low irradiance 300 W/m^2 with a temperature is 36 ℃ the current I$_{PV}$ is between 6.2A and 7.7A. This current have minimum fluctuations compared to during constant temperature current response. A high temperature that a PV cell can reach is 65 ℃ at this temperature with irradiance level is 700 W/m^2 the I$_{PV}$ is 17A, which is one Amp less than the I$_{MPP}$ of the PV Array.

When irradiance is 400 W/m^2 and the temperature also shifts to 28 ℃, the I$_{PV}$ is between 8.4A to 10.1A and fluctuates near I$_{MPP}$. When irradiance is increased to 600W/m^2 and the temperature shifts to 38 ℃, the I$_{PV}$ is 14.2A to 15.2A change and the current oscillations are minimum. Over-shoots occur at one stage in the current I$_{PV}$ of the PV Array when both irradiance and temperature are increasing. So, in this technique, high temperatures have a positive effect on the current of the PV Array and reduce the oscillations during high irradiance with high temperatures.

Power is the combination of the voltage and current value. The power P$_{PV}$ of the PV Array is shown in figure 5.13c. For high irradiance 1000 W/m^2 with temperature is around 40 ℃ to 45 ℃ the P$_{PV}$ is 877.6W which is less than the power value is extracted as compared to power extracted during fixed temperature. With the decrease in irradiance level (300 W/m^2 and 400 W/m^2) and the temperature is 28 ℃ to 36 ℃. The P$_{PV}$ has oscillations and the Ppv is between 252W to 282W and 351W to 391W respectively. Over-shoot occurs in P$_{PV}$ of the PV Array when both irradiance and temperature change their values from low to high. At temperature 65 ℃ that a PV cell can achieve and irradiance is 700 W/m^2, the P$_{PV}$ is settled at 592W with minimum oscillations.

When irradiance shifted towards 600 W/m^2 and the temperature is around 30 ℃ to 38 ℃, the P$_{PV}$ reaches 560W with 10W of oscillations. The thing worth mentioning

is that this Modified Inc.Cond technique under varying temperature and fast-dynamic irradiance levels shows satisfactory power, voltage, and current response which increases the performance efficiency with step-size is 0.008 and duty-max is 0.42. So, this technique is best during high temperature and irradiance levels. The technique is similar to method which is mention in chapter 2 in literature review. The only difference in both of these Inc.Cond MPPT algorithm is the slope error equation, one uses the slope value is 0.06 and the other is select 0.07.

5.2.6 An improved MPPT Control Strategy Based On Inc.Cond Algorithm

This modified Inc.Cond technique works slope value which is calculated by eq 4.10 and 4.11. These equations are explain in chapter 4.

Case 1:

In this case, the irradiance signal in figure 5.2 is given to the whole PV array, and the temperature is constant at 25 ℃ and the V_{PV} is changing between 21.5V to 46.1V. The fixed irradiance starts from 0 to 0.2 sec, at the start oscillations are occurs and then V_{PV} settles at 46.1V with zero oscillations. It can be observed from figure 5.14a that as fast-dynamic irradiance occurs from 0.2 to 1 sec. The V_{PV} is decreasing when irradiance level shifts. For high irradiance, the Vvp is between 40.2V to 46V. For low irradiance 300 W/m^2 and 400 W/m^2, the V_{PV} is 21.5V and 28V which is away from the V_{MPP} value.

Oscillations are generated only when the irradiance level is changed. For the irradiance level 700 W/m^2, the V_{PV} of the PV Array fluctuates at the start and V_{PV} is rising and it settles at 43V which is 2V greater than the V_{MPP} value at the available irradiance level.

No overshoots occur during shifting of irradiance level. For the 600W/m^2 irradiance level, the V_{PV} achieves the V_{MPP} value at settles at 40.2V. Initially, oscillations are present but after settling these oscillations become zero.

From figure 5.14b during the constant irradiance, the current of the PV Array have some oscillations and it settles at 17.1A with zero oscillations. With the start of dynamic irradiance from 0.2 sec, the current of PV Array is decreasing due to low irradiance level and I_{PV} is 7.8A and which is almost near to I_{MPP}. From 0.4sec to 0.6sec the current is increasing and settle at 15.9A and then from 0.6 sec to 0.8 sec the current is decreasing and reaches I_{MPP} value 10.3A, now from 0.8 sec to 1 sec the current is increasing and reached the 14.8A value which 2A less than I_{MPP} value at that available irradiance. The thing worth mentioning here is that this method is achieving its I_{MPP} during high irradiance levels with zero oscillations after settling and overshoot occurs only during irradiance is shifted from high to low level.

This power response is extracted by using proper tuning parameters. At the start from 0 to 0.2sec, the array Power P_{PV} is increasing and settle at 785.5W with zero oscillations which is clearly observed from figure 5.14c. But algorithm is not able to extract max. power against 1000 W/m². As irradiance is decreasing form 0.2 sec, the power of the PV array is decreasing and settle at 169W with zero oscillations. From 0.4 to 0.6 sec the P_{PV} is increasing, here extracted power is 687W which is near to Pmpp value.

During 0.6sec to 0.8sec the power P_{PV} is decreasing due to decrease in irradiance level and only able to achieve 293W. As irradiance increase to 600 W/m² from 0.8 sec to 1 sec the power is increasing. This power 596.6.2W is almost equal to Pmpp vlaue against 600W/m². The thing worth mentioning here is that if the step size with maximum delta are less than to a specific value the technique is not able to track the MPP. If the large value is selected than the output power of the PV array have large oscillations.

Case 2:

In this case, the same irradiance signal is given to the whole PV array, but the temperature is now varying shown in figure 5.3. The dynamic irradiance starts from 0.2 sec to 1 sec with a temperature of 45 ℃ at the start. The Vpv voltage of the PV Array is 43.6V, which is near to the V_{MPP} point against 1000 W/m²
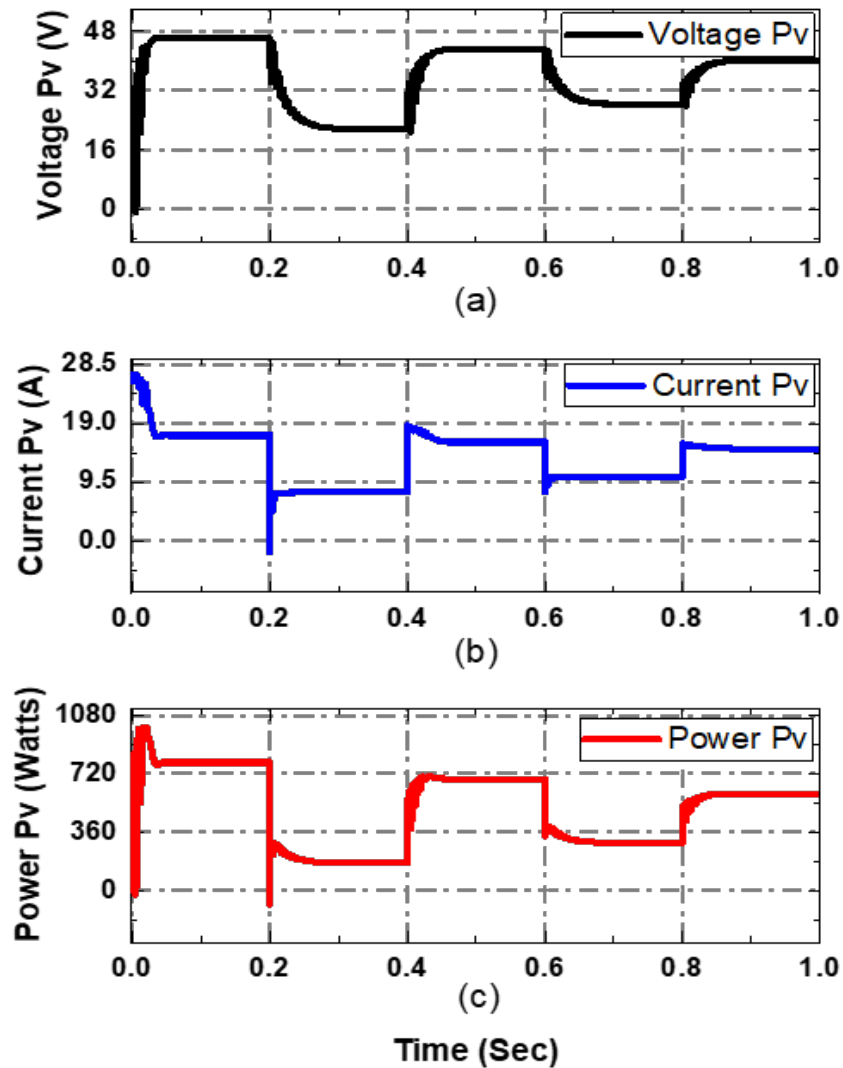
FIGURE 5.14: PV array output response of (a) voltage, (b) current & (c) power of Improved Inc.Cond technique against against fast-dynamic irradaince for case 1

irradiance level with oscillations at the start. For the whole irradiance and temperature signal, the V_{PV} is between 21.6V to 43.6V. When the irradiance level is high and the temperature is 65 ℃, the V_{PV} of the PV Array is away from its V_{MPP} value which is around 37.46V. During this time the algorithm performance efficiency is low.

For low irradiance between 300 to 400 W/m² with low temperature between 25 ℃ to 35 ℃, the voltage V_{PV} is between 21.6V to 28V which is far away from V_{MPP}. During the 600 W/m² irradiance at 38 ℃, the oscillations are zero at the

start and the algorithm manages to settle at 39V. Oscillations in voltage values only occur at the start when irradiance and temperature value is changed. Figure 5.15a shows the voltage response of the PV Array at varying temperatures with fast-dynamic irradiance. Here the voltage V_{PV} response is the same as compared to the voltage response at a fixed 25 ℃ temperature value. High temperature has not much affected the voltage of the PV Array in this technique, and this method manages the duty cycle which keeps its voltage response similar to fixed temperature voltage response.

The temperature will affect the performance of the PV Array. From figure 5.15b it can be observed that temperature limits the output current of the PV Array. At high irradiance with a temperature of 40 ℃, the current is decreasing from 27.4A and settles at 16A due to high temperature and the oscillations are zero. For low irradiance with temperature between 28 ℃ to 36 ℃ the current I_{PV} is between 7.9A and 10.9A, which is similar to the current response during constant temperature.

A high temperature that a PV cell can reach is 65 ℃, at this temperature with irradiance level is 700W/m2^2 the I_{PV} is 13.8A. Here current oscillations are zero after settling. But this current value is far away from the I_{MPP} value. When irradiance changes from 400 W/m^2 to 600 W/m^2 and the temperature also shifts from 28 ℃ to 40 ℃, I_{PV} is 10.4A and 14.5A respectively and I_{PV} shows a similar response compared to the fixed temperature response.

Over-shoots occur in the current I_{PV} of the PV Array when both irradiance and temperature are decreasing. The worth thing mentioning here is that the current value is low only during high irradiance with high temperature but for low irradiance with low temperature the current of the PV Array reaches near to I_{MPP} value. So, high temperatures have a negative effect on the current of the PV Array during high irradiance. Over-shoot occurs in the I_{PV} of the PV Array when both irradiance and temperature change their values from high to low.

Power is the combination of the voltage and current value. The power P_{PV} of the PV Array is shown in figure 5.15c. The P_{PV} value is different against each
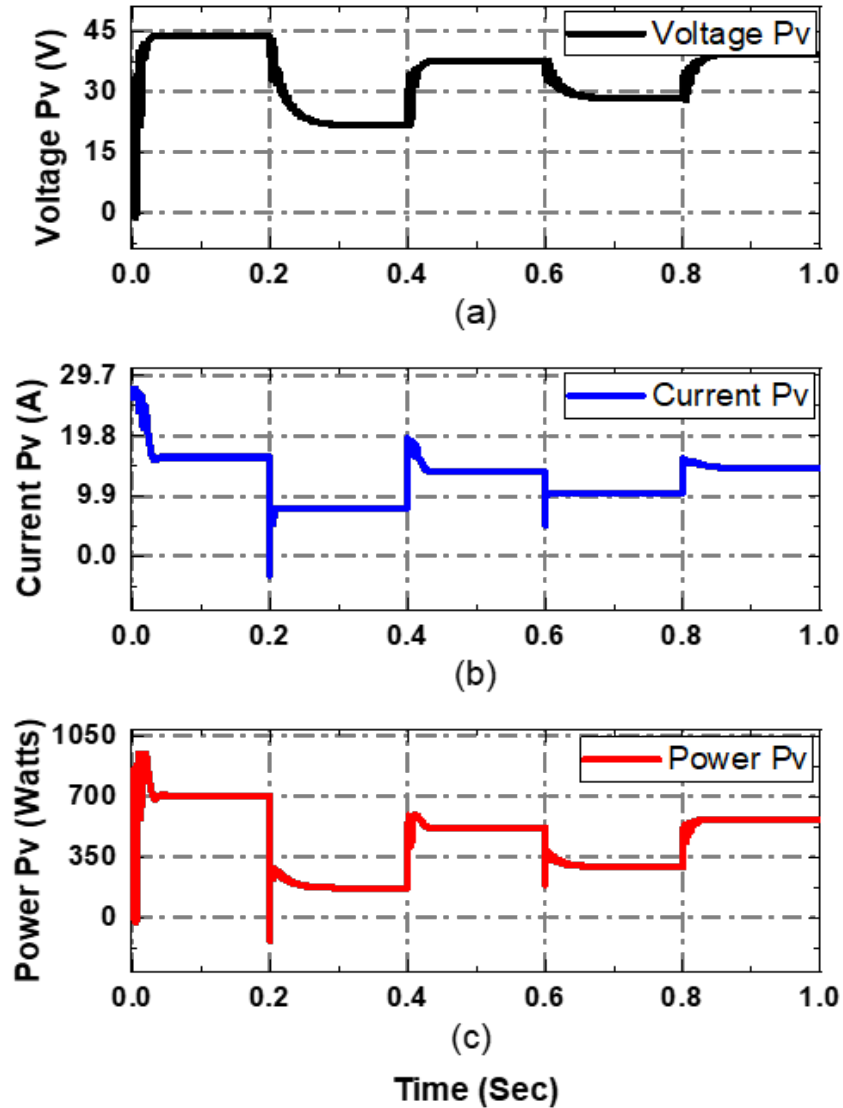
FIGURE 5.15: Tracking waveform of PV array (a) voltage, (b) current and (c) power of the improved Inc.Cond technique against varying temperature for case 2

irradiance level is due to the high temperature compared to the extracted power at a constant temperature.

For high irradiance with temperature is around 40 ℃ to 45 ℃ the P_{PV} is 709W which is less as compared to power extracted during fixed temperature and oscillations are occur at the start but it becomes zero after settling.

With the decrease in irradiance level (300 W/m² and 400 W/m²) and the temperature is 28 ℃ to 36 ℃ the P_{PV} value is between 172W and 294W respectively and

which are similar to the P_{PV} power value during fixed temperature. Over-shoot occurs in P_{PV} of the PV Array when both irradiance and temperature change their values from high to low. At temperature 65 ℃ and irradiance is 700 W/m^2, the P_{PV} is settled at 519W, it less than the power that is extracted under fixed temperature.

When irradiance shifted towards 600 W/m^2 and the temperature is around 30 ℃ to 38 ℃, the algorithm manages smoothly to reach 570W. The thing worth mentioning is that the extraction of power during high irradiance and at low temperature, the power response is similar to the P_{PV} response under fixed temperature. The algorithm performs better and has acceptable efficiency under low irradiance and low-temperature levels with setp-size equal to 0.08, duty-max is 0.52 and delta-in is $256e^-6$.

The overall power extraction is reduced due to high temperature level, because of temperature the PV Array voltage V_{PV} shows satisfactory response but the current is decreasing with the rise of the temperature and low irradiance level which causes the reduction in the extracted power of the PV Array.

5.3 Simulation results for Performance Testing Parameters

To make the comparison more authentic and close to realistic conditions five modified Inc.Cond MPPT algorithms were tested at the start of the chapter. To evaluate each technique under fast-dynamic irradiance and varying temperature values, eight Performance Testing Parameters (PTP) are proposed. In literature the modified Inc. Cond algorithms evaluated only under standard testing conditions (STC) and does not consider the fast-dynamic atmospheric conditions for the solar electric car.

Five distinctive irradiance levels (1000,300,700,400 and 600 W/m^2) with varying temperatures are considered in this thesis work to determine the efficiency of the modified Inc.Cond technique.

5.3.1 Rise and Settling Time

Rise and settling time is calculated for each modified Inc.Cond technique under two test cases. These cases are explain in detail at the start of this chapter. The case one include fast-dynamic irradiance signal at 25 ℃ and second case include five different irradaince level at varying temperature value. In this thesis, average rise time and settling time is calculated against the applied input irradaince and temperature signal.

Figure 5.16 shows the rise time of each modified Inc.Cond MPPT algorithms against case 1 and case 2. From figure 5.16a it can be observed that, during the fast-dynamic irradaince at 25 ℃ the minimum rise time is represented by NAVSS Inc.Cond technique which is 0.0034 sec. Modified Inc.Cond 1 and 2 have rise time equal to 0.0114 sec and 0.0124 sec respectively to reach the MPP point.
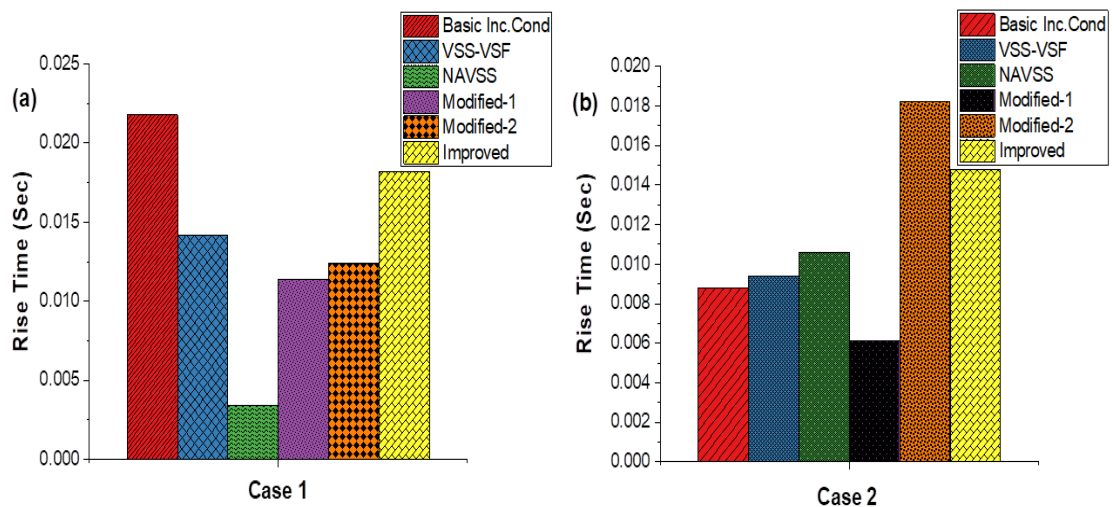
FIGURE 5.16: Rise time of each Modified Inc.Cond technique against case 1 and case 2

VSS-VSF and Improved Inc.Cond take almost 0.0145 sec to achieve the mpp point during fast-dynamic irradaince. The basic Inc.Cond have large rise time among all modified Inc.Cond techniques against case 1. The worth thing is mention here is that, the NAVSS Inc.Cond have minimum rise time among all modified Inc.Cond to achieve the mpp point against case 1. Both modified Inc.Cond techniques are

on second place and Improved and VSS-VSF Inc.Cond techniques are on the third in order to achieving mpp point against the applied signal under case 1.

When varying temperature signal is applied to PV array, the rise time of each modified Inc.Cond is reduce. Figure 5.16b show represent the rise time of basic and five modified Inc.Cond techniques against case 2. It can be clearly observe from figure 5.16b, the rise time is reduce due to temperature. Modified-1 Inc.Cond show quick rise time of 0.0061 sec against case 2 among all remaining Inc.Cond techniques.

The basic and VSS-VSF Inc.Cond show almost same rise time of 0.0092 sec to achieve the mpp point. NAVSS and modified-2 Inc.Cond take 0.0106 sec and 0.0182 sec respectively to get the mpp point during case 2. The large rise time of 0.0182 sec is shown by the Improved Inc.Cond technique. So, during the second case the minimum rise time is shown by the modified-1 Inc.Cond which is better then the other techniques. Basic and VSS-VSF Inc.Cond have less rise time during case 2 compared to case 1. But only NAVSS Inc.Cond take large rise time to achieve the mpp point compared to case 1.

Figure 5.17 shows the settling time of each modified Inc.Cond MPPT algorithms against case 1 and case 2. From figure 5.17a it can be observed that, during the fast-dynamic irradaince at 25 ℃ the average minimum settling time is given by NAVSS and Modified Inc.Cond 1 technique which is 0.0410 sec. Both techniques have small settling time compared to other techniques.

Modified-2 and VSS-VSF Inc.Cond have settling time equal to 0.0506 sec and 0.0540 sec respectively to reach the MPP point. Improved Inc.Cond take 0.0637 sec average settling time against the applied signal during case 1. But traditional Inc.Cond technique have large settling time among other techniques. The time taken by basic Inc.Cond is near to 0.075 sec to settle against the applied signal.

The worth thing is mention here is that, the two modified Inc.Cond have minimum settling time compared to other technique. VSS-VSF and modified-2 Inc.Cond techniques are on second place and Improved and basic Inc.Cond techniques are on the third place in order to settle against the applied signal under case 1.
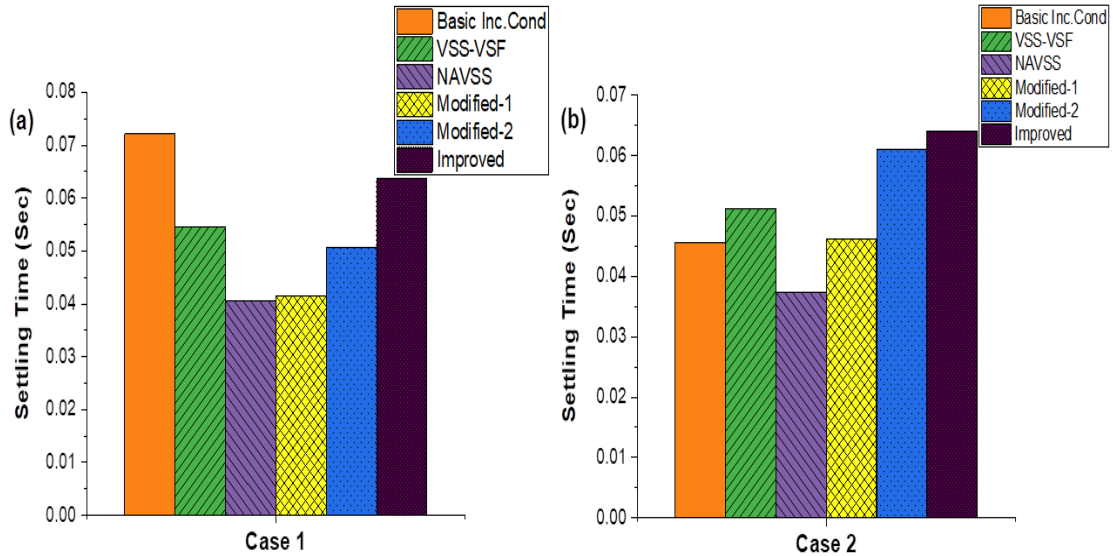
FIGURE 5.17: Settling time of each Modified Inc.Cond technique against case
1 and case 2

When varying temperature signal is applied to PV array, the settling time of some modified Inc.Cond techniques are reduced. Figure 5.17b show represent the settling time of basic and five modified Inc.Cond techniques during case 2. It can be clearly observe from figure 5.17b, the settling time is reduce due to temperature. NAVSS Inc.Cond show quick settling time of 0.0374 sec against case 2 among all remaining Inc.Cond techniques. The basic and modified-1 Inc.Cond show almost same settling time of 0.0458 sec at mpp point.

The VSS-VSF Inc.Cond take 0.0512 sec to settle at mpp point during case 2. The large settling time of 0.0640 sec is shown by the Improved Inc.Cond technique during case 2. So, during the varying temperature the settling time is reduce as it can observe from figure 5.17b. Based on minimum settling time the NAVSS is on first place during the case 2.

On the second place the basic and modified-1 Inc.Cond show less settling time compared to remaining techniques. The worth thing mention here is that, using varying temperature signal the settling time of each modified Inc.Cond is reduce compared to case 1. At different irradaince level with varying temperature the average settling is reduce due the the high temperature values. This is happened because of less power is extracted during high temperature.

5.3.2 Tracking Accuracy

The each modified inc.cond technique is simulated against 200W/m^2 to 1000W/m^2 irradiance level. Because in reality any irradaince value is the input irradiance of the PV module. For evaluating the tracking accuracy of each modified Inc.Cond algorithm, the irradaince is varying from low to high under constant temperature at 25 ℃. Figure 5.18 represent the tracking accuracy response of basic and each modified Inc.Cond techniques under normal conditions.

It can be observed that basic and Improved Inc.Cond has very low tracking accuracy when irradiance level is low. But with the increase in irradiance value, the tracking accuracy of basic and Improved Inc.Cond is start increasing. At high irradaince level these two techniques has 98.4% efficiency. It can be noticed from Figure 5.18, during low irradiance all modified inc.cond technique has the same tracking response around 75%. But at low irradiance level modified-1 Inc.Cond has tracking accuracy of 85% which is high conpared to remaining inc.cond technique.
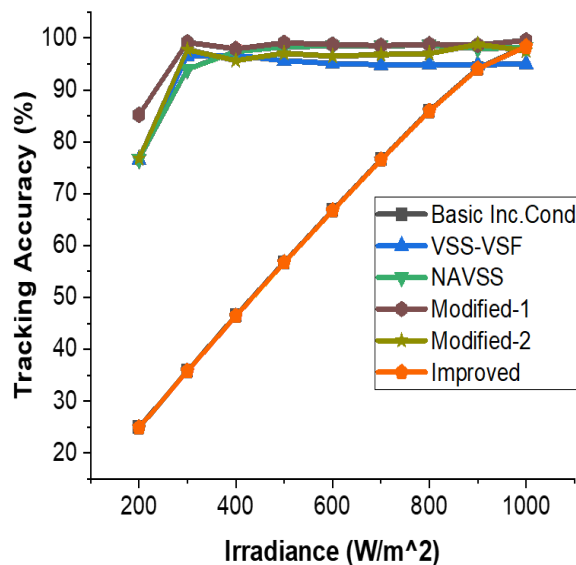
FIGURE 5.18: Tracking accuracy response of basic and modified Inc.Cond techniques under normal conditions

When irradiance level is between 300W/m^2 to 500W/m^2, the tracking accuracy of basic and Improved inc.cond is around 55%. The VSS-VSF and modified-2 show

the tracking accuracy between 92% to 95%. NAVSS has tracking accuracy of 95% between 300W/m² to 500W/m² irradaince level. But modified-1 Inc.Cond has 97% tracking accuracy. As irradiance level is shift towards 600W/m² to 800W/m², the tracking accuracy of VSS-VSF is reduces compared to previous tracking accuracy. But modified-2 Inc.Cond has 96% tracking accuracy. NAVSS and modified-1 show similar tracking accuracy against the 600W/m² to 800W/m² irradiance level.

Against high irradiance between 800W/m² to 1000W/m², the tracking accuracy of basic and Improved Inc.Cond is between 85% to 96%. Here again the tracking accuracy of VSS-VSF is reduce to 91%. But modified-2 show the tracking accuracy between 94% to 98% during 800W/m² to 1000W/m² irradaince level. NAVSS and modified-1 inc.cond has maximum tracking accuracy between 97% to 99% compared to other technique. The worth thing mention here is, during high irradaince level all modified and basic Inc.Cond methods have satisfactory tracking accuracy percentage. VSS-VSF and modified-2 Inc.COnd has acceptable tracking accuracy during high irradaince but they perform very well during low irradiance level. Among all of the Inc.Cond technique only modified-1 Inc.Cond show superior tracking accuracy against high and low irradiance.

5.3.3 Efficiency

The efficiency of basic and modified Inc.Cond techniques are generated by using the fast-dynamic irradiance signal which starts from 1000 W/m² and then changes to 300 W/m²,700 W/m²,400 W/m² and 600 W/m² in zero to one sec. This efficiency graph is extract against case 1 in which a fast-dynamic irradiance signal at 25 ℃is used. The efficiency against each irradiance level is calculated by dividing the average simulated power value by the real MPP power value. Figure 5.19 represents the tracking efficiency of basic and modified Inc.Cond algorithms against case 1. It can be clearly observe from figure 5.19, basic Inc.Cond and Improved Inc.Cond has same efficiency against the fast-dynamic irradiance signal. Both has 75% to 95% efficiency against the fast-dynamic irradiance signal in case 1. When irradiance level is low, their efficiency is lower than 50%. During low irradiance,
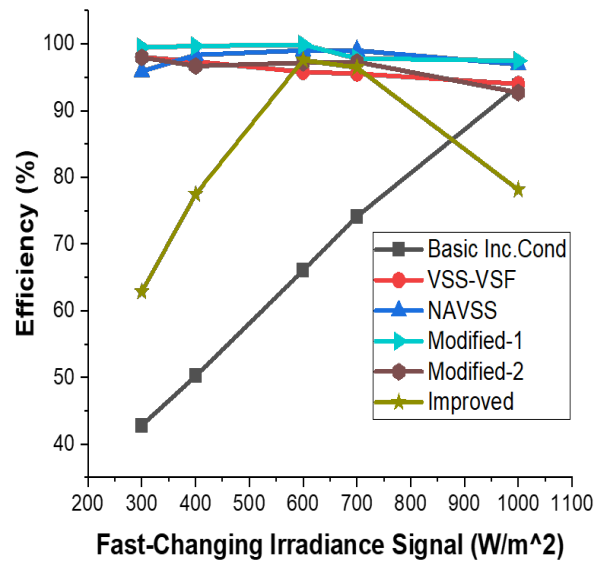
FIGURE 5.19: Efficiency of basic and modified Inc.Cond techniques against Fast-dynamic irradiance signal at 25 ℃

VSS-VSF and NAVSS Inc.Cond show 95% to 97% efficiency which is acceptable. But as fast-dynamic irradiance signal is shift towards the high irradaince level, their efficiency is reduced to 93%.

It can be observe from figure 5.19, modified-1 Inc.Cond has almost 97.82% to 99.9% efficiency against fast-changing irradiance levels and its show satisfactory efficiency against the high and low irradaince in case 1. Modified-2 Inc.Cond has an efficiency of 95% to 98% during low and medium irradiance levels. But as irradiance level is shifted toward a higher level the efficiency is reduced to 93%.

So, the worth thing mention here, during low irradiance levels VSS-VSF and NAVSS Inc.Cond has fine efficiency. But they struggle when irradiance level is high. Improved Inc.Cond has low efficiency during the low irradaince value of fast-dynamic irradiance signal under case 1. But it shows acceptable efficiency almost 95% when irradaince is between 600 W/m^2 to 800 W/m^2.

Against the complete fast-dynamic irradaince signal at 25 ℃, modified-1 Inc.Cond performance well and produce good efficiency among all remaining Inc.Cond techniques. On the second place, NAVSS show acceptable efficiency against case 1 input irradaince and temperature signal.

The efficiency of each modified IncCond MPPT algorithms against fast-changing irradiance signal is mention in Table 5.2. It can be observe from the Table 5.2 that modified-1 and NAVSS IncCond efficiently extract the max. power against each irradiance level. On the second place, the modified-2 and improved IncCond have good tracking against high irradiance level.

TABLE 5.2: Average efficiency of modified IncCond MPPT algorithms against case 1

IncCond Algorithms	Efficiency %
Traditional IncCond	65.43
VSS-VSF	95.7
NAVSS	98.28
Modified-1	99.1
Modified-2	96.34
Improved	82.42

5.3.4 Different Irradiance level signal with Varying Temperature for case 2

To evaluate the performance of basic and five modified versions of the Inc.Cond algorithms, a varying temperature with five differen irradiance levels signal is used to generate the power response of each technique under case 2. The reason behind the selection of this kind of signal is, just to observe the effect of different irradaince with different temperature value on PV array output power.

The initial irradiance leve is $1000W/m^2$ then its value is $300W/m^2$, $700W/m^2$, $400W/m^2$ and $600W/m^2$ and the temperature value is 40 ℃, 35 ℃, 65 ℃, 28 ℃, and 38℃ respectively.

In this thesis work an assumption is taken, about the simulations time which is divided onto five time interval. In each time interval the irradaince and temperature is constant and not related to fast-changing irradaince. Figure 5.20 shows the power response of the basic and each modified Inc.Cond against the Five different

irradiance level with varying temperature values.

At different irradiance level with varying temperatures value all modified Inc.Cond algorithms are not able to operate the PV Array system at its maximum efficiency due to high temperature. The basic Inc.Cond has an unsatisfactory response against high irradiance level with high temperature value. It can be observe from figure 5.20, the basic Inc.Cond algorithm operated the PV Array on constant power generation.

It has a large over-shoot in the negative direction when both irradiance and the temperature level change. VSS-VSF and NAVSS Inc.Cond have the same response during high irradiance and temperature. Both has oscillations around the mpp point, when irradaince value is $1000W/m^2$ and temperature in 40 ℃. But against low irradiance and temperature VSS-VSF and NAVSS Inc.Cond have satisfactory responses.

When irradaince and temperature shift from low to high value, the VSS-VSF and NAVSS Inc.Cond have overshoots and they settle with oscillations. It can be noticed from figure 5.20, modified-2 Inc.Cond show satisfactory power responses against high irradiance with high temperature values. It have fine power extraction during high & low irradiance and temperature level. The oscillations are present when irradiance and temperature level is change from low to high.

It is clearly observe from figure 5.20, modified-1 Inc.Cond has a very good response against each five irradiance level with varying temperature value compared to other Inc.Cond technique. Modified-1 Inc.Cond has fewer oscillations at the start but after settling these oscillations are zero. When irradiance and temperature level is a shift from high to low, the modified-1 Inc.Cond has very less overshoot compared to other techniques.

When the temperature is 65 ℃ and the irradiance level is high, VSS-VSF and NAVSS Inc.Cond produce oscillations and also have overshoots. At 65 ℃ and high irradiance level the basic Inc.Cond have zero oscillation but extracted power is very less compared to other techniques. But modified-1 and 2 Inc.Cond show quite well power response from remaining technique. The improved Inc.Cond have
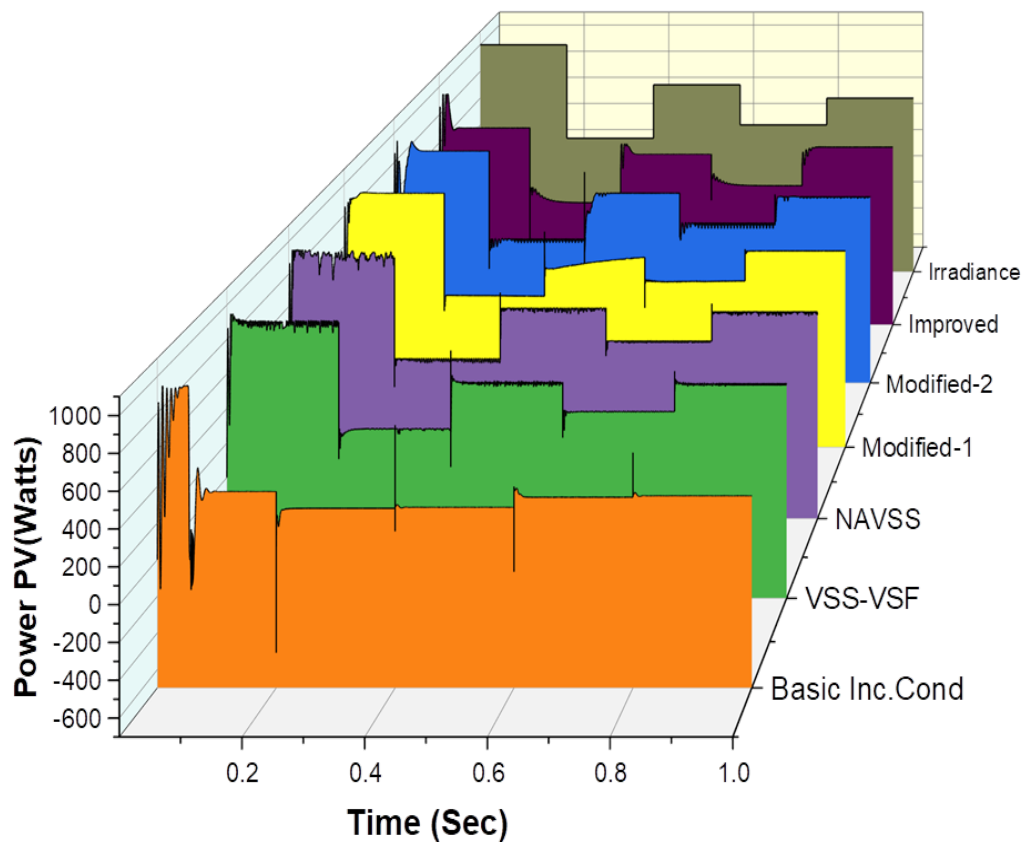
Figure 5.20: Power response of basic and modified Inc.Cond methods against five different irradiance levels and varying temperature for case 2

zero oscillations against high irradiance level at 65 ℃. But the extracted power is not upto the mark.

Improve Inc.Cond has an acceptable power response against the low irradiance and temperature. But this technique has less power extraction during high irradiance and temperature. Oscillations and overshoots are present when both irradaince and temperature level is shift from low to high. So, the worth thing mention here, VSS-VSF and NAVSS has a satisfactory response against low irradaince and temperature leve. They struggle and have oscillations and overshoot during high irradaince with high temperature. The basic inc.Cond completely fail to perform during high irradiance level with high temperature. Improved Inc.Cond show fine response against the low irradiance with low temperature. But when irradaince level is high and also the temperature, the improved inc.cond have oscillations which reduce the efficiency and cause power loss. Modified-1 and 2 Inc.Cond show better performance under five different irradiance level with varying

temperature values. They show better power response during high irradiance and temperature compared to other Inc.Cond. They have minimum oscillations and overshoot, when irradaince and temperature shift from low to high and high to low. So, modified-1 and 2 have superior power response under case 2. With less oscillations and overshoot their efficiency is large and power loss during tracking is less compared to other Inc.Cond algorithms.

5.4   Discussion

Sunlight energy is the leading and important renewable energy source for producing cheap, green, and emission-free electricity. The generation of electricity from the PV module is depend on the weather conditions. So, an algorithm is needed which operate the PV system at its maximum efficiency.

This thesis evaluate the modified versions of the Inc.Cond algorithm under more realistic testing conditions including fast-changing irradiance and varying temperature.

In this thesis, five modified Inc.Cond MPPT algorithms are compared, and suggest the best modified Inc.Cond as MPPT technique in the implementation of onboard solar-charger for solar electric vehicle. To examine the reliability, efficiency, and effectiveness of each Inc.Cond algorithm two test cases are used along with seven performance testing parameters (PTP).

In case 1, a fast-dynamic irradiance signal at 25 ℃ is used as the input of the PV syatem, and extract the voltage, current and power responses of each Inc.Cond algorithm. The case 2 have five different irradaince levels with varying temperature values as the of the PV array which shows the effect of the temperature on PV array output.

The main problem in previous work is, a fast-dynamic irradaince is not consider to evaluate the performance of the technique and also this kind of scenario is not consider for the solar electric car application. Most of the researchers not mention

their input irradaince. Most of the PV system rating is less than 100 watts with only one comparison with the basic Inc.Cond algorithm is given.

Few testing parameters are used mostly convergency speed, steady-state oscillations, and overshoot, etc. And no temperature variations are involved in simulations to determine the performance of their proposed technique under high temperature. To sort out above problem,two test cases with proposed performance testing parameters (PTP) are used to evaluate the performance of five modified Inc.Cond MPPT algorithms are simulationed in matlab/simulink.

The comparison of five modified Inc.Cond MPPT algorithms based on the Direct control under seven performance testing parameters have been done in this work. Two versions of the Inc.Cond algorithm works on the step size which is add or subtract in the duty cycle whenever changes occur in current, voltage, and power value. The remaining modified versions of the Inc.Cond used initial step size or initial delta value for the proper working of the technique.

The Matlab simulations represent that each Inc.Cond methods have fast rise time against the high irradiance level. But some of Inc.Cond technique have steady-state oscillations due to this their efficiency is less and power loss is large.

For low irradiance levels, each Inc.Cond methods have same rise and settling time responses. VSS-VSF and basic Inc.Cond have medium response time during high irradaince level. NAVSS have fast response time under low irradiance levels at STC. Modified-1 and 2 show better response time against high and low irradiance level compared to others. Improved Inc.Cond also have satisfactory time response against high irradiance level but it struggle against low irradaince. VSS-VSF, NAVSS and modified-2 have steady-state oscillations during high and low irradaince level. Due to this, the power loss at mpp point is large for these techniques.
Modified-1 and Improved Inc.Cond have zero oscillations against high and low irradiance level after settling at mpp point. So, their power loss around mpp point is almost negligible compared to other Inc.Cond techniques. Based on the MPP tracking accuracy, the rank of each Inc.Cond MPPT algorithm in this thesis

work is organized from better to unfavorable as fellow: modified-1, modified-2 and NAVSS, Improved Inc.Cond, VSS-VSF and basic Inc.Cond methods.

In terms of efficiency against case 1, the line-up of the modified versions of Inc.Cond MPPT algorithms is arranged from better to worst as fellow: modified-1, NAVSS, modified-2, VSS-VSF, Improved Inc.Cond and basic Inc.Cond. VSS-VSF has good efficiency during low irradiance level. NAVSS perform well during low irradiance level and against high irradaince level it produce oscillations which reduce its efficiency.

Modified-2 have satisfactory result during high irradiance level but it also produce oscillations which reduces its efficiency under high irradiance. Improved inc.cond have very fine response during high irradiance level because it have no oscillations around mpp point but its performance under low irradiance is unfavourable. Modified-1 have better performance under high and low irradiance compared to other Inc.Cond techniques.

During five different irradiance levels with varying temperatures, performance of each Inc.Cond technique is reduced due to the variations in temperature. Techniques which perform better against the case 2, are the modified-1 and 2 and NAVSS. They extract maximum power from PV Array during high irradiance and high temperature.
So, the suggested Inc.Cond method, as MPPT teachnique in the implementation of onboard solar charger for solar electric car, is must be the combination of above mention modified Inc.Cond. The combination or single technique must obtain maximum efficiency during high irradiance, high temperature or low irradiance, low temperature and also against fast-dynamic weather conditions. The combination maybe between Modified-1 and NAVSS or only modified-1 Inc.Cond, or VSS-VSF and modified-2 Inc.Cond etc.

The comparison of extracted power by each modified IncCond algorithm against case 1 and case 2 is given in tabular form. During case 1, it can be notice from Table 5.3 and Table 5.4, the basic and improved IncCond algorithm perform well against high irradaince level. VSS-VSF show good response against low irrdadiance level.

But NAVSS and modified-1 IncCond efficiently track the fast-changing irradaince signal. The extracted power by these two methods is greater then remaining algorithms. Modified-2 only manage to achieve max. power when irradaince is high and it produce oscillations during low irradiance.

TABLE 5.3: Power comparison of five modified Inc.Cond algorithms based-on direct control against case 1

Irrdiance Level	Step-size/Duty-max	Basic Inc.Cond	VSS-VSF	NAVSS
1000 W/m2	0.02 / 0.48	938.65	974.79	981.4
300 W/m2	0.011 / 0.49	126.56	289.04	291
700 W/m2	0.08 / 0.51	520.49	670.56	695.8
400 W/m2	0.008 / 0.42	198.91	386.5	390.6
600 W/m2	0.08 / 0.38	396.40	575.18	594.3

TABLE 5.4: Power comparison of five modified Inc.Cond algorithms based-on direct control against case 1

Irrdiance Level	Step-size/Duty-max	Modified-1	Modified-2	Improved
1000 W/m2	0.02 / 0.48	1002	931.8	785.1
300 W/m2	0.011 / 0.49	293.4	288.94	185.6
700 W/m2	0.08 / 0.51	690.9	683.05	677.28
400 W/m2	0.008 / 0.42	395.91	383.5	306.6
600 W/m2	0.08 / 0.38	599.40	585.18	586.03

During varying temperature conditions the extracted power is reduced and the efficiency of modified IncCond algorithm also reduced. Five different irradaince level with varying temperature is used in case 2. The Table 5.5 and Table 5.6 represent the extracted power comparison among modified IncCond algorithms against case 2. It ca be notic from the Table 5.5 and 5.6, basic IncCond generate constant power against case 2. VSS-VSF show good response against low temperature and irradiance level. NAVSS has power oscillations when temperature is high. Modified-1 IncCond manage to extract max. available power against varying temperature conditions but it struggle only against vary high temperature. Modified-2 and Improved IncCond only manage to achieve max. power when irradaince is high and they both produce oscillations during low irradiance.

TABLE 5.5: Power comparison of five modified Inc.Cond algorithms varying conditions against case 2

Irrdiance Level	Step-size/Duty-max	Basic Inc.Cond	VSS-VSF	NAVSS
1000 W/m2	0.02 / 0.48	480.5	880.3	898.8
300 W/m2	0.011 / 0.49	286	278.6	282.5
700 W/m2	0.08 / 0.51	277	547.09	583.7
400 W/m2	0.008 / 0.42	336.6	381.14	385.69
600 W/m2	0.08 / 0.38	348.40	541.55	564.9

TABLE 5.6: Power comparison of five modified Inc.Cond algorithms varying conditions against case 2

Irrdiance Level	Step-size/Duty-max	Modified-1	Modified-2	Improved
1000 W/m2	0.02 / 0.48	922.5	848.13	708.9
300 W/m2	0.011 / 0.49	283.4	271.02	187.6
700 W/m2	0.08 / 0.51	590.9	577	523.66
400 W/m2	0.008 / 0.42	384.91	376.15	303.16
600 W/m2	0.08 / 0.38	570.70	564.18	564.89

To summarize this work, overall performance against two test cases, the modified-1 Inc.Cond is superior to the remaining technique as this method effectively enhances the operation of the PV array at MPP point Under STC and fast-dynamic irradiance. It has better performance during varying temperature value.

It has less steady-state oscillations almost negligible, convergence speed, and efficiency. Modified-2 Inc.Cond and NAVSS are in second place and VSS-VSF are in third place.

According to these results, the pros and cons of each modified version of the Inc.Cond MPPT algorithms are summarized and simulation parameters are also given in this thesis work. It must be considered that performance differences among analyzed Inc.Cond MPPT technique is slight during STC.

Table 5.7 and Table 5.8 represented the comparison of basic and five modified versions of the Inc.Cond MPPT algorithm against seven performance indices. These

TABLE 5.7: Performance indices and Comparison of five variations in the Inc.Cond algorithm based on the direct control method

Performance indices	Basic Inc.Cond	VSS-VSF	NAVSS
Convergence speed	Slow	Slow	Fast
Complexity	Low	Low	Low
Efficiency	Low	High	High
Steady-state oscillations	Zero	Medium	Medium
Tracking Accuracy	Low	High	High
Fast-change detection	Yes	Yes	Yes
Length of algorithm	Small	Small	Small

TABLE 5.8: Performance indices and Comparison of five variations in the Inc.Cond algorithm based on the direct control method

Performance indices	Modified-1	Modified-2	Improved
Convergence speed	Very Fast	Fast	Slow
Complexity	Low	High	Medium
Efficiency	High	High	low
Steady-state oscillations	Zero	Medium	Zero
Tracking Accuracy	High	High	Low
Fast-change detection	Yes	Yes	Yes
Length of algorithm	Small	Large	Medium

performance indices including rising time, settling time around MPP, tracking accuracy, exact fast MPP detection during a continuous change in irradiance, oscillation at steady-state point, efficiency, complexity, and length of the proposed algorithm compared to basic Inc.Cond algorithm.

All five modified Inc.Cond MPPT methods including traditional Inc.Cond are summarized in Table 5.7 and Table 5.8. According to proposed PTP each Inc.Cond methods are explain along with their pros and cons and complete simulation parameters are mentioned in Table 5.1.

Chapter 6

Conclusion and Future Work

In this chapter conclusion and future work are discussed. There are many opportunities for new researchers in this area in order to develop improved and advanced incremental conductance technique for maximum power point tracking purpose.

6.1   Conclusion

In this thesis, five modified IncCond algorithms are compared in detail. These algorithms are tested against specific performance parameters. Like, convergence speed, steady-state oscillation, efficiency, accuracy, complexity, length of the algorithm, behavior under varying temperatures, and fast-changing solar irradiance. Moreover, simulation results of voltage, current, and power of each modified IncCond are also extracted and tested. This rigorous analysis of multiple algorithms will help to choose the best technique for solar electric cars.

There were a number of modified IncCond techniques in the literature that track the maximum power point of the PV module. Whereas, none of these algorithms were tested thoroughly against the realistic parameters. However, this presented work has an edge over the existing literature in terms of a thorough analysis of each modified IncCond algorithm and the detailed comparison of five modified IncCond algorithms. Afterward, the best algorithm for solar cars application is also

suggested on the basis of fast-changing irradiance signal and varying temperature conditions.

It can be concluded from this thesis that Modified-1 IncCond [33] has the best performance against the conversion speed, fast-tracking of irradiance, and zero oscillation against the high temperature. In the second place, the new advanced variable step size (NAVSS) [29] performed well having medium oscillations against high irradiance with less complexity. In the third place, modified-2 IncCond [34] performed better against very high temperature and high irradiance levels. However, it has oscillations around steady-state points which reduce its efficiency. The remaining modified IncCond have a quite well response against high irradiance levels but they struggled against high temperature and under low irradiance levels. Thus, the modified-1 IncCond is the best option for the MPPT algorithm in a solar electric car in order to increase its efficiency on the road in different weather conditions.

6.2 Future Work

In the future, this comparative study will facilitate further modifications in the IncCond MPPT algorithm. Researchers do not need to study all the proposed IncCond in literature to make a new and improved version of the IncCond technique. Furthermore, based on this work a physical system must be developed to validate the performance of each modified IncCond algorithm.

Moreover, the solar electric car can act as a small PV plant for power generation in a smart grid. It can also be part of hybrid electric vehicles applications. This concept is a more decentralized power generation system compared to the existing centralized power system.

Bibliography

[1] M. H. Uddin, M. A. Baig, & M. Ali, "Comparison of perturb & observe and incremental conductance, maximum power point tracking algorithms on real environmental conditions,"in *2016 International Conference on Computing, Electronic and Electrical Engineering (ICE Cube)*, pp. 1-6. IEEE

[2] "Golbal Energy Consumption Review", Apr. 4,2021. Accessed no: Dec. 29,2021. [Online]. Available: https://www.iea.org/reports/global-energy-review-2021

[3] "Solar Energy, largest solar plants and Renewable Energy", Aug. 15,2020. Accessed on: Dec. 29,2021. [Online]. Available: https://ourworldindata.org/renewable-energy

[4] "Passive Solar History", January ,2021. Accessed on: Dec. 29,2021. [Online]. Available:http://californiasolarcenter.org/old-pages-with-inbound-links/history-pv/.html

[5] N. H. Selman and J. R. Mahmood, "Comparison between perturb & observe, incremental conductance and fuzzy logic mppt techniques at different weather conditions", *International Journal of Innovative Research in Science, Engineering and Technology)* vol. no. 5, pp.12556-12569.

[6] M. Gul, Y. Kotak, & T. Muneer, "Review on recent trend of solar photovoltaic technology". *Energy Exploration and Exploitation* vol. no. 4, pp.485-526, 2016

[7] A. Zahedi, Solar photovoltaic (PV) energy; "latest developments in the building-integrated and hybrid PV systems",*Renewable Energy*, vol. no. 5, pp.711-718.

[8] C. Qi, & Z. Ming, "Photovoltaic Module Simulink Model for a Stand-alone PV System". *Physics Procedia* , 24, pp.94-100, 2012

[9] "Florida's Premier Energy Research Center at the University of Central Florida",May,2020. Accessed on:Dec.29,2021.[Online]. Available:https://energyresearch.ucf.edu/consumer/solar-technologies/solar-electricity-basics/cells-modules-panels-and-arrays.

[10] "PennState College of Earth and Mineral Science/Department of Energy and Mieral Engineering/", July ,2020. Accessed on: Dec. 29,2021. [Online]. Availabe: https://www.e-education.psu.edu/eme812/node/608

[11] "Most Efficient Solar Panels 2022/", Jan. 17,2022. Accessed on: Jan. 29,2022. [Online]. Availabe:https://www.cleanenergyreviews.info/blog/most-efficient-solar-panels

[12] P. Mohanty, T. Muneer, E. J. Gago, & Y. Kotak, "Solar Radiation Fundamentals and PV System Components,"In *Solar Photovoltaic System Applications,* pp. 7-47. Springer, Cham, 2016

[13] M. LokeshReddy, P. J. R. P. Kumar, S. A. M. Chandra, T. S. Babu, & N. Rajasekar, "Comparative study on charge controller techniques for solar PV system". *Energy Procedia* pp.1070-1077, 2017

[14] A. Kapoor, & A. Sharma, " Optimal Charge/Discharge Scheduling of Battery Storage Interconnected With Residential PV System". *IEEE Systems Journal,* vol. no. 3, pp. 3825-3835, 2020

[15] "Electronic Hub "What are the different types of batteries", May. 21,2021. Accessed on: Dec. 29,2021. [Online]. Available: https://www.electronicshub.org/types-of-batteries/

[16] M. Hlaili, & H. Mechergui, " Comparison of Different MPPT Algorithms with a Proposed One Using a Power Estimator for Grid Connected PV Systems". *International Journal of Photoenergy*, pp. 702-712, 2016.

[17] M. M. Rahman, M. Hasanuzzaman, & N. A. Rahim, "Effects of various parameters on PV-module power and efficiency. Energy Conversion and Management", *Energy Conversion and Management, 103,* pp.348-358, 2015

[18] A. R. Gxasheka, E. E. Van Dyk, E. L. & Meyer, "Evaluation of performance parameters of PV modules deployed outdoors". *Renewable Energy* vol. no. 5, pp. 611-620, 2005

[19] M. Suthar, G. K. Singh, & R. P. Saini, "Comparison of mathematical models of photo-voltaic (PV) module and effect of various parameters on its performance". In *2013 International Conference on Energy Efficient Technologies for Sustainability,* pp. 1354-1359. IEEE, 2013

[20] O. Singh, & S. K. Gupta , "A review on recent Mppt techniques for photovoltaic system", In *2018 IEEMA Engineer Infinite Conference (ETechNxT,* pp. 1-6. IEEE, 2018

[21] M. C. Argyrou, P. Christodoulides, & S. A. Kalogirou, "Modeling of a photovoltaic system with different MPPT techniques using MATLAB/Simulink". In *2018 IEEE International Energy Conference (ENERGYCON),* pp. 1-6. IEEE, 2018

[22] S. Pant, & R. P. Saini, "Comparative Study of MPPT Techniques for Solar Photovoltaic System". In *2019 International Conference on Electrical, Electronics and Computer Engineering (UPCON),* pp. 1-6. IEEE, 2019

[23] H. Zhang, & S. Cheng, "A New MPPT Algorithm Based on ANN in Solar PV Systems". In *Advances in Computer, Communication, Control and Automation,* pp. 77-84. Springer, Berlin, Heidelberg, 2011.

[24] A. Manmohan, A. Prasad, R. Dharavath, S. P. Karthikeyan, & I. J. Raglend, "Up and Down Conversion of Photons with modified Perturb and Observe MPPT technique for Efficient Solar Energy Generation". *Energy Procedia, 117,* pp.786-793, 2017

[25] O. Ezinwanne, F. Zhongwen, & L. Zhijun, "Energy Performance and Cost Comparison of MPPT Techniques for Photovoltaics and other Applications". *Energy Procedia,* vol. no. 107, pp.297-303, 2017

[26] C. C. Hua, & Y. Chen, "Modified perturb and observe MPPT with zero oscillation in steady-state for PV systems under partial shaded conditions". In *IEEE Conference on Energy Conversion (CENCON),* pp. 5-9. IEEE, 2017.

[27] M. Kamran, M. Mudassar, M. R. Fazal, M. U. Asghar, M. Bilal, & R. Asghar, "Implementation of improved Perturb & Observe MPPT technique with confined search space for standalone photovoltaic system". *Journal of King Saud University-Engineering Sciences,* vol. no. 7, pp.432-441.

[28] L. Yang, Z. Yunbo, L. Shengzhu, & Z. Hong, "Photovoltaic array MPPT based on improved variable step-size incremental conductance algorithm". In *2017 29th Chinese control and decision conference (CCDC),* pp. 2347-2351. IEEE, 2017.

[29] A. Loukriz, M. Haddadi, & S. Messalti, "Simulation and experimental design of a New Advanced Variable step size Incremental Conductance MPPT algorithm for PV systems". *ISA transactions,* vol. no. 62, pp. 30-38.

[30] N. A. Rahim, A. Amir, A. M. Amir, & J. Selvaraj, "Modified incremental conductance MPPT with direct control and Dual scaled Adaptive step-size method". In *4th IET Clean Energy and Technology Conference (CEAT 2016),* pp. 1-8. IET, 2016.

[31] K. S. Tey, & S. Mekhilef, "Modified incremental conductance MPPT algorithm to mitigate inaccurate responses under fast-changing solar irradiation level". *Solar Energy, 101,* pp.333-342

[32] S. Necaibia, M. S. Kelaiaia, H. Labar, A. Necaibia, & E. D. Castronuovo, "Enhanced auto-scaling incremental conductance MPPT method, implemented on low-cost microcontroller and SEPIC converter". *Solar Energy, 180,* pp.152-168.

[33] S. Bhattacharya, & S. Samanta, "Modified Incremental Conductance MPPT Algorithm for Very Fast-Changing Atmospheric Condition for Solar Electric Vehicle Application".In *2019 IEEE 16th India Council International Conference (INDICON),* pp. 1-4. IEEE, 2019

[34] S. Motahhir, A. El Ghzizal , S. Sebti, & A. Derouich, "Modeling of Photovoltaic System with Modified Incremental ConductanceAlgorithm for Fast Changes of Irradiance". *International Journal of Photoenergy,* 2018.

[35] L. Shang, H. Guo, & W. Zhu, "An improved MPPT control strategy based on incremental conductance algorithm". *Protection and Control of Modern Power Systems, 5(1),* pp.1-8,2020

[36] E. Prasetyono, D. O. Anggriawan, A. Z. Firmansyah, & N. A. Windarko, "A modified MPPT algorithm using incremental conductance for constant power generation of photovoltaic systems". In *2017 International Electronics Symposium on Engineering Technology and Applications (IES-ETA),* pp. 1-6. IEEE, 2017

[37] H. Shahid, M. Kamran, Z. Mehmood, M. Y. Saleem, M. Mudassar, & K. Haider, "Implementation of the novel temperature controller and incremental conductance MPPT algorithm for indoor photovoltaic system". *Solar Energy,* vol. no. 163, pp.235-242.

[38] A. Feroz Mirza, M. Mansoor , Q. Ling , M. I. Khan, & O. M. Aldossary, "Advanced Variable Step Size Incremental Conductance MPPT for a Standalone PV System Utilizing a GA-Tuned PID Controller." *Energies, 13*(16), p.4153-4159, 2020

[39] U. Chauhan, A. Rani, V. singh, & B. Kumar, "A Modified Incremental Conductance Maximum Power Point Technique for Standalone PV System." In *2020 7th International Conference on Signal Processing and Integrated Networks (SPIN),* pp. 61-64. IEEE, 2020.

[40] T. Radjai, L. Rahmani, S. Mekhilef, & J. P. Gaubert, "Implementation of a modified incremental conductance MPPT algorithm with direct control based

on a fuzzy duty cycle change estimator using dSPACE." *Solar Energy, 110,* pp. 325-337.

[41] U. Yilmaz, O. Turksoy, & A. Teke, "Improved MPPT method to increase accuracy and speed in photovoltaic systems under variable atmospheric conditions". *International Journal of Electrical Power and Energy Systems, 113,* pp. 634-651, 2019

[42] U. Yilmaz, A. Kircay, & S. Borekci, "PV system fuzzy logic MPPT method and PI control as a charge controller." *Renewable and Sustainable Energy Reviews, 81,* pp. 994-1001, 2018

[43] S. Ozdemir, N. Altin, & I. Sefa, "Fuzzy logic based MPPT controller for high conversion ratio quadratic boost converter." *International Journal of Hydrogen Energy,* 42(28), pp.17748-17759, 2017

[44] B. Bendib, F. Krim, H. Belmili, M. F. Almi, & S. Boulouma, "Advanced Fuzzy MPPT Controller for a Stand-alone PV System." *Energy Procedia,* 50, pp. 383-392, 2014

[45] S. Farajdadian, & S. M. H. Hosseini, "Optimization of fuzzy-based MPPT controller via metaheuristic techniques for stand-alone PV systems." *International Journal of Hydrogen Energy,* 44(47), pp. 25457-25472, 2019

[46] A. Jouda, F. Elyes, A. Rabhi, & M. Abdelkader, "Optimization of Scaling Factors of Fuzzy–MPPT Controller for Stand-alone Photovoltaic System by Particle Swarm Optimization." *Energy Procedia,* 111, pp. 954-963, 2017

[47] A. S. Saidi, C. B. Salah, A. Errachdi, M. F. Azeem, J. K. Bhutto, & V. P. Thafasal Ijyas, "A novel approach in stand-alone photovoltaic system using MPPT controllers & NNE." *Ain Shams Engineering Journal,* 12(2), pp. 1973-1984, 2021

[48] H. Yatimi, Y. Ouberri, S. Chahid, & E. Aroudam, "Control of an Off-Grid PV System based on the Backstepping MPPT Controller." *Procedia Manufacturing,* 46, pp. 715-723, 2020

[49] A. Mirzaei, M. Forooghi, A. A. Ghadimi, A. H. Abolmasoumi, & M. R. Riahi, "Design and construction of a charge controller for stand-alone PV/battery hybrid system by using a new control strategy and power management." *Solar Energy,* 149, pp. 132-144, 2017

[50] H. Yatimi, Y. Ouberri, & E. Aroudam, "Enhancement of Power Production of an Autonomous PV System Based on Robust MPPT Technique." *Procedia Manufacturing,* 32, pp. 397-404, 2019

[51] H. E. Fadil, & F. Giri, "Nonlinear Adaptive Control for MPPT in Photovoltaic Systems." *IFAC Proceedings* vol no. 9, pp. 392-397, 2009

[52] M. M. Rahman, M. Hasanuzzaman, & N. A. Rahim, "Effects of various parameters on PV-module power and efficiency." *Energy Conversion and Management,* vol. no. 103, pp. 348-358, 2015

[53] M. Hosenuzzaman, M. Hasanuzzaman, N. A. Rahim, & J. Selvaraj, "Factors affecting the pv based power generation."In *2014 3rd IET International Conference on Clean Energy and Technology (CEAT),* pp. 1-6. IET.

[54] Power Electronics: Circuits, Devices & Applications By Muhammad H. Rashid Book,Chapter 5: DC-DC Converters/ Boost Regulators/ page no 261.

[55] "Sigma launching solar-powered electric cars ", Dec. 24 ,2020-21. Accessed on: Jan. 29,2022. [Online]. Availabe: https://www.globalvillagespace.com/sigma-launching-solar-powered-electric-cars-in-pakistan/